

**ASSIMILATION OF FATTY ACIDS AND CHOLESTEROL
IN *MYCOBACTERIUM TUBERCULOSIS***

A Dissertation

Presented to the Faculty of the Graduate School
of Cornell University

In Partial Fulfillment of the Requirements for the Degree of
Doctor of Philosophy

by

Evgeniya Viktorovna Nazarova

August 2017

© 2017 Evgeniya Viktorovna Nazarova

ASSIMILATION OF FATTY ACIDS AND CHOLESTEROL IN *MYCOBACTERIUM TUBERCULOSIS*

Evgeniya Viktorovna Nazarova, Ph. D.

Cornell University 2017

Mycobacterium tuberculosis (Mtb) as a causative agent of human tuberculosis has successfully adapted to survive within the host for decades, and the bacterium's ability to metabolize host-derived lipids (fatty acids and cholesterol) is thought to enable this persistence. Here we provide insights into previously unknown regulatory mechanisms of lipid assimilation in Mtb.

Specifically, we identified a fatty acid transporter Mce1. We determined that previously uncharacterized protein Rv3723/LucA coordinates uptake of both fatty acids and cholesterol through its interaction with accessory subunits of Mce1 and Mce4, respectively. Rv3723/LucA or Mce accessory subunits provide stability to the lipid transporters by protecting from degradation with protease. Moreover, cholesterol and fatty acids imported into the cell send downstream signals to modulate assimilation of each other. Our results demonstrate that fatty acid and cholesterol import in Mtb is exquisitely coordinated through a network of proteins associated with Mce1 and Mce4.

Additionally, to further define genes required for assimilation of fatty acids during macrophage infection, we employed an unbiased approach of genetic screen using metabolic labeling. We identified a number of genes with

previously unknown link to lipid metabolism, and also determined that Mce1, Mce accessory protein OmamB and the ATPase MceG are required for import of fatty acids by Mtb inside the host.

Elucidation of the mechanisms for lipid uptake in Mtb will help us understand key survival strategies of the pathogen, and identify new points of vulnerability for drug discovery.

BIOGRAPHICAL SKETCH

Evgeniya V. Nazarova earned her Bachelors of Techniques and Technology in Chemical Technology and Biotechnology with Honors from Moscow Technological University (former Lomonosov Moscow State Academy of Fine Chemical Technology) in 2008. During her last year of college Evgeniya started working in the laboratory of Dr. Galina M. Sorokoumova where she became interested in lipid metabolism of mycobacteria. She continued her education in Moscow Technological University to receive a Masters of Techniques and Technology in Molecular and Cell Biotechnology with Honors in 2010. Her research was focused on identification of changes in *Mycobacterium smegmatis* lipid metabolism during transition into a nonculturable state. To complete her work she learned microbiological techniques in the lab of Dr. Arseny S Kaprelyants at Russian Academy of Sciences. In parallel, Evgeniya has earned her Bachelors of Management with Honors from the same school for studying methods of motivation of highly qualified employees. She continued working with nonculturable mycobacteria in Dr. Galina Sorokoumova's laboratory for an additional year, after which she came to Cornell to start her graduate studies in 2011. She joined David Russell lab in 2012, where after exploring multiple research avenues, she focused her interest on regulation of lipid assimilation in *Mycobacterium tuberculosis*.

This dissertation is dedicated to my high school chemistry teacher Ekaterina
M. Gelman for instilling her love for science in me.

ACKNOWLEDGMENTS

I would like to thank my PhD advisor Dr. David Russell for believing in me and for his support through my years here. David has inspired me by his excitement about research, his eagerness to always move science forward, to discover the unknown and his unconventional way of thinking. He set up an exceptional example of a great scientist for me.

I would also like to thank my committee members Dr. Brian Crane and Dr. Holger Sondermann for their guidance.

My project would have never existed without Dr. Brian VanderVen, who is simply obsessed with *Mycobacterium tuberculosis* (in a good way). He taught me a great deal of perseverance in our relentless attempts to understand how LucA contributes to lipid metabolism of mycobacteria. He helped me develop as a scientist on an everyday basis through working side-by-side with me, our countless discussions, and his on point questions. These lessons will stay with me for the rest of my life.

Thank you to all the members of David's and Brian's labs whom I had fortune to work with. Special thanks to Wonsik Lee, Maria Podinovskaia, Shumin Tan, Sarah Sidnam, David Gludish, Christine Montague, Thuy La, and last but not least Lu Huang, the best labmate ever. Thanks to Monique Theriault for her help with editing of this dissertation. Linda Bennett's and Shannon Caldwell's technical support is impeccable.

I would like to thank faculty members of the Department of Microbiology and Immunology and the Department of Microbiology. I greatly appreciate everything that Helene Marquis had done for me during my first year here. Also thanks to the brave professors David Lin, James Casey and Holger Sondermann for their BIOAP 6100 Skill Building for Career in Life Sciences. They set up a high bar of expectations for us. Thanks to Joe Peters for being a

caring DGS, and to Shirley Cramer, Sachiko Funaba, Kelly Boyko, Janna S. Lamey, Arla Hourigan, Cindy Grey, for creating such a welcoming atmosphere for graduate students. I highly appreciate all the work of Paul Jennette and Andrew Amodeo in maintaining our BSL-3 labs and making them as comfortable as they can be.

Many thanks to the friends I met here, in Ithaca: Jennifer and Tom Pinello, Chantal Koechli and David Flannelly, Olga Lastovetsky and Marc Barker, and many-many others. Thanks to my friends from back home, especially Aleftina Murashkina, Alyona Shilova and Anastasiya Romanova. I am very thankful to my former PI's Galina Sorokoumova, Margarita Shleeva and Arseny Kaprelyants for making me interested in science.

I am grateful to my parents, Marina Nazarova and Viktor Nazarov, and to my grandmother Valentina Prokaeva for endless love, support and forgiveness. Having these people in my life helped me to push myself further. Thanks to the love of my life Jeff Lovett for putting up with me for so long. I am so lucky I met you, and I cherish every moment we spend together. Finally, thanks to my three J's for keeping me sane.

TABLE OF CONTENTS

Chapter 1: Introduction	1
<i>Mycobacterium tuberculosis</i> pathogenesis	2
Lipid diet of Mtb during infection	3
Known lipid transporters in bacteria	6
Mtb Mce1-4 proteins are ABC transporters	8
Transcriptional regulation of the <i>mce</i> loci.....	11
Importance of Mce complexes for infection	13
Substrates for Mce transporters in Mtb	15
Role of SBPs and accessory proteins in Mce transporters.....	17
Summary.....	20
References.....	21
Chapter 2: Rv3723/LucA coordinates fatty acid and cholesterol uptake in <i>Mycobacterium tuberculosis</i>	31
Abstract	32
Introduction	33
Materials and methods	37
Results	47
<i>lucA</i> encodes a membrane protein involved in cholesterol metabolism... ..	47
LucA facilitates cholesterol uptake and metabolism	49
The Δ <i>lucA</i> :: <i>hyg</i> mutant is defective in cholesterol utilization during infection in macrophages.....	53
The Mtb Δ <i>lucA</i> :: <i>hyg</i> mutant does not assimilate fatty acids during macrophage infection	57
LucA facilitates fatty acid uptake	63
Mce1 is a fatty acid transporter.....	66
LucA interacts with Mce1- and Mce4-associated proteins	68
LucA stabilizes subunits of the Mce1 and Mce4 complexes.	72
LucA contributes to the <i>in vivo</i> fitness of Mtb.....	76

Discussion	78
Acknowledgements	84
References	85
Chapter 3: Insights into mechanisms of inter-regulation of cholesterol and fatty acid transport in <i>Mycobacterium tuberculosis</i>	93
Abstract	94
Introduction	95
Materials and methods	98
Results	101
3.1. Cholesterol catabolites regulate transcription of the <i>mce1</i> locus ...	101
Cholesterol downregulates transcription of the <i>mce1</i> locus.	101
Early catabolites of cholesterol downregulate transcription Of the <i>mce1</i> locus.	105
Cholesterol breakdown product propionate downregulates transcription of the <i>mce1</i> locus.	109
3.2. Long chain fatty acids induce an increase in cholesterol uptake by Mtb.....	110
3.3. Mce accessory proteins are essential for lipid import in Mtb, likely through protection from activity of specialized proteases	113
Mam4B facilitates internalization of cholesterol but not its binding to the bacterial surface.....	114
OmamA facilitates import of fatty acids	116
Deletion of Zmp1/Rv0198c restores fatty acid uptake in $\Delta omamA::hyg$	118
Discussion	120
Acknowledgements	125
References	126
Chapter 4: Identification of genes required for fatty acid assimilation by <i>Mycobacterium tuberculosis</i> during macrophage infection	130
Abstract	131
Introduction	132
Materials and methods	135

Results	139
Validation of the proposed genetic screen	139
Two rounds of genetic screen to identify mutants deficient in uptake of fatty acids during macrophage infection	141
Characterization of lipid metabolism defect in selected mutants.....	154
MceG is required for both fatty acid and cholesterol uptake.	163
Discussion	165
Acknowledgements	169
References	170
Chapter 5: Summary and future directions	175
References.....	183

LIST OF FIGURES

Chapter 1

Figure 1.1. Organization of the <i>mce1-4</i> loci in Mtb	9
Figure 1.2. Mechanism of import for Type I ABC transporter	10
Figure 1.3. Cell wall structures of gram-negative, gram-positive bacteria and mycobacteria	17

Chapter 2

Figure 2.1. LucA facilitates cholesterol uptake in Mtb	51
Figure 2.2. Transcriptional profile of the $\Delta lucA::hyg$ mutant during infection in macrophages.....	54
Figure 2.3. Inactivation of LucA leads to defect in <i>prpD</i> expression	56
Figure 2.4. LucA facilitates fatty acid uptake during macrophage infection	58
Figure 2.5. LucA facilitates accumulation of lipid inclusions in Mtb during macrophage infection	61
Figure 2.6. LucA facilitates fatty acid uptake in axenic culture	64
Figure 2.7. Deletion of the full Mce1 operon leads to fatty acid uptake defect.....	67
Figure 2.8. LucA interacts with subunits of Mce1 and Mce4 transporters.	70
Figure 2.9. LucA is required for stability of Mce1 and Mce4 subunits.....	74
Figure 2.10. Schematic of LucA function in fatty acid and cholesterol uptake	75
Figure 2.11. LucA is required for the full fitness of Mtb in macrophages and survival in mouse lungs.	77

Chapter 3

Figure 3.1. Cholesterol negatively regulates expression of the <i>mce1</i> operon in wild type Mtb.	102
Figure 3.2. Cholesterol catabolic pathway in Mtb	106
Figure 3.3. Cholesterol metabolites regulate expression of the <i>mce1</i> genes	108

Figure 3.4. Fatty acids induce an increase in cholesterol uptake in Mtb.	112
Figure 3.5. Deletion of the Mam4B leads to cholesterol metabolism defect but does not affect cholesterol uptake.....	115
Figure 3.6. Deletion of Zmp1 reverses lipid uptake/metabolism in $\Delta omamA::hyg$	117
Figure 3.7. Proposed model for fatty acid and cholesterol uptake co-regulation in Mtb.....	122

Chapter 4

Figure 4.1. Bacterial populations with low Bodipy-palmitate uptake during macrophage infection can be sorted out with high level of purity.	140
Figure 4.2. Two rounds of genetic screen to identify mutants deficient in uptake of fatty acids during macrophage infection.	143
Figure 4.3. Flow cytometry analysis of Bodipy-palmitate incorporation by original unsorted transposon mutant library, transposon mutants purified in the first round of screen, and transposon mutants purified in the second round of screen.	146
Figure 4.4. Pulse labeling of transposon mutants with Bodipy-palmitate on third day of macrophage infection.	155
Figure 4.5. Quantification of Bodipy-palmitate uptake by transposon mutants on third day of macrophage infection	159
Figure 4.6. Analysis of selected mutants for their ability to metabolize fatty acids and cholesterol.....	162
Figure 4.7. Tn:: <i>mceG</i> mutant has a significant defect in uptake and metabolism of fatty acids and cholesterol.....	164

Chapter 5

Figure 5.1. Model for Mce mediated transport of lipids in Mtb.....	178
--	-----

LIST OF TABLES

Chapter 2

Table 2.1. Strains used in the study 38

Table 2.2. Protein interaction constructs 71

Chapter 3

Table 3.1. Strains used in the study 99

Chapter 4

Table 4.1. Randomly selected mutants from the first round of the screen tested for their ability to assimilate Bodipy-palmitate during macrophage infection 145

Table 4.2. Mutants identified in the first round of screen. 148

Table 4.3. Mutants identified in the second round of screen. 151

Table 4.4. Mutants identified in both first and second rounds of screen 153

LIST OF ABBREVIATIONS

ABC	ATP-binding cassette
Bodipy-C16 (BC16)	Bodipy palmitate
CFU	Colony forming units
FACS	Fluorescence-activated cell sorting
FAS	Fatty acid synthase
mDHFR	Murine dihydrofolate reductase
M Φ	Macrophage
Mlep	<i>Mycobacterium leprae</i>
MOI	Multiplicity of infection
Msm	<i>Mycobacterium smegmatis</i>
Mtb	<i>Mycobacterium tuberculosis</i>
PDIM	Phthiocerol dimycocerosates
SBP	Substrate binding protein
SD	Standard deviation
SEM	Standard error of the mean
TAG	Triacylglycerol
TB	Tuberculosis
TCA	Tricarboxylic acid cycle
THL	Tetrahydrolipstatin
TM	Transmembrane

CHAPTER 1

Introduction

***Mycobacterium tuberculosis* pathogenesis**

Gram-positive *Mycobacterium tuberculosis* (Mtb), the causative agent of tuberculosis (TB), is the number one killer among pathogens, with over 1.5 million deaths every year (WHO, 2016). TB infection is initiated after Mtb is inhaled as aerosol droplets and is engulfed by resident lung phagocytes, prevalently by alveolar macrophages. These leukocytes are designed to degrade all the small foreign objects that reach the lungs, but Mtb perturbs function of macrophages to transform them into a niche for the pathogen's survival. Initial infection leads to infiltration of other immune cells, including neutrophils, monocytes and lymphocytes. As infection progresses, Th1 lymphocytes produce IFN- γ to activate macrophages which causes more inflammation through production of TNF, while IL-10 production reduces inflammation. This balanced inflammation is believed to be the main contributor in formation and progression of granuloma (Mayer-Barber et al., 2014; Gideon et al., 2015; Lin et al., 2016) – a cluster of cells that surround the infection site. This structure serves dual purpose: it contains the infection at the local level, but it also protects Mtb from elimination (Ramakrishnan, 2012). Infected individuals contain granulomas of differing states: from newly formed, healed, to cavitating (i.e. releasing Mtb for reinfection), and bacteria experience very distinct environments within these lesions (Flynn et al., 2015). The outcome of infection is determined at the level of individual granuloma (Lin et al., 2013), making treatment of disease extremely difficult (Via et al., 2015).

Lipid diet of Mtb during infection

With the complicated spectrum of niches that Mtb has to adapt to, it seems that the pathogen always secures availability of its preferred nutrient – lipids (Russell et al., 2010). Mtb infection causes induction of a foamy phenotype in macrophages (Almeida, et al., 2012; Singh et al., 2012), the hallmark of which is accumulation of lipid bodies most likely comprised of triacylglycerols and cholesterol esters. Mtb can acquire fatty acids directly from the macrophage (Lee et al., 2013) or as products of triacylglycerol breakdown (Daniel et al., 2011). Mycobacteria-containing vacuoles can be found fused with these lipid bodies as revealed by electron microscopy, suggesting lipid bodies as a possible route of fatty acid delivery to the pathogen (Peyron et al., 2008; Podinovskaia, et al., 2013; Caire-Brändli et al., 2014). Foamy macrophages are abundant in Mtb granulomas (Hunter et al., 2007; Cáceres et al., 2009), and these lesions are comprised of cholesterol, cholesterol ester and triacylglycerols (Kim et al., 2010), providing an excellent source of nutrients to the pathogen. Importantly, Mtb isolated from the mouse lungs had higher preference for metabolism of fatty acids compared to bacteria grown in axenic culture, indicating metabolic shift towards fatty acids in Mtb *in vivo* (Segal & Bloch, 1956).

Importance of lipid metabolism for Mtb is supported by strikingly high prevalence of lipid metabolism genes in its genome: ~250 compared to only 50 in *E. coli* (Cole et al., 1998), with 100 devoted to beta-oxidation. Mtb is among few bacteria possessing full enzymatic machinery required for

cholesterol breakdown (Van der Geize et al., 2007; Chang et al., 2009) inherited from its saprophytic ancestors (Wipperman et al., 2014; Olive & Sasseti, 2016). These cholesterol catabolism pathways are part of 89 genes of KstR1 and KstR2 regulons that respond transcriptionally to cholesterol. Importantly, these cholesterol and fatty acid metabolism-related genes are upregulated by Mtb in macrophage, in murine model of infection and in the human lung tissue (Schnappinger et al., 2003; Rachman et al., 2006; Rohde et al., 2007; Fontán et al., 2008; Tailleux et al., 2008; Homolka et al., 2010; Rohde, et al., 2012).

Both fatty acids and cholesterol are used by Mtb for energy production and for synthesis of essential lipids. Importance of cholesterol metabolism during infection was supported recently by identification of new antituberculosis compounds inhibiting cholesterol metabolism (VanderVen et al., 2015). Inactivation of isocitrate lyase that integrates cholesterol and fatty acids into central carbon metabolism results in a severe survival defect of the pathogen in mouse infection and in macrophages (McKinney et al., 2000; Muñoz-Elías & McKinney, 2005). Preferential utilization of fatty acids versus carbohydrates by Mtb during infection is supported by the pathogen's dependency on the gluconeogenic pathway (Marrero et al., 2010). Synthesis of important virulence factors of Mtb, such as phthiocerol dimycocerosates (PDIM) and sulfolipid-1, is dependent on both fatty acids and cholesterol (Rainwater & Kolattukudy, 1982; Cox et al., 1999; Jain et al., 2007; Kaur et al., 2009; Lee, et al., 2013). Additionally, excess of fatty acids can be esterified

and stored within Mtb in the form of triacylglycerol (TAG) (Daniel et al., 2011). Induction of TAG synthesis is also triggered by stress conditions suggesting that this pathway is used to reduce bacterial growth by diverting fatty acids from TCA cycle (Baek et al., 2011).

Although significance of lipid metabolism for Mtb pathogenesis is undeniable, specific mechanisms of fatty acid and cholesterol acquisition are not well understood. We provide an overview of literature on this topic further on.

Known lipid transporters in bacteria

Lipid metabolism in bacteria has been studied for decades, however, not that much is known about mechanisms of lipid transport. There was a long standing presumption that lipids can simply diffuse through the lipid bilayer of the cytosolic or outer membrane, but once the exquisite mechanisms of fatty acid metabolism regulation were described in gram-negative *E. coli* (overviewed in Fujita et al., 2007), it became obvious that import of fatty acids had to be transporter-mediated (Abumrad et al., 1998). Long-chain fatty acids are transported by *E.coli* in two-steps: outer membrane-associated protein FadL in the form of β -barrel binds and translocates the substrate by means of the lateral opening in the barrel wall from extracellular space into the outer membrane with subsequent diffusion into the periplasmic space, followed by transfer by cytosolic membrane protein acyl-CoA synthase, FadD, which feeds acyl CoA thioester to cytosolic enzymes for further metabolism (Black, 1991; Black et al., 1992; Lepore et al., 2011). This transport is dependent on intracellular ATP pools and on an energized inner membrane. Homologs of FadD exist in almost every animal kingdom, including one Rv1206/FadD6 in *Mtb* (Hirsch et al., 1998). This protein was found to function as acyl-CoA synthase with preference towards oleic acid to provide building blocks for triacylglycerol synthesis in *Mtb*, however no significant role in fatty acid uptake was determined (Daniel et al., 2014). *Mtb* does not have any proteins homologous to FadL.

Recently, the first cholesterol transport system was identified in another gram-negative bacterium *Sterolibacterium denitrificans* (Lin et al., 2015). Cholesterol and similar sterols are first transferred through the outer membrane by a FadL-like transport system. Then multiple modifications of the sterol molecule take place, products of which are then delivered into the cytosol for catabolism. Interestingly, this import is not ATP-dependent.

Finally, gram-positive actinobacteria *Mtb* and *Rhodococcus jostii* were found to transport cholesterol through the ABC (ATP-binding cassette) transporter Mce4 (Mohn et al., 2008; Pandey & Sasseti, 2008). The rest of this review will focus on this type of transporter in *Mtb*.

Mtb Mce1-4 proteins are ABC transporters

The genome of Mtb contains four homologous unlinked *mce* loci (*mce1-mce4*). The name Mce stands for mammalian cell entry and was assigned based on the role of these proteins in invasion of nonphagocytic HeLa cells (Arruda et al., 1993; Chitale et al., 2001). These loci share homology to ABC (ATP binding cassette) transporters, where each *mce* locus consists of two *yrbE* genes, encoding ABC transporter permeases, six *mce* genes for substrate-binding proteins (SBPs), plus varying numbers of accessory *mam* genes (Mce associated membrane proteins or in old nomenclature *mas* – Mce associated proteins), encoding proteins of unknown function (Figure 1.1). Additionally, five proteins homologous to accessory Mam subunits were encoded by genes scattered throughout the Mtb genome (Perkowski et al., 2016). These proteins were termed OmamA-E for orphaned Mce-associated membrane proteins. All ABC transporters require ATPase for their activity, and genetic epistasis studies predicted Rv0655/MceG to perform this function for all of the four Mce transporters in Mtb (Joshi et al., 2006). The *rv0655/mceG* is located separately from all of the *mce1-4* loci in Mtb genome.

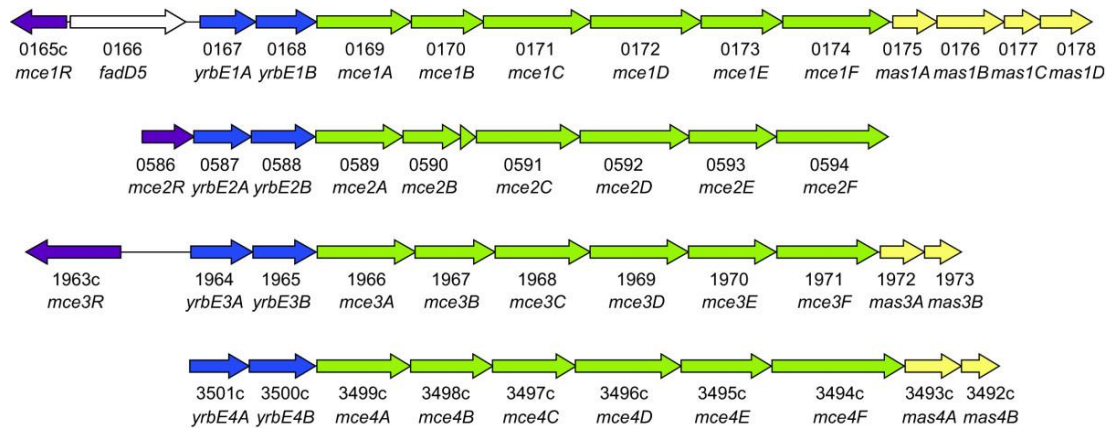


Figure 1.1. Organization of the *mce1-4* loci in *Mtb*. Adapted from (Casali & Riley, 2007).

Import through ABC transporters begins when a substrate binding protein (SBP) delivers the substrate to the two permease domains that span across the cytoplasmic membrane and are inward-facing in the idle position (Figure 1.2). ATPase dimers located in the cytosol always have ATP bound to them with negligible futile activity. The ATPase dimer begins ATP hydrolysis only when its two domains come in close contact with each other, exposing ATP to the active site of the enzyme. Because protrusions of the two permeases are physically inserted into ATPases, this closed position of two ATPases pushes permeases towards each other, which results in outward-facing conformation of the transporter. Due to resulting physical constraints, SBP releases substrate that binds to a specific site formed by two permeases. When ATP hydrolysis is complete, two ATPase subunits dissociate from each other, pulling the permease subunits apart so that they release the substrate into the cytoplasm (Locher, 2016).

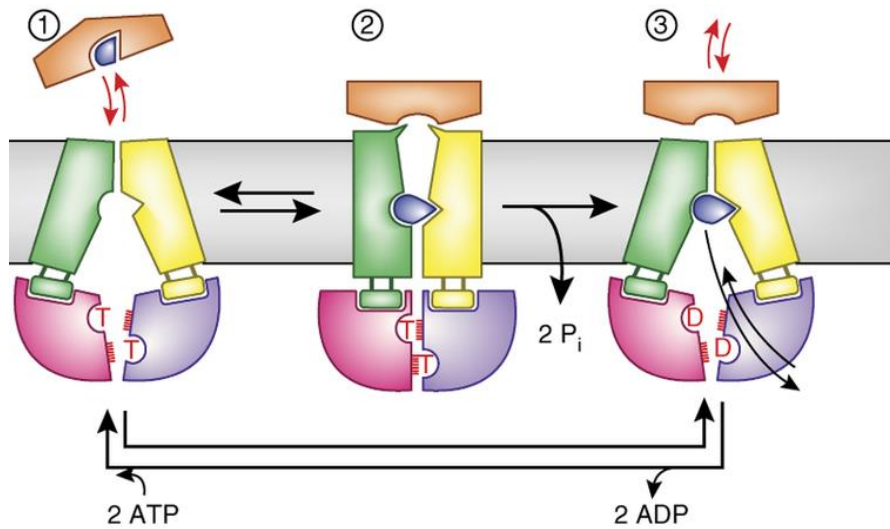


Figure 1.2. Mechanism of import for Type I ABC transporter. Step 1 – binding of a substrate by substrate-binding protein (SBP). Step 2 – Transfer of a substrate from the SBP to permease/transmembrane domains. Step 3. Release of the substrate in cytosol due to hydrolysis of ATP by ATPase/nucleotide binding domain. Nucleotide binding domains or ATPases (analogous to MceG of Mtb) are shown in magenta and purple, permeases (analogous to YrbEA and YrbEB) are in yellow and green, SBP – in brown, and substrate – in blue. Adapted from (Locher, 2016).

Transcriptional regulation of the *mce* loci

The *mce* loci can be transcribed as a singular operon (spanning from *yrbE* genes all the way through accessory *mam* genes), or as smaller regions (Casali et al., 2006; Mohn et al., 2008). The *mce1*, *mce3* and *mce4* genes are expressed in bacilli isolated from the lungs of rabbits (Kumar et al., 2003).

Interestingly, *mce1-3* loci have transcriptional repressors *mce1R-3R* upstream, while *mce4* locus is void of it (Figure 1.1). Specifically, Mce1R and Mce2R share homology with FadR repressor, which consists of a DNA-binding N-terminal, and acyl-CoA-binding C-terminal domains. In *E coli*, FadR is a global regulator of fatty acid metabolism, performing this function through de-repression upon binding of long-chain fatty acid (>14 carbons) CoA thioester (Fujita et al., 2007). The *mce1* operon is downregulated in Mtb during macrophage infection due to Mce1R repressor function (Casali et al., 2006), and Mce2R was shown to negatively regulate the *mce2* operon (Santangelo et al., 2009). However effectors of Mce1R and Mce2R are unknown. Recently, stress-responsive transcription factor DosR was found to increase *mce1R* expression, which in turn would downregulate bacterial growth genes, implying a complicated network of regulation of bacterial replication and Mce1 function (Zeng et al., 2012).

Mce3R is homologous to TetR-transcriptional factors, including FadR, but it's 3D structure is more distinct from Mce1R and Mce2R (Kelly et al., 2015). Intriguingly, 3D structure analysis revealed that its DNA-binding N-terminal domain (8-195 aa) is identical to the one of KstR, and substrate

binding C-terminal domain (217-402 aa) aligns to acyl-CoA binding domains of Mtb Fad35R and *Nacillus halodurans* FadR. In addition to *mce3* Mce3R negatively regulates 2 operons *rv1933c–rv1935c* and *rv1936–rv1941* (Santangelo et al., 2008; de La Paz et al., 2009). Interestingly, *rv1933c–rv1935c* genes are also under control of the KstR repressor, supporting prediction of DNA-binding domain homology between Mce3R and KstR. This analysis reveals possible regulation of cholesterol metabolism by Mce3R (Wipperman et al., 2014).

Finally, *mce4* genes are regulated by cholesterol-sensing KstR repressor, and are induced by cholesterol (Wipperman et al., 2014; Rathor et al., 2016).

Importance of Mce complexes for infection

Genes of the *mce1* and *mce4* loci were found to be a part of the genetic requirements for Mtb's survival in mouse infection (Sasseti & Rubin, 2003). Interestingly, inactivation of *mce1* produced a growth defect of Mtb during the first 2 weeks of infection, while *mce4* mutation does not affect bacterial survival until after 2 weeks of infection when a T cell immune response has developed, enabling activation of the host leukocytes. Additionally, Pandey & Sasseti showed that Mce4 is required for bacterial growth only in IFN- γ activated macrophages (Pandey & Sasseti, 2008), and not in resting macrophages.

Inactivation of both *mce1* and *mce4* loci has a synergistic effect on Mtb survival in mice (Joshi et al., 2006).

Inactivation of *mce2* and *mce3* operons in Mtb results in attenuation of Mtb in mouse infection, manifested in no increase of bacterial counts compared to initial inoculum and in better survival of infected mice (Gioffré et al., 2005; Marjanovic et al., 2010).

Inactivation of *mceG*, encoding a putative ATPase predicted to be required for function of all Mce1-4 transporters, leads to ~10 fold decrease in Mtb numbers in murine lungs (compared to the initial inoculum) by the end of 5 weeks of infection which manifests in ~4 log difference compared to the infection with the wild type strain (Joshi et al., 2006). This data indicates the essential role of MceG and possibly linked to it Mce1-4 transporters for Mtb during infection.

We should point out that the majority of these experiments were performed with an intravenous or intraperitoneal route of infection (as opposed to the natural aerosol route), and CFU counts were determined from the spleen, not from the lung.

Substrates for Mce transporters in Mtb

The first Mce protein complex for which function was characterized in Mtb was Mce4, a cholesterol transporter. However, mutants defective in *mce4* showed residual cholesterol uptake activity and ability to grow in media with cholesterol as a single carbon source (Pandey & Sassetti, 2008). This indicates presence of an alternative cholesterol transporter in Mtb, possibly Mce3 (Wipperman et al., 2014).

The *mce1* locus is preceded by *fadD5* encoding fatty acyl-coenzyme A synthetase (Figure 1.1), responsible for the first modification that fatty acid undergoes once it enters the cytosol which solubilizes it for downstream reactions. FadD5 is important in controlling bacterial numbers in a mouse infection (Dunphy et al., 2010). Taken together with similarity of Mce1R to the FadR repressor, we could suggest that Mce1 functions as a fatty acids transporter. Given the importance of Mce1 for Mtb in a mouse infection, there were few attempts to assign function to this ABC transporter complex. As inactivation of *mce1* in Mtb causes perturbation in mycolic acid content (Dunphy et al., 2010; Forrellad et al., 2014; Queiroz et al., 2015), which results in the inability of infected macrophages to produce a proinflammatory response (Shimono et al., 2003), it was suggested that Mce1 moves mycolic acids in the mycobacterial cell wall to maintain its homeostasis. Additionally, a marginal defect in palmitic acid transport was found in the $\Delta mce1$ mutant (Forrellad et al., 2014). It is important to note that inability to import fatty acids could result in changes of mycobacterial mycolic acid content, since Mtb uses

long-chain fatty acids as substrates for FASII elongation to produce these lipids. In the absence of the extracellular fatty acids, Mtb would have to either synthesize fatty acids *de novo* or to recycle them from other lipids, which would be energy-costly. Further investigation of substrate specificity for Mce1 is needed.

Similarly, changes in sulfolipid-1 content observed in Mtb with disrupted *mce2* could result from a defect in fatty acid/cholesterol uptake causing an imbalance in their metabolism (Marjanovic et al., 2011). Considering the homology of the transcriptional repressor Mce2R to FadR, we hypothesize that Mce2 functions as an alternative fatty acid transporter.

The genome of the pathogen *Mycobacterium leprae*, a close relative of Mtb, contains only one *mce* operon, a homologue of *mce1*. *M. leprae* is fully capable of importing and metabolizing palmitate when the bacteria are recovered from animal tissues (Franzblau, 1988), supporting the role of Mce1 as a fatty acid transporter. *M. leprae* lacks almost all of the genes encoding for cholesterol catabolic pathways, except for the very first one, which converts cholesterol to cholestenone. Interestingly, this pathogen still imports cholesterol, and performs this very first reaction (Marques et al., 2015), indicating that cholestenone might serve as a signal molecule, and raising a question of which alternative cholesterol transporter is used in *M. leprae*.

Role of SBPs and accessory proteins in Mce transporters

In addition to actinobacteria, Mce proteins are also found in double-membraned bacteria (Casali & Riley, 2007) and eukaryotic chloroplasts (Awai et al., 2006). Although Mtb is considered a gram-positive bacterium, its outer layer of the cell wall is comprised of complex lipids, resembling the cell wall structure of gram-negative bacteria (Figure 1.3). Therefore analysis of organization of Mce complexes in gram-negative bacteria could allow better understanding of mechanisms of lipid transport through these transporters in Mtb.

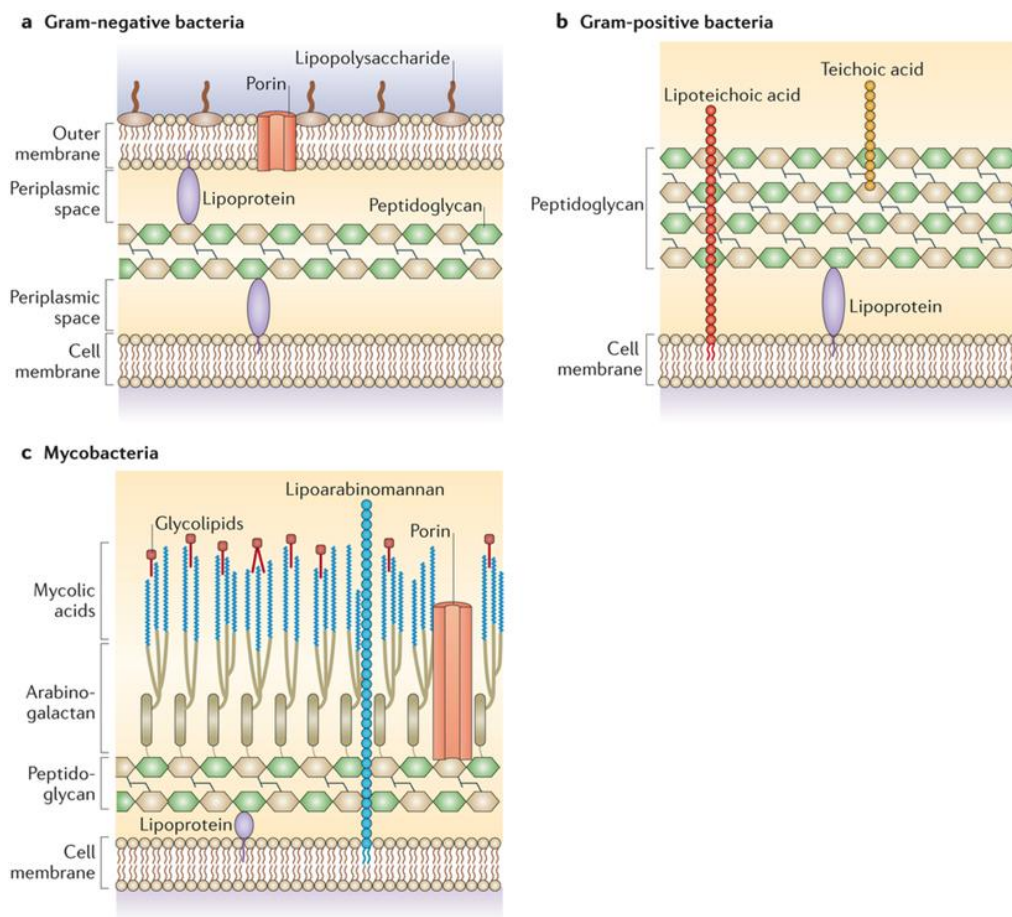


Figure 1.3. Cell wall structures of gram-negative, gram-positive bacteria and mycobacteria. Adapted from (Brown et al., 2015).

E. coli complex homologous to Mce that is involved in delivery of lipids from the outer to the cytoplasmic membrane was recently characterized (Ekiert et al., 2016; Thong et al., 2016). It consists of MlaE permease and MlaF ATPase subunits along with additional proteins MlaD and MlaC. MlaD in the form of a homo-hexamer along with MlaC bind lipids and resemble SBPs of the Mce complex. These SBPs were proposed to function in binding and shuttling of the substrates between the outer membrane and inner membrane, however directionality of this transport has not been determined.

Mce1 and Mce4 protein complexes are secreted onto the surface of Mtb through the SecA2-dependent protein export system (McCann et al., 2011; Feltcher et al., 2015). YrbE1B permease is localized in cytoplasmic membrane, while SBPs Mce1A, Mce1B, Mce1C and Mce1E are found preferentially in the cell wall with partial localization to the cytoplasmic membrane (Forrellad et al., 2014). Interestingly, six Mce SBP's found in each Mce1-4 transporter complex resemble homo-hexamer structure of MlaD in *E. coli*. Therefore, by comparing Mce transporters of Mtb to the Mla complex of *E. coli*, we can hypothesize that Mce SBP's are responsible for binding/shuttling of substrates across the cell wall of Mtb to deliver them to YrbE permease, which will complete the import by pushing substrates through the cytoplasmic membrane into the cytosol.

Activity of ABC transporters for the most part is determined through interaction with accessory subunits that can perform a variety of functions (Biemans-Oldehinkel et al., 2006). For instance, membrane-embedded

accessory proteins of endoplasmic reticulum membrane transporter associated with antigen processing (TAP) complex are essential for recruitment of tapasin, a glycoprotein responsible for interaction between TAP and MHC class I molecules (Procko et al., 2005). Therefore, such membrane accessory proteins can perform an adapter function to recruit interacting partners to the transporter. The cytosolic accessory domain of ATPase MalK, which supplies energy for maltose transporter in enteric bacteria, performs dual function (Böhm & Boos, 2004). First, it serves as a binding site for regulatory enzyme IIA^{glc} when glucose is abundant, which results in inactivation of maltose import. Second, it inhibits activity of MlaT, a positive transcription regulator of maltose regulon. In result, bacteria metabolize glucose (a better energy source) when it is available, halting import of maltose.

The exact function of accessory subunits in Mtb still needs to be determined. Orphaned accessory Rv0199/OmamA protects Mce1 SBPs from degradation in Mtb (Perkowski et al., 2016). Mtb cultures grown in rich media demonstrated an abundant presence of Mce1C degradation products in the cell membrane and extracellularly, suggesting possible regulation of Mce1 function by protease activity (Forrellad et al., 2014).

Summary

One of the mechanisms of Mtb's adaptation to infection is its ability to acquire host-derived lipids: fatty acids and cholesterol. Mce4 ABC transporter was found to be responsible for cholesterol import in Mtb, however a fatty acid transporter still needs to be identified. How Mce transporters are regulated is also unknown. Improved understanding of mechanisms used by Mtb for lipid assimilation will determine points of vulnerability of Mtb inside its host.

References

Abumrad, N., Harmon, C., & Ibrahimi, A. (1998). Membrane transport of long-chain fatty acids: evidence for a facilitated process. *J. Lipid Res.*, 39, 2309–2318.

Almeida, P. E., Carneiro, A. B., Silva, A. R., & Bozza, P. T. (2012). PPAR-gamma expression and function in mycobacterial infection: Roles in lipid metabolism, immunity, and bacterial killing. *PPAR Research.*, 2012, 383829.

Arruda, S., Bomfim, G., Knights, R., Huima-Byron, T., & Riley, L. W. (1993). Cloning of an *M. tuberculosis* DNA fragment associated with entry and survival inside cells. *Science*, 261, 1454–1457.

Awai, K., Xu, C., Tamot, B., & Benning, C. (2006). A phosphatidic acid-binding protein of the chloroplast inner envelope membrane involved in lipid trafficking. *Proceedings of the National Academy of Sciences*, 103, 10817–10822.

Baek, S. H., Li, A. H., & Sassetti, C. M. (2011). Metabolic regulation of mycobacterial growth and antibiotic sensitivity. *PLoS Biology*, 9, e1001065.

Beatty, W. L., Rhoades, E. R., Ullrich, H.-J., Chatterjee, D., Heuser, J. E., & Russell, D. G. (2000). Trafficking and release of mycobacterial lipids from infected macrophages. *Traffic*, 1, 235–247.

Biemans-Oldehinkel, E., Doeven, M. K., & Poolman, B. (2006). ABC transporter architecture and regulatory roles of accessory domains. *FEBS Letters*, 580, 1023-1035.

Black, P. N. (1991). Primary sequence of the *Escherichia coli fadL* gene encoding an outer membrane protein required for long-chain fatty acid transport. *Journal of Bacteriology*, 173, 435–442.

Black, P. N., DiRusso, C. C., Metzger, A. K., & Heimert, T. L. (1992). Cloning, sequencing, and expression of the *fadD* gene of *Escherichia coli* encoding acyl coenzyme A synthetase. *Journal of Biological Chemistry*, 267, 25513–25520.

Böhm, A., & Boos, W. (2004). Gene regulation in prokaryotes by subcellular relocalization of transcription factors. *Curr Opin in Microbiology*, 7, 151-156.

Brown, L., Wolf, J. M., Prados-Rosales, R., & Casadevall, A. (2015). Through the wall: extracellular vesicles in Gram-positive bacteria, mycobacteria and fungi. *Nature Reviews Microbiology*, 13, 620–630.

Cáceres, N., Tapia, G., Ojanguren, I., Altare, F., Gil, O., Pinto, S., ... Cardona, P. J. (2009). Evolution of foamy macrophages in the pulmonary granulomas of experimental tuberculosis models. *Tuberculosis*, 89, 175–182.

Caire-Brändli, I. B., Papadopoulos, A., Malaga, W., Marais, D., Canaan, S., Thilo, L., & De Chastelliera, C. (2014). Reversible lipid accumulation and associated division arrest of *Mycobacterium avium* in lipoprotein-induced foamy macrophages may resemble key events during latency and reactivation of tuberculosis. *Infection and Immunity*, 82, 476–490.

Casali, N., & Riley, L. W. (2007). A phylogenomic analysis of the *Actinomycetales mce* operons. *BMC Genomics*, 8, 60.

Casali, N., White, A. M., & Riley, L. W. (2006). Regulation of the *Mycobacterium tuberculosis mce1* operon. *Journal of Bacteriology*, 188, 441–449.

Chang, J. C., Miner, M. D., Pandey, A. K., Gill, W. P., Harik, N. S., Sasseti, C. M., & Sherman, D. R. (2009). *igr* genes and *Mycobacterium tuberculosis* cholesterol metabolism. *Journal of Bacteriology*, 191, 5232–5239.

Chitale, S., Ehrt, S., Kawamura, I., Fujimura, T., Shimono, N., Anand, N., ... Riley, L. W. (2001). Recombinant *Mycobacterium tuberculosis* protein associated with mammalian cell entry. *Cellular Microbiology*, 3, 247–254.

Cole, S. T., Brosch, R., Parkhill, J., Garnier, T., Churcher, C., Harris, D., ... Barrell, B. G. (1998). Deciphering the biology of *Mycobacterium tuberculosis* from the complete genome sequence. *Nature*, 393, 537–544.

Cox, J. S., Chen, B., McNeil, M., & Jacobs, W. R. (1999). Complex lipid determines tissue-specific replication of *Mycobacterium tuberculosis* in mice. *Nature*, 402, 79–83.

Daniel, J., Maamar, H., Deb, C., Sirakova, T. D., & Kolattukudy, P. E. (2011). *Mycobacterium tuberculosis* uses host triacylglycerol to accumulate lipid droplets and acquires a dormancy-like phenotype in lipid-loaded macrophages. *PLoS Pathogens*, 7, e1002093.

Daniel, J., Sirakova, T., & Kolattukudy, P. (2014). An Acyl-CoA synthetase in *Mycobacterium tuberculosis* involved in triacylglycerol accumulation during dormancy. *PLoS ONE*, 9, e114877.

de La Paz, M., Klepp, L., Nuñez-García, J., Blanco, F. C., Soria, M., del Carmen García-Polayo, M., ... Bigi, F. (2009). Mce3R, a TetR-type transcriptional repressor, controls the expression of a regulon involved in lipid metabolism in *Mycobacterium tuberculosis*. *Microbiology*, 155, 2245–2255.

Dunphy, K. Y., Senaratne, R. H., Masuzawa, M., Kendall, L. V., & Riley, L. W. (2010). Attenuation of *Mycobacterium tuberculosis* functionally disrupted in a fatty acyl-coenzyme A synthetase gene *fadD5*. *The Journal of Infectious Diseases*, 201, 1232–1239.

Ekiert, D. C., Bhabha, G., Greenan, G., Ovchinnikov, S., Cox, J. S., & Vale, R. D. (2016). Architectures of a lipid transport systems for the bacterial outer membrane. *Cell*, 169, 273-285.

Feltcher, M. E., Gunawardena, H. P., Zulauf, K. E., Malik, S., Griffin, J. E., Sasseti, C. M., ... Braunstein, M. (2015). Label-free quantitative proteomics reveals a role for the *Mycobacterium tuberculosis* SecA2 pathway in exporting solute binding proteins and Mce transporters to the cell wall. *Molecular & Cellular Proteomics*, 14, 1501–1516.

Flynn, J. L., Gideon, H. P., Mattila, J. T., & Lin, P. ling. (2015). Immunology studies in non-human primate models of tuberculosis. *Immunological Reviews*, 264, 60–73.

Fontán, P., Aris, V., Ghanny, S., Soteropoulos, P., & Smith, I. (2008). Global transcriptional profile of *Mycobacterium tuberculosis* during THP-1 human macrophage infection. *Infection and Immunity*, 76, 717–725.

Forrellad, M. A., McNeil, M., Santangelo, M. D. L. P., Blanco, F. C., Garcia, E., Klepp, L. I., ... Bigi, F. (2014). Role of the Mce1 transporter in the lipid homeostasis of *Mycobacterium tuberculosis*. *Tuberculosis*, 94, 170–177.

Franzblau, S. G. (1988). Oxidation of palmitic acid by *Mycobacterium leprae* in an axenic medium. *Journal of Clinical Microbiology*, 26, 18–21.

Fujita, Y., Matsuoka, H., & Hirooka, K. (2007). Regulation of fatty acid metabolism in bacteria. *Molecular Microbiology*, 66, 829-839.

Gideon, H. P., Phuah, J. Y., Myers, A. J., Bryson, B. D., Rodgers, M. A., Coleman, M. T., ... Flynn, J. A. L. (2015). Variability in tuberculosis granuloma T cell responses exists, but a balance of pro- and anti-inflammatory cytokines is associated with sterilization. *PLoS Pathogens*, 11, e1004603.

Gioffré, A., Infante, E., Aguilar, D., De La Paz Santangelo, M., Klepp, L., Amadio, A., ... Bigi, F. (2005). Mutation in *mce* operons attenuates *Mycobacterium tuberculosis* virulence. *Microbes and Infection*, 7, 325–334.

Hirsch, D., Stahl, A., & Lodish, H. F. (1998). A family of fatty acid transporters conserved from mycobacterium to man. *Proceedings of the National Academy of Sciences of the United States of America*, 95, 8625–8629.

Homolka, S., Niemann, S., Russell, D. G., & Rohde, K. H. (2010). Functional genetic diversity among *Mycobacterium tuberculosis* complex clinical isolates: Delineation of conserved core and lineage-specific transcriptomes during intracellular survival. *PLoS Pathogens*, 6, 1–17.

Hunter, R. L., Jagannath, C., & Actor, J. K. (2007). Pathology of postprimary tuberculosis in humans and mice: Contradiction of long-held beliefs. *Tuberculosis*, 87, 267–278.

Jain, M., Petzold, C. J., Schelle, M. W., Leavell, M. D., Mougous, J. D., Bertozzi, C. R., ... Cox, J. S. (2007). Lipidomics reveals control of *Mycobacterium tuberculosis* virulence lipids via metabolic coupling. *Proceedings of the National Academy of Sciences*, 104, 5133–5138.

Joshi, S. M., Pandey, A. K., Capite, N., Fortune, S. M., Rubin, E. J., & Sasseti, C. M. (2006). Characterization of mycobacterial virulence genes through genetic interaction mapping. *Proceedings of the National Academy of Sciences*, 103, 11760–11765.

Kaur, D., Guerin, M. E., Skovierová, H., Brennan, P. J., & Jackson, M. (2009). Chapter 2 Biogenesis of the cell wall and other glycoconjugates of *Mycobacterium tuberculosis*. *Advances in Applied Microbiology*, 69, 23-78.

Kelly, L. A., Mezulis, S., Yates, C., Wass, M., & Sternberg, M. (2015). The Phyre2 web portal for protein modelling, prediction, and analysis. *Nature Protocols*, 10, 845–858.

Kim, M. J., Wainwright, H. C., Locketz, M., Bekker, L. G., Walther, G. B., Dittrich, C., ... Russell, D. G. (2010). Caseation of human tuberculosis granulomas correlates with elevated host lipid metabolism. *EMBO Molecular Medicine*, 2, 258–274.

Kumar, A., Bose, M., & Brahmachari, V. (2003). Analysis of expression profile of mammalian cell entry (*mce*) operons of *Mycobacterium tuberculosis*. *Infect Immun*, 71, 6083–6087.

Lee, W., VanderVen, B. C., Fahey, R. J., & Russell, D. G. (2013). Intracellular *Mycobacterium tuberculosis* exploits host-derived fatty acids to limit metabolic stress. *Journal of Biological Chemistry*, 288, 6788–6800.

Lepore, B. W., Indic, M., Pham, H., Hearn, E. M., Patel, D. R., & van den Berg, B. (2011). Ligand-gated diffusion across the bacterial outer membrane. *Proceedings of the National Academy of Sciences*, 108, 10121–10126.

Lin, C. W., Wang, P. H., Ismail, W., Tsai, Y. W., Nayal, A. El, Yang, C. Y., ... Chiang, Y. R. (2015). Substrate uptake and subcellular compartmentation of anoxic cholesterol catabolism in *Sterolibacterium denitrificans*. *Journal of Biological Chemistry*, 290, 1155–1169.

Lin, P. L., Ford, C. B., Coleman, M. T., Myers, A. J., Gawande, R., Ioerger, T., ... Flynn, J. L. (2013). Sterilization of granulomas is common in active and latent tuberculosis despite within-host variability in bacterial killing. *Nature Medicine*, 20, 75–79.

Lin, P. L., Maiello, P., Gideon, H. P., Coleman, M. T., Cadena, A. M., Rodgers, M. A., ... Flynn, J. A. L. (2016). PET CT identifies reactivation risk in cynomolgus macaques with latent *M. tuberculosis*. *PLoS Pathogens*, 12, e1005739.

Locher, K. P. (2016). Mechanistic diversity in ATP-binding cassette (ABC) transporters. *Nature Structural & Molecular Biology*, 23, 487–493.

Marjanovic, O., Iavarone, A. T., & Riley, L. W. (2011). Sulfolipid accumulation in *Mycobacterium tuberculosis* disrupted in the *mce2* operon. *Journal of Microbiology*, 49, 441–447.

Marjanovic, O., Miyata, T., Goodridge, A., Kendall, L. V., & Riley, L. W. (2010). *Mce2* operon mutant strain of *Mycobacterium tuberculosis* is attenuated in C57BL/6 mice. *Tuberculosis*, 90, 50–56.

Marques, M. A. M., Berrêdo-Pinho, M., Rosa, T. L. S. A., Pujari, V., Lemes, R. M. R., Lery, L. M. S., ... Pessolani, M. C. V. (2015). The essential role of cholesterol metabolism in the intracellular survival of *Mycobacterium leprae* is not coupled to central carbon metabolism and energy production. *Journal of Bacteriology*, 197, 3698–3707.

Marrero, J., Rhee, K. Y., Schnappinger, D., Pethe, K., & Ehrt, S. (2010). Gluconeogenic carbon flow of tricarboxylic acid cycle intermediates is critical for *Mycobacterium tuberculosis* to establish and maintain infection. *Proceedings of the National Academy of Sciences*, 107, 9819–9824.

Mayer-Barber, K. D., Andrade, B. B., Oland, S. D., Amaral, E. P., Barber, D. L., Gonzales, J., ... Sher, A. (2014). Host-directed therapy of tuberculosis based on interleukin-1 and type I interferon crosstalk. *Nature*, 511, 99–103.

McKinney, J. D., Höner zu Bentrup, K., Muñoz-Elías, E. J., Miczak, a, Chen, B., Chan, W. T., ... Russell, D. G. (2000). Persistence of *Mycobacterium tuberculosis* in macrophages and mice requires the glyoxylate shunt enzyme isocitrate lyase. *Nature*, 406, 735–738.

Mohn, W. W., Van Der Geize, R., Stewart, G. R., Okamoto, S., Liu, J., Dijkhuizen, L., & Eltis, L. D. (2008). The actinobacterial *mce4* locus encodes a steroid transporter. *Journal of Biological Chemistry*, 283, 35368–35374.

Muñoz-Elías, E. J., & McKinney, J. D. (2005). *Mycobacterium tuberculosis* isocitrate lyases 1 and 2 are jointly required for *in vivo* growth and virulence. *Nature Medicine*, 11, 638–644.

Olive, A. J., & Sasseti, C. M. (2016). Metabolic crosstalk between host and pathogen: sensing, adapting and competing. *Nature Reviews Microbiology*, 14, 221–234.

Pandey, A. K., & Sasseti, C. M. (2008). Mycobacterial persistence requires the utilization of host cholesterol. *Proceedings of the National Academy of Sciences*, 105, 4376–4380.

Perkowski, E. F., Miller, B. K., Mccann, J. R., Sullivan, J. T., Malik, S., Allen, I. C., ... Braunstein, M. (2016). An orphaned Mce-associated membrane protein of *Mycobacterium tuberculosis* is a virulence factor that stabilizes Mce transporters. *Molecular Microbiology*, 100, 90–107.

Peyron, P., Vaubourgeix, J., Poquet, Y., Levillain, F., Botanch, C., Bardou, F., ... Altare, F. (2008). Foamy macrophages from tuberculous patients' granulomas constitute a nutrient-rich reservoir for *M. tuberculosis* persistence. *PLoS Pathogens*, 4, e1000204.

Podinovskaia, M., Lee, W., Caldwell, S., & Russell, D. G. (2013). Infection of macrophages with *Mycobacterium tuberculosis* induces global modifications to phagosomal function. *Cellular Microbiology*, 15, 843–859.

Procko, E., Raghuraman, G., Wiley, D. C., Raghavan, M., & Gaudet, R. (2005). Identification of domain boundaries within the N-termini of TAP1 and TAP2 and their importance in tapasin binding and tapasin-mediated increase in peptide loading of MHC class I. *Immunology and Cell Biology*, 83, 475–482.

Queiroz, A., Medina-Cleghorn, D., Marjanovic, O., Nomura, D. K., & Riley, L. W. (2015). Comparative metabolic profiling of *mce1* operon mutant vs wild-type *Mycobacterium tuberculosis* strains. *Pathogens and Disease*, 73, ftt066.

Rachman, H., Strong, M., Ulrichs, T., Grode, L., Schuchhardt, J., Mollenkopf, H., ... Kaufmann, S. H. E. (2006). Unique transcriptome signature of *Mycobacterium tuberculosis* in pulmonary tuberculosis. *Infection and Immunity*, 74, 1233–1242.

Rainwater, D. L., & Kolattukudy, P. E. (1982). Isolation and characterization of acyl coenzyme A carboxylases from *Mycobacterium tuberculosis* and *Mycobacterium bovis*, which produce multiple ethyl-branched mycocerosic acids. *Journal of Bacteriology*, 151, 905–911.

Ramakrishnan, L. (2012). Revisiting the role of the granuloma in tuberculosis. *Nature Reviews Immunology*, 12, 352-366.

Rathor, N., Garima, K., Sharma, N. K., Narang, A., Varma-Basil, M., & Bose, M. (2016). Expression profile of *mce4* operon of *Mycobacterium tuberculosis* following environmental stress. *International Journal of Mycobacteriology*, 5, 328–332.

Rohde, K. H., Abramovitch, R. B., & Russell, D. G. (2007). *Mycobacterium tuberculosis* invasion of macrophages: linking bacterial gene expression to environmental cues. *Cell Host and Microbe*, 2, 352–364.

Rohde, K. H., Veiga, D. F. T., Caldwell, S., Balázsi, G., & Russell, D. G. (2012). Linking the transcriptional profiles and the physiological states of *Mycobacterium tuberculosis* during an extended intracellular infection. *PLoS Pathogens*, 8, e1002769.

Russell, D. G., VanderVen, B. C., Lee, W., Abramovitch, R. B., Kim, M. J., Homolka, S., ... Rohde, K. H. (2010). *Mycobacterium tuberculosis* wears what it eats. *Cell Host and Microbe*, 8, 68-76.

Santangelo, M. P., Blanco, F. C., Bianco, M. V., Klepp, L. I., Zabal, O., Cataldi, A. A., & Bigi, F. (2008). Study of the role of Mce3R on the transcription of *mce* genes of *Mycobacterium tuberculosis*. *BMC Microbiology*, 8, 38.

Santangelo, M. de la P., Blanco, F., Campos, E., Soria, M., Bianco, M. V., Klepp, L., ... Bigi, F. (2009). Mce2R from *Mycobacterium tuberculosis* represses the expression of the *mce2* operon. *Tuberculosis*, 89, 22–28.

Sasseti, C. M., & Rubin, E. J. (2003). Genetic requirements for mycobacterial survival during infection. *Proceedings of the National Academy of Sciences*, 100, 12989–12994.

Schnappinger, D., Ehrt, S., Voskuil, M. I., Liu, Y., Mangan, J. A., Monahan, I. M., ... Schoolnik, G. K. (2003). Transcriptional adaptation of *Mycobacterium tuberculosis* within macrophages: Insights into the phagosomal environment. *The Journal of Experimental Medicine*, 198, 693–704.

Segal, W., Bloch, H. (1956). Biochemical differentiation of *Mycobacterium tuberculosis* grown *in vivo* and *in vitro*. *Journal of Bacteriology*, 72, 132–141.

Shimono, N., Morici, L., Casali, N., Cantrell, S., Sidders, B., Ehrt, S., & Riley, L. W. (2003). Hypervirulent mutant of *Mycobacterium tuberculosis* resulting from disruption of the *mce1* operon. *Proceedings of the National Academy of Sciences*, 100, 15918–15923.

Singh, V., Jamwal, S., Jain, R., Verma, P., Gokhale, R., & Rao, K. V. S. (2012). *Mycobacterium tuberculosis*-driven targeted recalibration of macrophage lipid homeostasis promotes the foamy phenotype. *Cell Host and Microbe*, 12, 669–681.

Tailleux, L., Waddell, S. J., Pelizzola, M., Mortellaro, A., Withers, M., Tanne, A., ... Neyrolles, O. (2008). Probing host pathogen cross-talk by transcriptional profiling of both *Mycobacterium tuberculosis* and infected human dendritic cells and macrophages. *PLoS ONE*, 3, e1403.

Thong, S., Ercan, B., Torta, F., Fong, Z. Y., Alvina Wong, H. Y., Wenk, M. R., & Chng, S. S. (2016). Defining key roles for auxiliary proteins in an ABC transporter that maintains bacterial outer membrane lipid asymmetry. *eLife*, 5, e19042.

Van der Geize, R., Yam, K., Heuser, T., Wilbrink, M. H., Hara, H., Anderton, M. C., ... Eltis, L. D. (2007). A gene cluster encoding cholesterol catabolism in a soil actinomycete provides insight into *Mycobacterium tuberculosis* survival in macrophages. *PNAS*, 104, 1947–1952.

VanderVen, B. C., Fahey, R. J., Lee, W., Liu, Y., Abramovitch, R. B., Memmott, C., ... Russell, D. G. (2015). Novel inhibitors of cholesterol degradation in *Mycobacterium tuberculosis* reveal how the bacterium's metabolism is constrained by the intracellular environment. *PLoS Pathogens*, 11, e1004679.

Via, L. E., England, K., Weiner, D. M., Schimel, D., Zimmerman, M. D., Dayao, E., ... Barry, C. E. (2015). A sterilizing tuberculosis treatment regimen is associated with faster clearance of bacteria in cavitory lesions in marmosets. *Antimicrobial Agents and Chemotherapy*, 59, 4181–4189.

WHO (World Health Organization). (2016). *Global tuberculosis report 2016*.

Wipperman, M. F., Sampson, N. S., & Thomas, S. T. (2014). Pathogen roid rage: Cholesterol utilization by *Mycobacterium tuberculosis*. *Critical Reviews in Biochemistry and Molecular Biology*, 49, 269–293.

Zeng, J., Cui, T., & He, Z. G. (2012). A Genome-Wide Regulator-DNA Interaction Network in the Human Pathogen *Mycobacterium tuberculosis* H37Rv. *J Proteome Res*, 11, 4682–4692.

CHAPTER 2

Rv3723/LucA coordinates fatty acid and cholesterol uptake in *Mycobacterium tuberculosis*¹

¹ Nazarova, E.V., Montague C.R., La, T.M., Wilburn, K., Sukumar, N., Lee, W., Caldwell, S., Russell, D.G., VanderVen, B.C. (2017). Rv3723/LucA coordinates fatty acid and cholesterol uptake in *Mycobacterium tuberculosis*. eLife, 6, e26969.

Abstract

Pathogenic bacteria have evolved highly specialized systems to extract essential nutrients from their hosts and *Mycobacterium tuberculosis* (Mtb) scavenges lipids (cholesterol and fatty acids) to maintain infections in mammals. The mechanisms and proteins responsible for the import of fatty acids in Mtb were previously unknown. Here, we identify and determine that the previously uncharacterized protein Rv3723/LucA functions to integrate cholesterol and fatty acid uptake in Mtb. Rv3723/LucA interacts with subunits of the Mce1 and Mce4 complexes to coordinate the activities of these nutrient transporters by maintaining their stability. We also demonstrate that Mce1 functions as a fatty acid transporter in Mtb and determine that facilitating cholesterol and fatty acid import via Rv3723/LucA is required for full bacterial virulence *in vivo*. These data establish that fatty acid and cholesterol assimilation are inexorably linked in Mtb and reveals a key function for Rv3723/LucA in coordinating both transport activities.

Introduction

Mycobacterium tuberculosis (Mtb), the causative agent of human tuberculosis (TB), is responsible for more than 1 million deaths each year and the bacterium currently infects nearly ~1.5 billion individuals. A hallmark of TB is that infected individuals rarely develop active TB disease and most infections (~90%) remain in a latent or asymptomatic state. Mtb is exquisitely adapted to survive within the human host and the bacterium's ability to metabolize host-derived lipids (fatty acids and cholesterol) is thought to enable bacterial persistence for long periods of time. Thus, elucidating the mechanisms involved in nutrient uptake and metabolism in Mtb will help us better understand important host-pathogen interactions of this disease and may identify new vulnerabilities for drug discovery.

Multiple lines of evidence indicate that host lipids (fatty acids and cholesterol) serve as critical carbon sources for Mtb during infection. In the 1950's it was determined that Mtb propagated in mammalian tissues preferentially metabolizes fatty acids (Bloch & Segal, 1956) and numerous studies since have repeatedly demonstrated that lipid metabolism promotes Mtb survival during infection (McKinney et al., 2000; Muñoz-Elías et al., 2006; Marrero et al., 2010). Mtb also has the ability to metabolize cholesterol (Van der Geize et al., 2007) and the utilization of this nutrient is critical for Mtb survival within macrophages (VanderVen et al., 2015) and in various *in vivo* infection models (Chang et al., 2007; Pandey and Sasseti, 2008; Yam et al., 2009; Hu et al., 2010; Nesbitt et al., 2010).

Although Mtb's remarkable capacity to assimilate and metabolize lipids is considered a defining characteristic of this pathogen (Cole et al., 1998), the mechanisms underlying fatty acid uptake by Mtb have remained unknown. The mycolic acid-containing cell envelope of Mtb constitutes a unique barrier for the import of hydrophobic molecules and likely explains why the Mtb genome does not encode canonical fatty acid transporters that are typically found in other bacterial systems (Black et al., 1987; Theodoulou et al., 2016; van den Berg et al., 2004). Instead, it is thought that Mtb uses Mce proteins to import hydrophobic nutrients across the bacterial cell envelope. The Mce family of proteins in Mtb were originally associated with mammalian cell entry (Arruda et al., 1993) and are classified as part of the MlaD superfamily (cl27420) based on the presence of one or more Mce domains (Casali & Riley, 2007). Proteins containing Mce domains have been implicated in the transport of hydrophobic molecules in various bacteria and chloroplasts (Awai et al., 2006; Mohn et al., 2008; Xu et al., 2008; Malinverni & Silhavy, 2009; Roston et al., 2011; Sutterlin et al., 2016). The aggregate data now indicate that Mce proteins mediate transport of hydrophobic molecules across double-membranous structures in cells (Thong et al., 2016; Ekiert et al., 2017). Mtb imports cholesterol across the mycobacterial cell envelope via the multi-subunit Mce transporter, termed Mce4 (Pandey & Sassetti, 2008) and the Mtb genome contains four total unlinked *mce* loci (*mce1-mce4*). Although the functions of proteins encoded in the *mce1-mce3* loci are unknown; the similarities shared across the *mce1-4*

loci suggest that these loci all encode transporters responsible for the assimilation of hydrophobic substrates in Mtb.

Most of the genes required for the growth of Mtb on cholesterol as a sole carbon source have been mapped (Griffin et al., 2011) but little is known about how Mtb utilizes cholesterol in the presence of other nutrients. Mtb can co-metabolize simple carbon substrates *in vitro* (de Carvalho et al., 2010), which suggests that the bacterium has the capacity to utilize fatty acids and cholesterol simultaneously *in vivo*. Mtb likely encounters both fatty acids and cholesterol during infection. For example, Mtb can induce foamy macrophage formation and can reside within these fatty acid and cholesterol-loaded cells (Peyron et al., 2008). It is also thought that Mtb is capable of persisting within the necrotic centers of human granulomas, an environment that is rich in fatty acids and cholesterol (Kim et al., 2010). Mtb also has the capacity to metabolically integrate the utilization of fatty acids and cholesterol when growing in macrophages where Mtb utilizes fatty acids to balance the incorporation of cholesterol-derived metabolic intermediates into biosynthesis of bacterial cell wall lipids (Lee et al., 2013).

Here we performed a forward genetic screen to identify Mtb mutants defective in cholesterol utilization when the bacteria are grown in the presence of fatty acids. We identified Rv3723, a protein of unknown function, and determined that this protein is required for the import of both fatty acids and cholesterol by Mtb during growth in macrophages and in axenic culture. Thus, we renamed this previously uncharacterized protein Rv3723, as LucA (lipid

uptake coordinator A). We determined that LucA facilitates fatty acid and cholesterol uptake in Mtb by stabilizing protein subunits of the Mce1 and Mce4 transporters. These studies also establish that the Mce1 complex transports fatty acids into Mtb and that LucA is required for full virulence *in vivo*. Together, these findings demonstrate that fatty acid and cholesterol import in Mtb is integrated via LucA and that coordination of these activities is necessary to support Mtb pathogenesis.

Materials and Methods

Bacteria and growth conditions

M. tuberculosis strains were routinely grown at 37°C in 7H9 (broth) or 7H11 (agar) media supplemented with OAD enrichment (oleate-albumin-dextrose-NaCl), 0.05% glycerol and 0.05% tyloxapol (broth). AD enrichment consisted of fatty acid free albumin-dextrose-NaCl. 7H9-based minimal medium is composed of Difco Middlebrook 7H9 powder 4.7 g/liter, 100 mM 2-(*N*-morpholino)ethanesulfonic acid pH 6.6, and carbon sources as indicated. Cholesterol was added to the liquid and solid media as tyloxapol:ethanol micelles as described (Lee et al., 2013). Hygromycin 100 µg/ml, kanamycin 25 µg/ml, streptomycin 50 µg/ml, and apramycin 50 µg/ml were used for selection. For *E. coli* selection hygromycin was used at 150 µg/ml.

Transposon screen and strain construction

A library of transposon mutants ($\sim 10^5$) in a $\Delta icl1$ deficient strain of Mtb described by (Lee et al., 2013) was plated onto 7H11 OAD agar containing 100 µM cholesterol. Individual mutants were recovered in culture. Chromosomal DNA was isolated and the transposon insertion sites were PCR amplified and sequenced according to (Prod'hom et al., 1998). Mutant strains of Mtb were generated by allelic exchange (Mann et al., 2011) using a hygromycin resistance cassette mutant. Allelic exchange was confirmed by sequencing and/or Southern analysis using the Direct nucleic acid labeling and detection kit, GE Health Care. All the strains used in the study are summarized in Table 2.1.

Table 2.1. Strains used in the study

Strain	Location of hygromycin resistance cassette insertion	Background
<i>Δicl1</i> ::hyg	McKinney <i>et al.</i> (2000) Nature 406, 735-738	<i>M. tuberculosis</i> H37Rv
<i>Δicl1</i> ::hyg, <i>lucA</i> ::TnHimar	Mycomar transposon insertion at 67 bp of <i>rv3723</i>	<i>M. tuberculosis</i> H37Rv <i>Δicl1</i>
<i>ΔlucA</i> ::hyg	(283-469 bp) of <i>rv3723</i>	<i>M. tuberculosis</i> Erdman
<i>Δmce1</i> ::hyg	(551 bp of <i>rv0167</i> - 493 bp of <i>Rv0174</i>) in the <i>mce1</i> loci	<i>M. tuberculosis</i> Erdman
<i>ΔyrbE1A</i> ::hyg	(67-778 bp) of <i>rv0167</i>	<i>M. tuberculosis</i> Erdman
<i>ΔyrbE4A</i> ::hyg	(1-764 bp) of <i>rv3501c</i>	<i>M. tuberculosis</i> Erdman

Strain	Genetic features	Background
<i>Δicl1</i> Tn::lucA comp	pMV306 + aacC4 (apramycin resistance) + <i>hsp60'</i> :: <i>rv3723</i>	<i>Δicl1</i> ::hyg, <i>lucA</i> ::TnHimar
wild type	pMV306 <i>smyc'</i> :: <i>mCherry</i>	<i>M. tuberculosis</i> Erdman
<i>ΔlucA</i> ::hyg comp	pMV306 <i>hsp60'</i> :: <i>rv3723</i> and <i>smyc'</i> :: <i>mCherry</i>	<i>ΔlucA</i> ::hyg
<i>Δmce1</i> ::hyg comp	pMV306 <i>hsp60'</i> :: <i>rv0167-rv0177</i>	<i>Δmce1</i> ::hyg
<i>ΔyrbE1A</i> ::hyg comp	pMV306 <i>hsp60'</i> :: <i>rv0167-rv0177</i>	<i>ΔyrbE1A</i> ::hyg
<i>ΔyrbE4A</i> ::hyg comp	pMV306 <i>hsp60'</i> :: <i>rv3501c</i>	<i>ΔyrbE4A</i> ::hyg
LucA-GFP	pVV16 + <i>hsp60'</i> :: <i>rv3723</i> ::GFP + <i>smyc'</i> :: <i>mCherry</i>	<i>M. tuberculosis</i> CDC1551
wild type (<i>prpD'</i> ::GFP <i>smyc'</i> :: <i>mCherry</i>)	pVV16 + aacC4 (apramycin resistance) + <i>prpD'</i> ::GFP + <i>smyc'</i> :: <i>mCherry</i>	<i>M. tuberculosis</i> Erdman
<i>ΔlucA</i> ::hyg (<i>prpD'</i> ::GFP <i>smyc'</i> :: <i>mCherry</i>)	pVV16 + aacC4 (apramycin resistance) + <i>prpD'</i> ::GFP + <i>smyc'</i> :: <i>mCherry</i>	<i>ΔlucA</i> ::hyg
<i>ΔlucA</i> ::hyg comp (<i>prpD'</i> ::GFP <i>smyc'</i> :: <i>mCherry</i>)	pVV16 + aacC4 (apramycin resistance) + <i>hsp60'</i> :: <i>rv3723</i> + <i>prpD'</i> ::GFP + <i>smyc'</i> :: <i>mCherry</i>	<i>ΔlucA</i> ::hyg

Radiorespirometry assays

Lipid oxidation was monitored by quantifying the release of $^{14}\text{CO}_2$ from [4- ^{14}C]-cholesterol, [^{14}C (U)]-palmitate, and [1- ^{14}C]-oleate by radiorespirometry as described (VanderVen *et al.*, 2015). Briefly, Mtb cultures were pre-grown in 7H9 AD for 5 days. Then they were incubated at OD₆₀₀ of 0.7 in 5 ml 7H9 AD spent medium supplemented with 1.0 μCi of radiolabeled substrates in vented standing T-25 tissue culture flasks placed in a sealed air-tight vessel with an open vial containing 0.5 ml 1.0 M NaOH at 37°C. After 5 hours, the NaOH vial was recovered, neutralized with 0.5 ml 1.0 M HCl, and the amount of base soluble Na₂¹⁴CO₃ was quantified by scintillation counting. The radioactive signal was normalized to the relative levels of bacterial growth by determining the OD₆₀₀ for the bacterial cultures. % CO₂ release was expressed as a ratio of normalized radioactive signal for each strain relative to the wild type control.

Lipid uptake assays

Lipid uptake was quantified as described previously (Pandey & Sassetti, 2008; Forrellad et al., 2014) with slight modifications. Briefly, Mtb was cultured at an initial OD₆₀₀ of 0.1 in 7H9 AD medium in vented standing T-75 tissue culture flasks. After 5 days, cultures were normalized to OD₆₀₀ of 0.7 in 8ml using spent medium, and 0.2 µCi of radiolabeled substrates was added to bacteria. After 5, 30, 60 and 120 min of incubation at 37°C 1.5 ml of the bacterial cultures were collected by centrifugation. Each bacterial pellet was washed thrice in 1 ml of ice-cold wash buffer (0.1% Fatty acid free-BSA and 0.1% Triton X-100 in PBS), fixed in 0.2 ml of 4% PFA for 1h. The total amount of radioactive label associated with the fixed pellet was quantified by scintillation counting. The radioactive signal was normalized to the relative levels of bacterial growth, i.e. to the OD₆₀₀ of the bacterial cultures before addition of radioactive label. The uptake rate was calculated by applying linear regression to the normalized radioactive counts over time, and uptake efficiency was expressed as a ratio of uptake rate for each strain relative to the wild type control.

Macrophage isolation and culturing

Macrophages were differentiated using bone marrow cells from BALB/c mice (Jackson Laboratories, USA) and maintained in DMEM supplemented with 10% heat inactivated fetal calf serum, 2.0 mM L-glutamine, 1.0 mM sodium pyruvate, 10% L-cell-conditioned media and antibiotics (100 U/ml penicillin and 100 mg/ml streptomycin) at 37°C and 7.0% CO₂ for 10 days

before infection. Human macrophages were differentiated from purified human peripheral blood mononuclear cells obtained from Elutriation Core Facility, University of Nebraska Medical Center and maintained in DMEM supplemented with 10% pooled heat inactivated human serum (SeraCare), 2.0 mM L-glutamine, 1.0 mM sodium pyruvate and antibiotics (100 U/ml penicillin and 100 mg/ml streptomycin) at 37°C and 7.0% CO₂ for 7 days before infection. Media without antibiotics was used for infections with Mtb.

Transcriptional profiling

Murine bone marrow-derived macrophages were seeded into two T-75 tissue culture flasks (1.5×10^7 cells per flask) and infected with Mtb at a MOI of 4:1 for 3 days. Bacterial RNA was isolated, amplified, dye labeled, and hybridized to the microarray as described (Rohde et al., 2007; Liu et al., 2016). Gene expression data has been deposited in the NCBI Gene Expression Omnibus database accession number (GSE98792) (Edgar et al., 2002).

***prpD*::GFP reporter assays**

The promoter of *rv1130/prpD* was fused to GFP in a replicating vector that constitutively expresses mCherry (Supplementary file 1) To detect *prpD* promoter activity bacteria were grown in 7H9-based minimal medium containing 10 mM glucose for 5 days, washed twice with PBS 0.05% tyloxapol, and passed to medium containing 100 μM cholesterol or propionate at the indicated concentration for 24 hr. The bacteria were fixed with 4% paraformaldehyde (PFA) and GFP expression was quantified by flow cytometry on a BD Biosciences *LSR II* flow cytometer. To detect *prpD*

promoter activity during infection bacteria grown in 7H9-based minimal medium containing 10 mM glucose were used to infect murine macrophages at an MOI of 5:1. After 24 hr infection the macrophages were fixed with 4% PFA, scraped into 10 ml of PBS and suspended in 1 ml of lysis buffer (0.1% SDS, 0.1 mg/ml Proteinase K in H₂O). Macrophages were lysed by 25 passages through a 25-gauge needle, the bacteria containing cell lysate was centrifuged, the pellet was retained and analyzed on a BD Biosciences *LSR II* flow cytometer. Flow cytometry data was analyzed using FlowJo (Tree Star, Inc).

Imaging of intracellular lipid inclusions

Confluent monolayers of macrophages in Ibidi eight-well glass-bottom chambers were infected with bacteria at a MOI of 4:1. Extracellular bacteria were removed after 4 hours of infection. Infected macrophages were maintained in cell culture medium at 37°C and 7% CO₂ for 3 days. Lipid inclusions of bacteria in macrophages were metabolically labeled with Bodipy-C16 (final concentration 20 µM) conjugated to 1.0% de-fatted bovine serum albumin (BSA) for a 30 minute pulse followed by a 1 hour chase with fresh media. Live-cell images were acquired as described (Podinovskaia et al., 2013). For lipid staining, macrophages were transferred onto sterile coverslips in 24-well plates, infected with Mtb for 3 days and fixed in 4% PFA followed by staining with Bodipy-493/503 (1.0 µg/ml, at room temperature for 1 hour). Post-acquisition, images were analyzed using Volocity (PerkinElmer Life Sciences).

Flow cytometric quantification of assimilated lipids

Murine bone marrow-derived macrophages were seeded into T-150 tissue culture flasks (3×10^7 cells per flask) and infected with Mtb at a MOI of 4:1. After 3 days of infection Bodipy-palmitate (final concentration 8 μ M) conjugated to de-fatted 1% BSA was added to the cells for 1 hour pulse and then chased with cell media for another hour. The infected macrophages were scraped into 15 ml of homogenization buffer (250 mM sucrose, 0.5 mM EGTA, 20 mM HEPES, 0.05% gelatin, pH 7.0) and pelleted by centrifugation at 514xG (1,500 rpm, Beckman Allegra 6KR centrifuge, GH-3.8 rotor), followed by cell lysis by 70 passages through a 25 gauge needle. 5 ml of cell lysate was centrifuged at 146xG (800 rpm) for 10 minutes, supernatant (suspensions of phagosomes) was retained and treated with 0.1% Tween-80 at 4°C for 15 minutes to break-open Mtb containing vacuoles. Isolated bacteria were washed once in PBS+0.05% tyloxapol and fixed in 4% PFA. Flow cytometry data was collected on BD FACS LSR II and analyzed using FlowJo (Tree Star, Inc).

Colocalization studies with Alexa647-dextran labeled lysosomes

At day 3 of infection, bone marrow derived macrophages were pulse labeled with 50 μ g/ml Alexa647-dextran for 45 minutes and chased in fresh media for an additional 45 minutes. Following the chase period the infected cells were fixed and imaged by confocal microscopy. An extended focus merge of the two channels and the background was used to threshold the data

as described (Costes et al., 2004) and colocalization was calculated using Volocity (PerkinElmer Life Sciences).

Transmission electron microscopy

Imaging was conducted as described (Podinovskaia et al., 2013).

Tetrahydrolipstatin treatment of infected macrophages

100 μ M tetrahydrolipstatin was added to infected bone marrow derived macrophages at 4 hours post infection and maintained in the medium throughout the infection. Cells were fixed at day 3, stained with Bodipy-493/503, and imaged by confocal microscopy.

Protein fragment complementation screen

Library construction and the screen were performed as described (Singh et al., 2006). Briefly, Mtb genomic DNA was isolated and partially digested with Acil and HpaII, size fractionated (0.5-2 kb), and cloned into the ClaI site of pUAB300 upstream of the F_{1,2} domain of murine dihydrofolate reductase. *E. coli* MegaXTM DH10BTM T1 (Life Technologies) electrocompetent cells were used for transformation. In total 5x10⁵ independent clones were selected on LB hygromycin agar plates. The clone library was isolated by QIAGEN QIAfilter Plasmid Giga Kit and used to transform Msm mc²155 containing pUAB200 which co-expresses the bait protein LucA fused to the F₃ (LucA-F₃) domain of murine dihydrofolate reductase. In total 2x10⁶ clones were screened on plates containing trimethoprim 30 μ g/ml. Clones containing fragments of the Mtb dihydrofolate reductase (*rv2763c/dfrA*) were identified by PCR and removed (85.8%). Inserts from the *dfrA*-negative clones were

sequenced, and the only in-frame clone that was identified more than once (4 times) contained first 225 bp of *rv3492c/mam4B*.

Spotting two-hybrid interaction assay

Msm was grown in modified 7H9-OAD media containing 2% glycerol, 0.5% additional glucose and 0.05% Tween-80 shaking at 37°C. $\sim 8.3 \times 10^6$ bacteria/ml culture was grown for 5 hours before serial dilutions were made to spot onto agar plates containing trimethoprim at 0, 15, and 30 $\mu\text{g/mL}$.

Quantification of protein interactions

To quantify the strength of interactions (IC_{50}) we used an AlamarBlue based approach modified from (Singh et al., 2006). Briefly, log-phase cultures of Msm clones were transferred into 96-well microtiter plates at a density of 10^6 of cells per well. Eight 2-fold serial dilutions of trimethoprim were made for each clone, from 600 to 4.69 $\mu\text{g/ml}$. The final volume in the wells was 200 μl . After 41 hours of incubation at 37°C, 30 μl 50% AlamarBlue (Life Technologies) (diluted with the media) was added to the wells and after incubating for 20 hours the fluorescence intensity was measured in Gemini EM Microplate Reader (Molecular Devices) with excitation at 530nm and emission at 590nm. 100% inhibition was assigned to the wells without bacterial cells, and 0% inhibition to the wells with cells without trimethoprim.

Antibody generation and western analysis

Antibody for MceG was generated in rabbits using the peptide KAQAAILDDL conjugated to keyhole limpet hemocyanin by (Cocalico Biologicals). This peptide was used for antibody purification by immunoaffinity

chromatography. To generate the lysate bacteria were grown as for the lipid uptake assays. In the cases of chloramphenicol treatment, the antibiotic was added at 20 µg/ml 2 days prior to harvesting the bacteria. To generate lysates bacteria were washed twice with PBS 0.05% tyloxapol and fixed with 4% PFA for 1 hour. Fixed cells were washed twice in PBS 0.05% tyloxapol and lysed by sonication. Protein concentrations were determined by BCA (Thermo Fisher Scientific) and equivalent amounts of protein were resolved by SDS-PAGE and transferred to nitrocellulose membranes. The primary anti-Mce1A, anti-Mce1D and, anti-Mce1E antibodies were obtained from Christopher Sasseti (Feltcher et al., 2015), and the anti-GroEL antibody was obtained from BEI resources. A HRP-conjugated goat-anti rabbit IgG (Jackson ImmunoResearch) was used as the secondary antibody. ImageJ was used to quantify signals on Western blots.

qPCR

Bacteria were cultured as described for western analysis and the RNA was extracted and analyzed as previously described (Abramovitch et al., 2011).

Bacterial survival assay in macrophages

Confluent macrophage (human and murine) monolayers in 24-well dishes were infected with Mtb at a MOI 4:1 for murine cells and a MOI of 0.5:1 for the human cells. Extracellular bacteria were removed by washing with fresh media after 4 hours of infection. At indicated time points macrophages were lysed with 0.1% Tween-80 in water and the lysates were serially diluted in

0.05% Tween-80 in water. The lysates were plated on 7H11 OAD agar and CFU were quantified after 3-4 weeks incubation at 37°C.

Mouse infections

Eight-week-old female C57BL/6J WT mice (Jackson Laboratories) were infected with 1,000 CFU of Mtb Erdman (wild type, $\Delta lucA::hyg$, complemented strain) via an intranasal delivery method as described (Sukumar et al., 2014). This was accomplished by lightly anesthetizing the mice with isoflurane and administering the bacteria in a 25 μ l volume onto both nares. At sacrifice, the lungs were removed and half of the lungs were fixed in 4% PFA overnight, while another half was used for bacterial load quantification. For the latter, lungs were homogenized in PBS 0.05% Tween-80 and plated on 7H11 OAD agar. CFU were quantified after 3-4 weeks incubation at 37°C.

Lung histopathology

PFA fixed lung lobes were stained with hematoxylin and eosin by the Cornell Histology Laboratory. Stained sections were imaged using a Zeiss Axio Imager M1 equipped with an AxioCam Hrc camera.

Ethics Statement

All animal care and experimental protocols were in accordance with the NIH “Guide for the Care and Use of the laboratory Animals” and were approved by the Institutional Animal Care and Use Committee of Cornell University (protocol number 2013-0030).

Results

***lucA* encodes a membrane protein involved in cholesterol metabolism.**

Using a forward genetic screen we identified genes involved in cholesterol utilization when Mtb is grown in media containing a mixture of fatty acids and carbohydrates. To do this we used the Mtb H37Rv mutant ($\Delta icl1::hyg$) (McKinney et al., 2000) which has a synthetic lethal phenotype and fails to grow in rich media containing cholesterol. This growth inhibition is linked to the accumulation of one or more toxic cholesterol-derived intermediates produced by the methylcitrate cycle, which accumulate in the bacteria when *icl1* is nonfunctional (Lee et al., 2013; Eoh & Rhee, 2014; VanderVen et al., 2015). We reasoned that mutations in the cholesterol utilization pathway would rescue the growth inhibition of $\Delta icl1::hyg$ by preventing the formation of the cholesterol-dependent toxic methylcitrate cycle intermediate(s) (Figure 2.1. A). Therefore, we isolated transposon rescue mutants in a $\Delta icl1::hyg$ background that gained the ability to grow on media containing cholesterol.

17 sibling mutants carrying Himar transposon insertions in the *lucA* gene ($\Delta icl1::hyg$, *lucA::TnHimar*) were identified with the screen, suggesting that *lucA* is required for cholesterol utilization by Mtb. Orthologs of *lucA* are restricted to *Mycobacterium* spp., and this gene encodes an uncharacterized putative integral membrane protein. Additionally, previous genetic epistasis studies implicated *lucA* in cholesterol utilization *in vivo* (Joshi et al., 2006), but, the function of this gene/protein has not yet been described. Using genetic

complementation we confirmed that the transposon insertion in the *lucA* gene is responsible for the growth rescue of the $\Delta icl1::hyg$, *lucA::TnHimar* mutant in cholesterol-containing media (Figure 2.1. B). To ascertain subcellular localization, the LucA protein was fused to green fluorescent protein (LucA-GFP) and expressed in a wild type strain of Mtb that constitutively expresses a cytosolic mCherry fluorescent protein. Confocal microscopy revealed a peripheral distribution for LucA-GFP, which is consistent with LucA having a cell membrane or cell envelope localization (Figure 2.1. C).

LucA facilitates cholesterol uptake and metabolism.

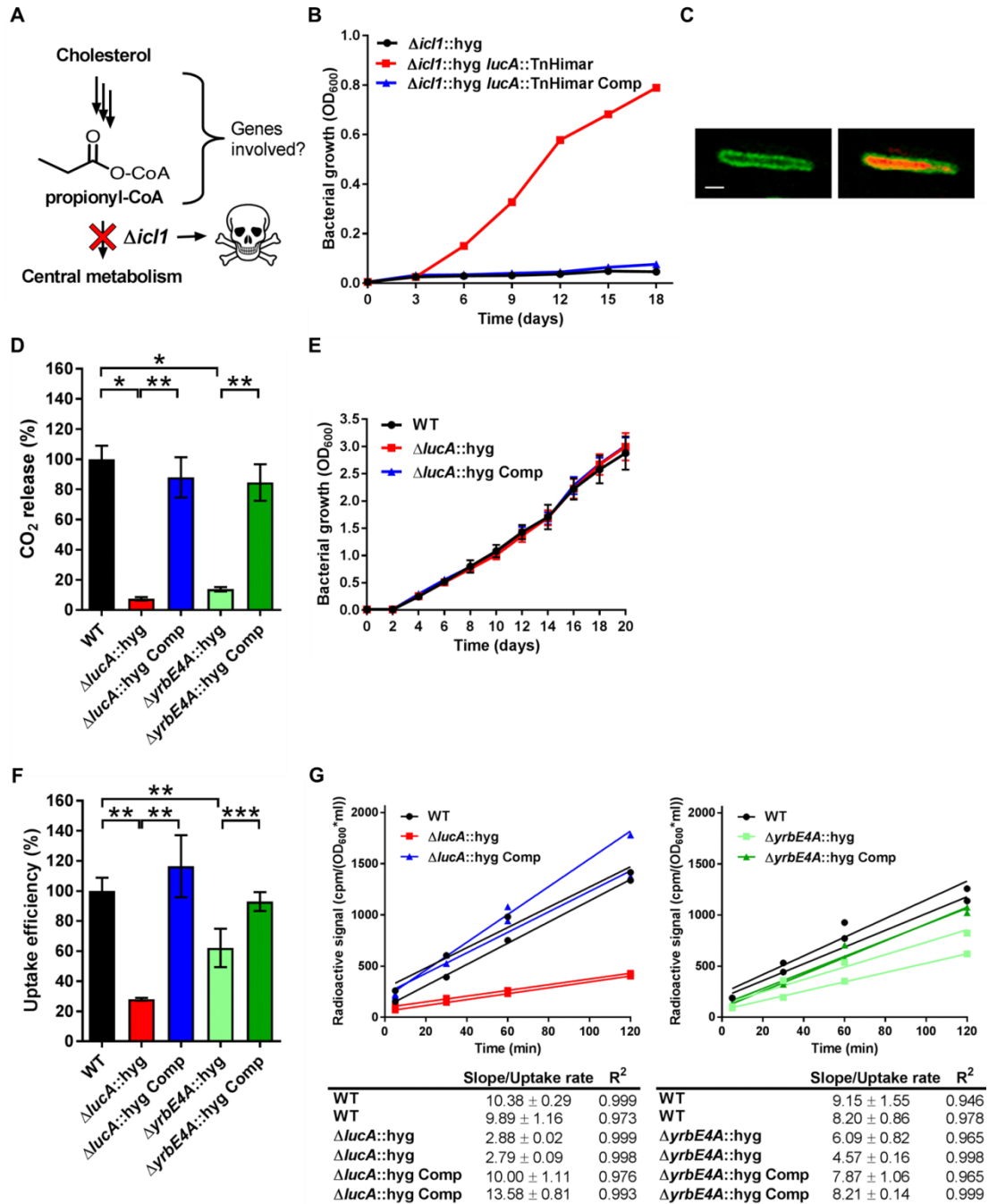
Given the potential role of LucA in cholesterol metabolism, we constructed a *lucA* mutant in Mtb Erdman by allelic exchange (Mtb Δ *lucA*::hyg). We first quantified cholesterol metabolism in the Δ *lucA*::hyg mutant by measuring the catabolic release of $^{14}\text{CO}_2$ from [4- ^{14}C]-cholesterol (VanderVen et al., 2015). This assay detected a ~90% reduction in the amount of $^{14}\text{CO}_2$ released from [4- ^{14}C]-cholesterol in the Δ *lucA*::hyg mutant relative to the wild type and the complemented strains (Figure 2.1. D). The reduction in $^{14}\text{CO}_2$ release was not due to a growth defect of the mutant (Figure 2.1. E) and the percent $^{14}\text{CO}_2$ released was normalized to bacterial biomass.

To determine if *lucA* is required for cholesterol uptake in Mtb we next quantified the rate of [4- ^{14}C]-cholesterol uptake using an established assay (Pandey & Sassetti, 2008). We found that the Δ *lucA*::hyg mutant assimilates ~70% less cholesterol relative to the wild type and complemented controls (Figure 2.1. F). The cholesterol uptake rates were derived from the bacterial associated radioactive counts (Figure 2.1. G) and the cholesterol uptake rate in wild type was set to 100% and the rates for the other strains were expressed as a ratio relative to wild type. The levels of cholesterol metabolism and uptake in the Δ *lucA*::hyg strain was comparable to a Mtb Erdman mutant lacking the permease subunit of the Mce4 cholesterol transporter Rv3501c/YrbE4A (Δ *yrbE4A*::hyg) (Figure 2.1. D,F,G). The residual cholesterol that is imported in the Δ *yrbE4A*::hyg mutant may be transported by an unknown alternative cholesterol transporter in Mtb. Together these data

demonstrate that *lucA* is required for the uptake of cholesterol and the subsequent metabolism of the sterol.

Figure 2.1. LucA facilitates cholesterol uptake in Mtb. **A** Schematic detailing cholesterol toxicity in $\Delta icl1::hyg$ Mtb. **B** Complementation with *lucA* restores cholesterol toxicity in the $\Delta icl1::hyg$ *lucA::TnHimar* mutant. **C** Wild type Mtb constitutively expressing cytosolic mCherry and LucA-GFP. Left panel, a z-slice in the green channel alone (green = LucA-GFP) and the right panel, overlaid green and red channels (red = mCherry Mtb) for the same optical slice. Scale bar 1.0 μm **D** The $\Delta lucA::hyg$ and $\Delta yrbE4A::hyg$ mutants are defective in the catabolic release of $^{14}\text{CO}_2$ from $[4-^{14}\text{C}]$ -cholesterol. Data are means \pm SD (n = 4). **E** The $\Delta lucA::hyg$ mutant has no growth defect in the 7H9 AD media used for uptake and metabolism experiments. Data are means \pm SD (n = 3). **F** The $\Delta lucA::hyg$ and $\Delta yrbE4A::hyg$ mutants are defective in cholesterol uptake. Data are means \pm SD (n = 4). **G** Representative ^{14}C -cholesterol uptake data used to calculate cholesterol uptake rates. Data shown is representative of one independent experiment with two biological replicates.

*p < 0.0005, **p < 0.005, ***p < 0.05 (Student's t test).



The $\Delta lucA::hyg$ mutant is defective in cholesterol utilization during infection in macrophages.

We next analyzed the transcriptional profile of the $\Delta lucA::hyg$ mutant during macrophage infection. These experiments revealed that the KstR regulon was strongly down-regulated in the $\Delta lucA::hyg$ mutant (Figure 2.2). The KstR regulon is controlled by the transcriptional repressor, KstR which regulates expression of the genes encoding enzymes responsible for metabolizing the side chain and A/B rings of cholesterol (Kendall et al., 2007). The KstR regulon is activated in a “feed forward” manner when KstR is de-repressed by binding to the second cholesterol degradation intermediate, 3-oxocholest-4-en-26-oyl-CoA (3OCh-CoA) (Ho et al., 2016). Thus, down-regulation of the KstR regulon in the $\Delta lucA::hyg$ mutant is consistent with a decrease in cholesterol uptake by the $\Delta lucA::hyg$ mutant and suggests that 3OCh-CoA may not be produced to levels that are sufficient to de-repress the KstR regulon in the mutant during infection in macrophages.

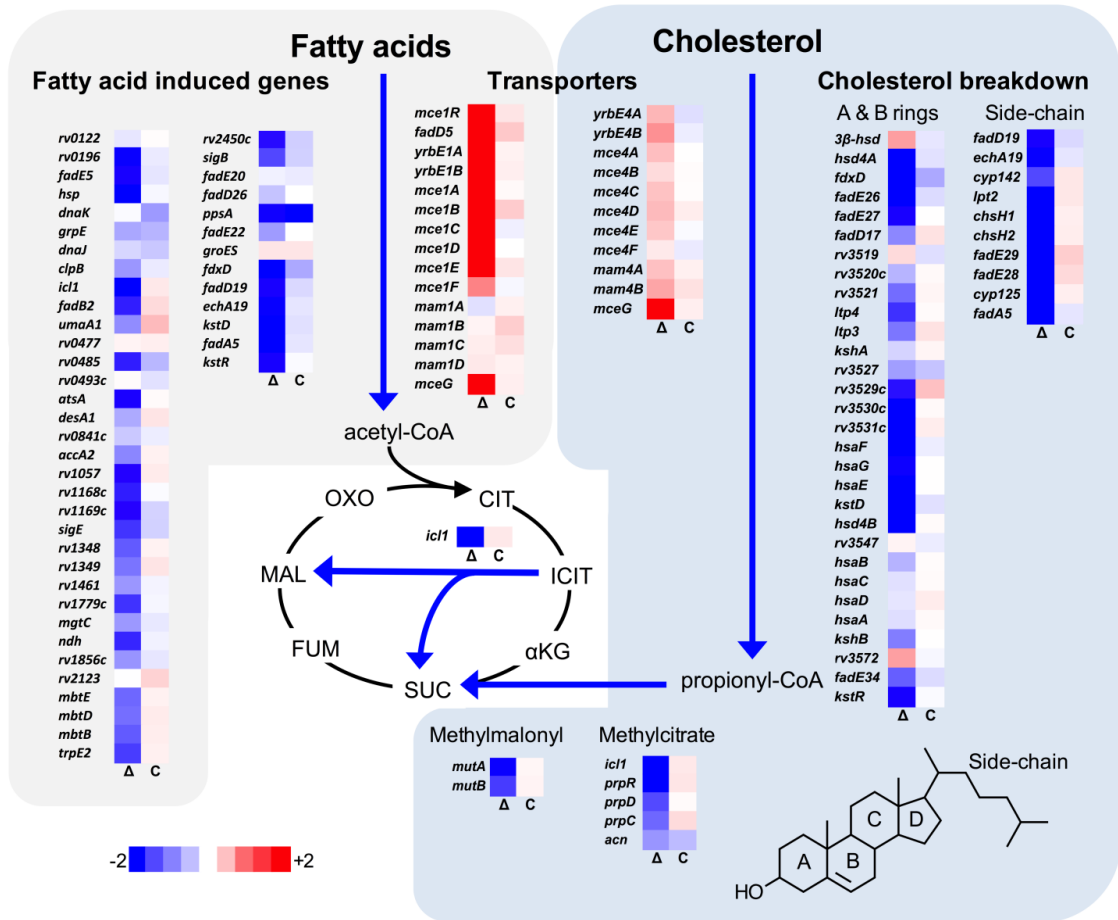


Figure. 2.2. Transcriptional profile of the $\Delta lucA::hyg$ mutant during infection in macrophages. Bacterial gene expression profiles were determined at day 3-post infection in resting murine macrophages. Gene expression values from the $\Delta lucA::hyg$ mutant (Δ) and complement (C) strains were normalized to wild type. Data represent means (n = 3).

Mtb assimilates cholesterol-derived propionyl-CoA into its central metabolism via the methyl-malonyl pathway and the methylcitrate cycle and the genes encoding enzymes of these pathways are normally highly expressed when Mtb metabolizes cholesterol (Savvi et al., 2008; Griffin et al., 2012). We found that expression of the methyl-malonyl and the methylcitrate cycle genes were also down-regulated in the Mtb $\Delta lucA::hyg$ mutant (Figure 2.2). In Mtb propionyl-CoA, activates the *rv1130/prpD* promoter to enhance the bacterium's ability to assimilate cholesterol-derived metabolic intermediates via the methyl-citrate pathway (Griffin et al., 2012; Masiewicz et al., 2012). Thus, to monitor cholesterol breakdown in Mtb during infection in macrophages we constructed a reporter vector where the *rv1130/prpD* promoter controls GFP expression while mCherry is constitutively expressed (*prpD':GFP smyc':mCherry*). We validated this reporter strain and determined by flow cytometry that GFP fluorescence increased >20-fold in wild type Mtb when the bacteria were grown in media containing cholesterol or propionate (Figure 2.3. A,B). Using this reporter we observed a ~75% reduction in GFP fluorescence in the $\Delta lucA::hyg$ strain relative to the wild type and complemented strain controls when the bacteria were grown in media containing cholesterol (Figure 2.3. C). We also quantified GFP fluorescence in the Mtb $\Delta lucA::hyg$ strain during infection in macrophages. To do this, intracellular bacteria were isolated from the infected macrophages and bacterial GFP fluorescence was quantified by flow cytometry. This analysis also demonstrated a ~75% reduction in GFP fluorescence in the Mtb

$\Delta lucA::hyg$ strain (Figure 2.3. D) supporting the idea that the Mtb $\Delta lucA::hyg$ mutant is defective in assimilating cholesterol during infection in macrophages.

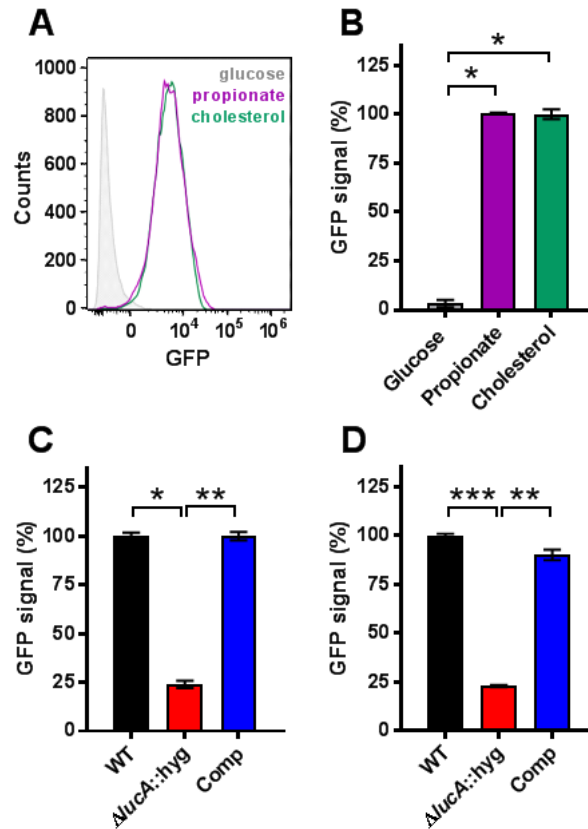


Figure 2.3. Inactivation of *LucA* leads to defect in *prpD* expression. **A** Flow cytometry-based analysis of wild type Mtb carrying the *prpD* promoter reporter (*prpD*::GFP *smyc*::mCherry) confirms that this strain expresses GFP in response to cholesterol (100 μ M) or propionate (300 μ M) but not glucose (200 μ M). **B** Quantification of GFP expression of wild type Mtb carrying the *prpD* promoter reporter in media containing the indicated carbon source. **C** The $\Delta lucA::hyg$ mutant carrying the *prpD* reporter has a decrease in GFP expression in cholesterol media. **D** The $\Delta lucA::hyg$ mutant carrying the *prpD* reporter has a decrease in GFP expression during infection of murine macrophages. Data are means \pm SD (n=3) and for flow cytometry analysis, >10,000 individual bacteria were analyzed.

* $p < 1 \cdot 10^{-6}$, ** $p < 5 \cdot 10^{-6}$, *** $p < 5 \cdot 10^{-8}$ (Student's t test).

The Mtb $\Delta lucA::hyg$ mutant does not assimilate fatty acids during macrophage infection.

Unexpectedly, the transcriptional response of the Mtb $\Delta lucA::hyg$ mutant also revealed a gene expression signature that is consistent with a defect in fatty acid utilization. For these analyses, we focused on the Mtb genes that are induced during infection in macrophages and during growth in axenic media containing palmitate (Schnappinger et al., 2003). The majority of these genes were strongly down-regulated in the $\Delta lucA::hyg$ mutant indicating a defect in fatty acid assimilation by the mutant (Figure 2.2).

To confirm that the $\Delta lucA::hyg$ mutant has a fatty acid utilization defect during infection in macrophages, we next quantified import of fluorescently labelled palmitate (Bodipy-C16) by the intracellular bacteria. Resting murine macrophages were infected with wild type, $\Delta lucA::hyg$ mutant, and complemented strains, all of which constitutively express mCherry. On day 3, the infected macrophages were pulsed with Bodipy-C16 and confocal analysis revealed that the wild type and the complemented bacteria accumulated intracellular Bodipy-C16 as visible punctate inclusions, while the $\Delta lucA::hyg$ mutant did not (Figure 2.4. A). To corroborate this finding, the bacteria were isolated from Bodipy-C16 pulse-labeled macrophages and we quantified the amount of Bodipy-C16 assimilation by flow-cytometry. This analysis revealed a 10-fold reduction in the amount of Bodipy-C16 assimilated by the Mtb $\Delta lucA::hyg$ mutant relative to the wild type and complemented strains (Figure 2.4. B). The decrease in Bodipy-C16 assimilation by the $\Delta lucA::hyg$ mutant is

not due to a loss of bacterial viability since there was minimal difference in bacterial colony forming units (CFU) at day 3 of these experiments (Figure 2.4. C).

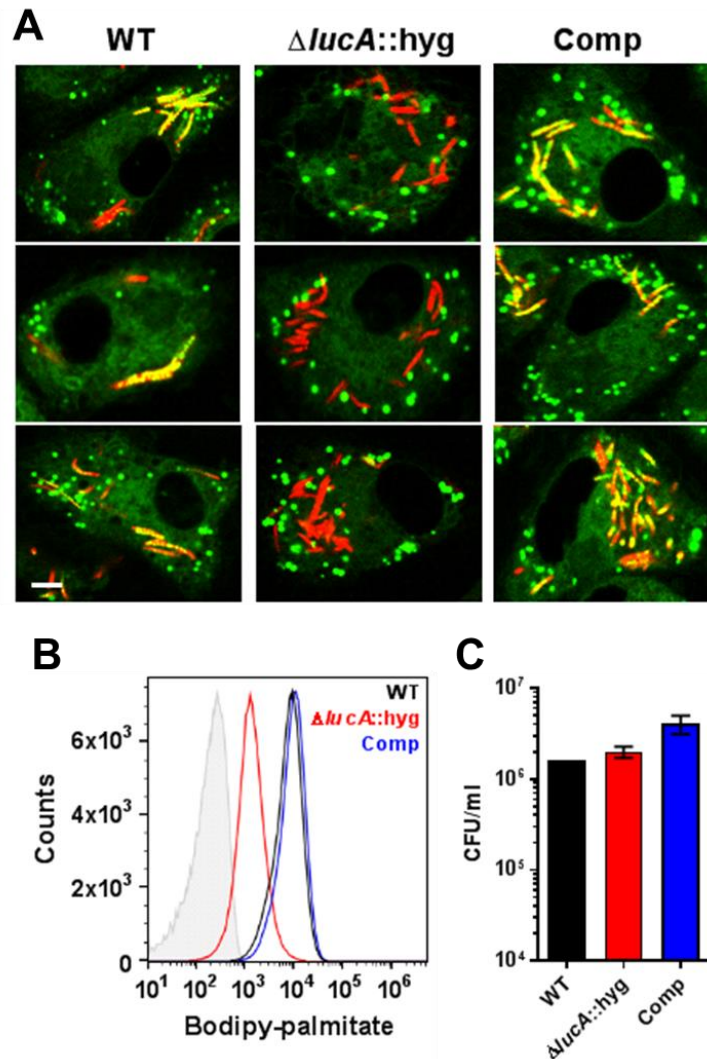


Figure 2.4. LucA facilitates fatty acid uptake during macrophage infection. **A** Bodipy-C16 does not accumulate in $\Delta lucA::hyg$ mutant as cytosolic lipid inclusions. Representative confocal images of infected macrophages (red = mCherry Mtb, green = Bodipy-C16). Scale bar 5.0 μ m. **B** Flow cytometry quantification of Bodipy-C16 incorporation by Mtb isolated from pulse labeled macrophages. Shaded histogram represents autofluorescence in the green channel. **C** Bacterial viability determined at day 3-post infection from infected macrophages. Data are means \pm SD (n = 3).

Mtb principally resides in an intracellular macrophage compartment that resembles an early endosome that fails to fuse with lysosomes (Russell et al., 2010). It is possible that the $\Delta lucA::hyg$ mutant is aberrantly trafficked to lysosomal compartments in the macrophage and this could potentially restrict access of Bodipy-C16 to the intracellular mutant. To rule this out, lysosomes were pulse labeled with Alexa647-dextran and at day 3 of infection we determined that wild type, the $\Delta lucA::hyg$ mutant, and complemented strain did not co-localize with the Alexa647-dextran-loaded lysosomes with Pearson coefficient of correlation values of 0.052 ± 0.062 (wild type), 0.101 ± 0.054 ($\Delta lucA::hyg$), and 0.190 ± 0.174 (complemented strain) (Figure 2.5. A).

During infection Mtb can sequester and store fatty acids as triacylglycerol (TAG) within cytosolic intracellular lipid inclusions in the bacteria (Daniel et al., 2011). Therefore, the presence of lipid inclusions can serve as an indicator of fatty acid assimilation by Mtb during infection. To image intracellular lipid inclusions in Mtb we used the neutral lipid stain Bodipy-493/503 (Listenberger & Brown, 2007). Staining infected murine macrophages with Bodipy-493/503 revealed a punctate staining pattern in the wild type and complemented strains while no staining was observed in the Mtb $\Delta lucA::hyg$ mutant (Figure 2.5. B). The lack of Bodipy-493/503 staining in the $\Delta lucA::hyg$ mutant indicates that this strain does not accumulate fatty acids during infection in macrophages. Lipid inclusions in Mtb can also be visualized by transmission electron microscopy and we observed that only ~5% of the $\Delta lucA::hyg$ mutant cells had identifiable lipid inclusions, while ~25% of the wild

type and ~35% of complemented bacteria had visible cytosolic lipid inclusions during infection in macrophages (Figure 2.5. C,D).

The apparent decrease in cytosolic lipid inclusions within the $\Delta lucA::hyg$ mutant during infection in macrophages could also be due to enhanced bacterial turnover of the intracellular TAG in the mutant strain. To rule this possibility out, we treated the $\Delta lucA::hyg$ mutant bacteria with the broad-spectrum lipase inhibitor, tetrahydrolipstatin (THL) during infection in macrophages. It has been reported that THL can inhibit TAG turnover in Mtb (Baek et al., 2011). We predicted that if TAG were more efficiently degraded in the Mtb $\Delta lucA::hyg$ mutant, THL treatment would restore the presence of intracellular lipid inclusions in this mutant. Visualizing cytosolic bacterial lipid inclusions with Bodipy-493/503 following THL treatment revealed that THL had no effect on presence of intracellular lipid inclusions in the $\Delta lucA::hyg$ mutant (Figure 2.5. E). Together, these observations indicate that the Mtb $\Delta lucA::hyg$ mutant is unable to utilize both fatty acids and cholesterol during infection in macrophages.

Figure 2.5. LucA facilitates accumulation of lipid inclusions in Mtb during macrophage infection. **A** Three-dimensional reconstructions of infected macrophages labeled with Alexa647-dextran (green = lysosomes, red = Mtb). **B** The $\Delta lucA::hyg$ mutant does not accumulate Bodipy-493/503 positive intracellular lipid inclusions (red = Mtb, green = Bodipy-493/503). Scale bar, 5.0 μm . **C** Transmission electron microscopy reveals that lipid inclusions (indicated by asterisks) are not apparent in the $\Delta lucA::hyg$ mutant. Scale bar 0.5 μm . **D** Quantification of intracellular Mtb containing lipid inclusions per macrophage section. Horizontal bars are means \pm SD (n = 20). **E** THL treating of the $\Delta lucA::hyg$ strain does not induce intracellular lipid inclusions that are positive with Bodipy-493/503 (red = Mtb, green = Bodipy-493/503). *p < 0.0005, **p < 0.0001 (Student's t test)

LucA facilitates fatty acid uptake.

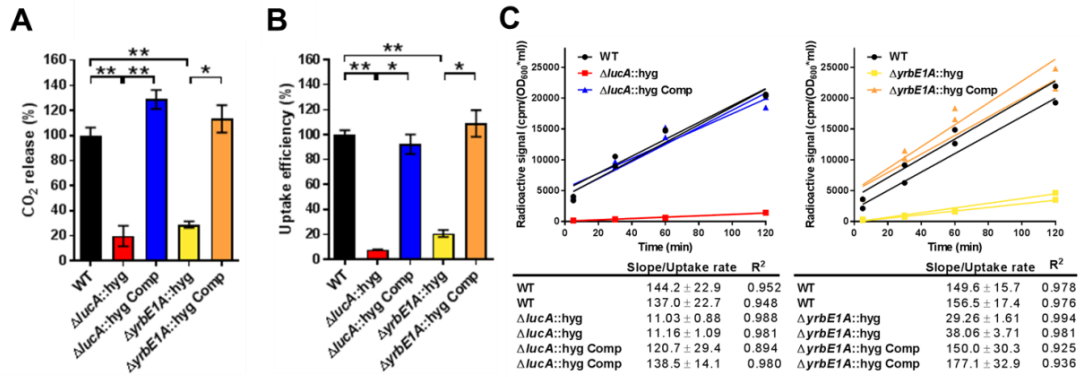
Our studies using the macrophage infection model indicate that the $\Delta lucA::hyg$ mutant has a defect in fatty acid assimilation. Therefore, we next quantified fatty acid metabolism and uptake in the Mtb $\Delta lucA::hyg$ mutant using radiolabeled fatty acids in axenic culture. Fatty acid metabolism was measured by quantifying the catabolic release of $^{14}\text{C-CO}_2$ from [$^{14}\text{C(U)}$]-palmitate and [1- ^{14}C]-oleate. This assay detected a ~80% and ~95% reduction in the $\Delta lucA::hyg$ mutant's ability to metabolize the [$^{14}\text{C(U)}$]-palmitate and [1- ^{14}C]-oleate, respectively (Figure 2.6. A,D). We used both of these lipid substrates because palmitate and oleate are the dominant fatty acid species found in mammalian cell membranes and we wanted to evaluate uptake of both saturated (palmitate) and unsaturated (oleate) substrates.

Fatty acid uptake was quantified with [$^{14}\text{C(U)}$]-palmitate and [1- ^{14}C]-oleate similar to cholesterol uptake experiments. Relative to the wild type and complemented strains we observed a ~90% and ~95% reduction in the $\Delta lucA::hyg$ mutant's ability to assimilate [$^{14}\text{C(U)}$]-palmitate and [1- ^{14}C]-oleate, respectively (Figure 2.6. B,C,E,F). Based on these results we conclude that inactivating *lucA* perturbs fatty acid uptake by Mtb, which decreases the bacterium's ability to metabolize fatty acids.

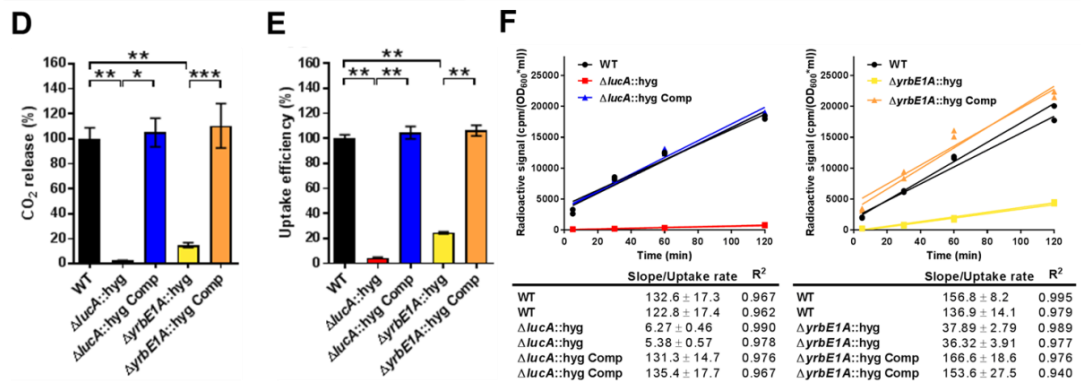
Figure 2.6. LucA facilitates fatty acid uptake in axenic culture. **A** and **D** Catabolic release of $^{14}\text{CO}_2$ from [$^{14}\text{C}(\text{U})$]-palmitic acid or [$1\text{-}^{14}\text{C}$]-oleic acid. Data are means \pm SD ($n \geq 4$). **B** and **E** Uptake of [$^{14}\text{C}(\text{U})$]-palmitic acid or [$1\text{-}^{14}\text{C}$]-oleic acid. Data are means \pm SD ($n \geq 4$). **C** and **F** Representative ^{14}C -palmitate and ^{14}C -oleate uptake data used to calculate fatty acid uptake rates. **G** The catabolic release of $^{14}\text{CO}_2$ from [$4\text{-}^{14}\text{C}$]-cholesterol by the $\Delta yrbE1A::\text{hyg}$ mutant. Data are means \pm SD ($n \geq 4$). **H** Uptake of [$4\text{-}^{14}\text{C}$]-cholesterol for the $\Delta yrbE1A::\text{hyg}$ mutant (data are means \pm SD ($n \geq 4$)) **I** representative [$4\text{-}^{14}\text{C}$]-cholesterol uptake data used to calculate cholesterol uptake rates in the $\Delta yrbE1A::\text{hyg}$ mutant.

* $p < 0.0005$, ** $p < 0.0001$, *** $p < 0.005$ (Student's t test).

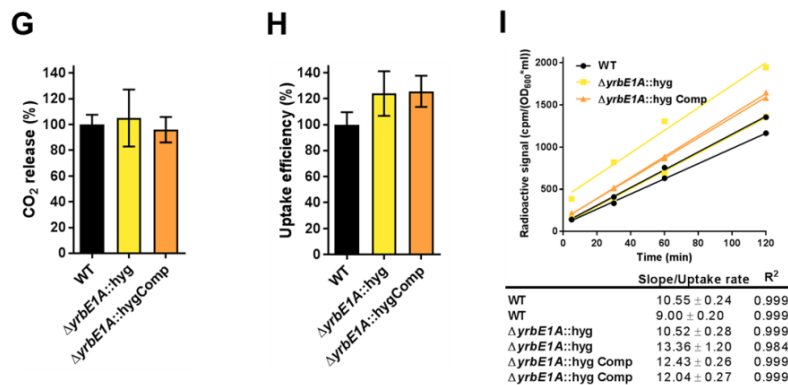
palmitate



oleate



cholesterol



Mce1 is a fatty acid transporter.

The system(s) responsible for fatty acid import in Mtb have remained elusive. While the $\Delta lucA::hyg$ mutant is defective in fatty acid uptake, the LucA protein lacks any recognizable domains that would predict a transport function for the protein. Thus, we hypothesized that, in the absence of *lucA*, Mtb may up-regulate expression of an actual fatty acid transporter to compensate for the fatty acid uptake defect observed in the mutant. Analyses of the up-regulated genes in the $\Delta lucA::hyg$ mutant during infection in macrophages revealed that genes in the *mce1* locus are strongly induced (Figure 2.2). Thus, we hypothesized that Mce1 functions as a fatty acid transporter in Mtb. To test this hypothesis we inactivated the Mce1 permease Rv0167/YrbE1A subunit by allelic exchange ($\Delta yrbE1A::hyg$) and quantified fatty acid uptake and metabolism in this mutant. We found that the $\Delta yrbE1A::hyg$ mutant displayed a ~70% and ~85% reduction in its ability to metabolize [$^{14}\text{C}(\text{U})$]-palmitate and [1- ^{14}C]-oleate, respectively (Figure 2.6. A,D). Relative to the wild type and complemented strains we detected a ~80% and ~75% reduction in the $\Delta yrbE1A::hyg$ mutant's ability to import [$^{14}\text{C}(\text{U})$]-palmitate and [1- ^{14}C]-oleate (Figure 2.6. B,C,E,F). Notably, $\Delta yrbE1A::hyg$ was still able to metabolize and import cholesterol to wild type levels (Figure 2.6. G,H,I). Lastly, we generated a separated mutant and inactivated 8 genes of the *mce1* locus by allelic exchange ($\Delta mce1::hyg$). We found that the $\Delta mce1::hyg$ mutant was also defective in fatty acid uptake and metabolism, while this mutant had no detectable defect in cholesterol uptake or metabolism (Figure 2.7). Based on

these results we conclude that the Mce1 complex functions as a dedicated fatty acid transporter in Mtb.

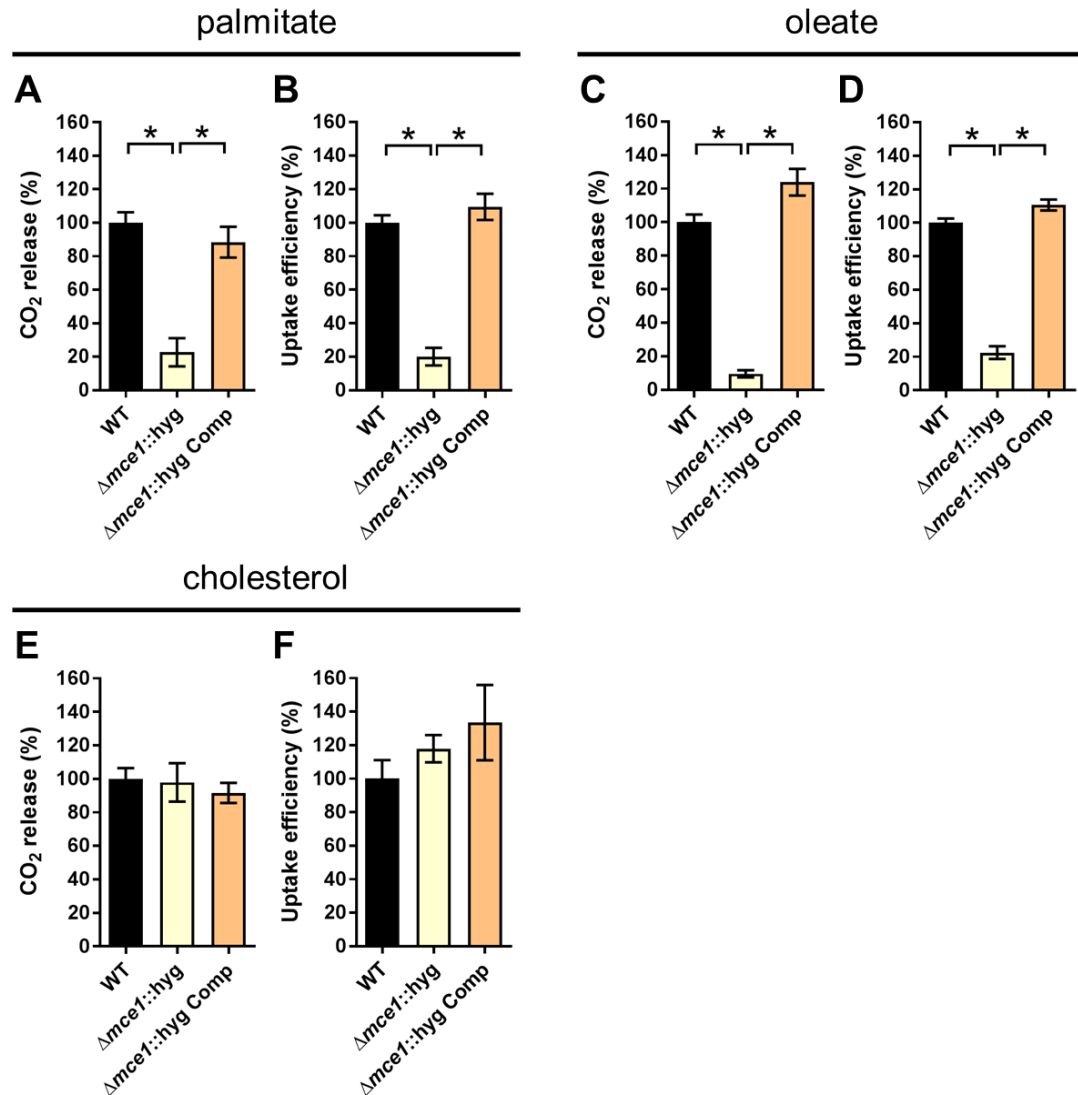


Figure 2.7. Deletion of the full *mce1* operon leads to fatty acid uptake defect. **A** and **B** the $\Delta mce1::hyg$ is defective in palmitic acid metabolism and uptake. **C** and **D** the $\Delta mce1::hyg$ mutant is defective in oleic acid metabolism and uptake. **E** and **F** the $\Delta mce1::hyg$ mutant can metabolize and import cholesterol.

Data are means \pm SD (n \geq 4). *p < 0.0001 (Student's t test).

LucA interacts with Mce1- and Mce4-associated proteins.

To shed light on the function of LucA we next conducted an unbiased mycobacterial 2-hybrid screen to identify protein fragments that interact with LucA (Singh et al., 2006). For this, the F₃ domain of murine dihydrofolate reductase (mDHFR) was fused to the C-terminus of a full length LucA (LucA-F₃) (Table 2.2). We co-expressed LucA-F₃ in *M. smegmatis* (Msm) along with a library (2x10⁶) of random Mtb protein fragments fused to the F_{1,2} domain of mDHFR (Figure 2.8. A). Interactions between bait and prey fusions that carry the split domains of mDHFR confer resistance to trimethoprim in Msm. This protein interaction screen identified 4 sibling clones which all encode an in-frame N-terminal fragment (1-75 aa) of the Rv3492c/Mam4B protein fused to the F_{1,2} domain of mDHFR. Mam4B is encoded by a gene within the *mce4* operon (Figure 2.8. A) and this protein is predicted to function as a subunit of the Mce4 cholesterol transporter complex. To validate this screen result we engineered a new truncated (TR) Mam4B fusion with the F_{1,2} domain of mDHFR (Mam4B(TR)-F_{1,2}) (1-75 aa) and confirmed that co-expressing Mam4B(TR)-F_{1,2} with LucA-F₃ in Msm conferred resistance to trimethoprim (Figure 2.8. B, Table 2.2). We found that the transmembrane (TM) segment of Mam4B is the portion of the Mam4B protein that interacts with LucA. Co-expressing just the transmembrane domain (1-30 aa) of Mam4B fused to the F_{1,2} domain of mDHFR (Mam4B(TM)-F_{1,2}) conferred trimethoprim resistance (Figure 2.8. B, Table 2.2).

The Mtb genome encodes additional homologs of Rv3492c/Mam4B that are associated with the Mce1 transporter. Given that the $\Delta lucA::hyg$ mutant is also defective in the import of fatty acids we hypothesized that LucA could also interact with homologous subunits of the Mce1 transporter. We focused on the homologous Mtb proteins Rv0175/Mam1A, Rv0177/Mam1C, Rv0178/Mam1D and Rv0199/OmamA because these proteins are predicted to be part of the Mce1 transporter (Casali & Riley, 2007; Perkowski et al., 2016) and conserve a similar transmembrane topology as Rv3492c/Mam4B (Figure 2.8. A). To determine if these subunits also interact with LucA we engineered F_{1,2} fusions with various homologs of Rv3492c/Mam4B. We found that co-expressing LucA-F₃ with full length (FL) versions of Rv0177/Mam1C and Rv0199/OmamA fused to F_{1,2} conferred trimethoprim resistance (Figure 2.8. B, Table 2.2). Additionally, we found that LucA-F₃ with transmembrane domains (TM) of Rv0177/Mam1C and Rv0199/OmamA fused to F_{1,2} conferred trimethoprim resistance (Figure 2.8. B, Table 2.2). These data indicate that LucA physically interacts with subunits of the Mce1 and Mce4 transporters and suggests that the LucA protein participates in the function of these complexes.

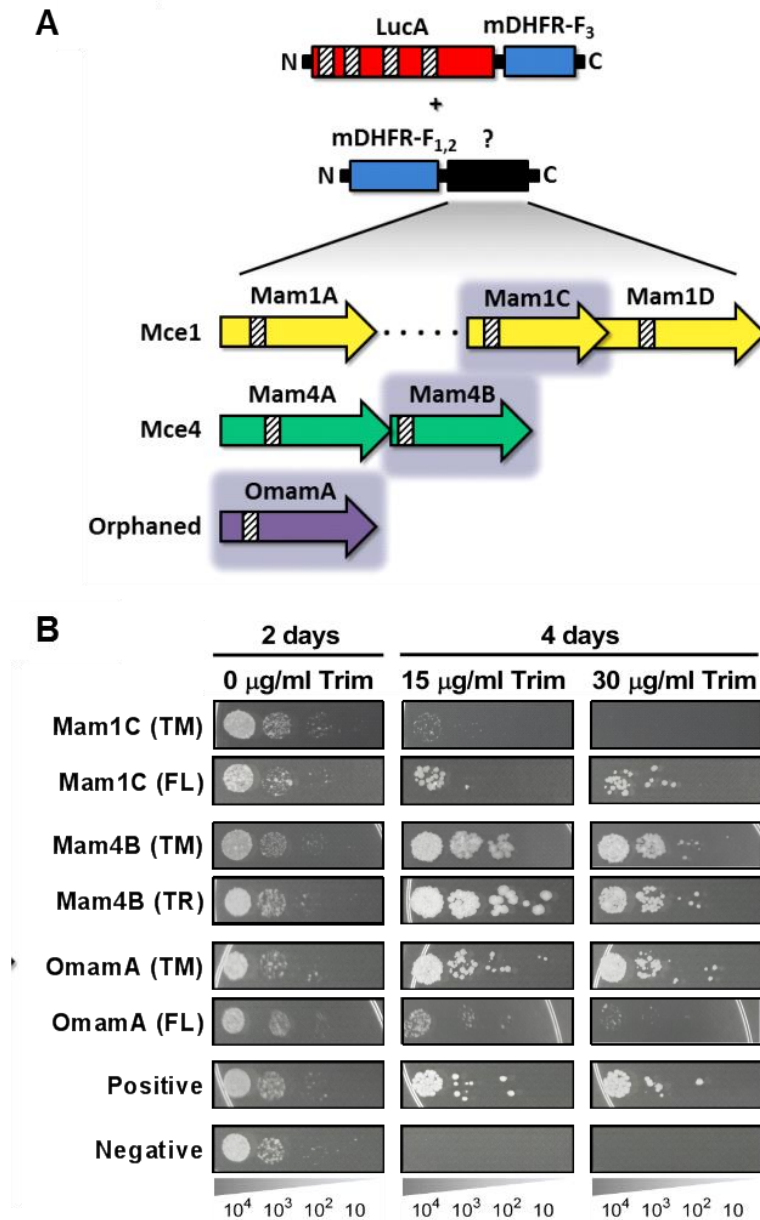


Figure 2.8. LucA interacts with subunits of Mce1 and Mce4 transporters.
A Schematic of split-DFHR protein constructs, shading indicates proteins that interact with LucA and striped boxes indicate predicted transmembrane domains. **B** Serial dilutions of Msm co-expressing the LucA-F₃ bait and the indicated prey were plated onto plates without antibiotic or plates containing trimethoprim at the indicated concentration. Growth on trimethoprim indicates protein-protein interaction. Positive is the positive control strain of Msm that co-expresses *Saccharomyces cerevisiae* homodimeric leucine zipper subunits (GCN4-F_{1,2} and GCN4-F₃). Negative is the negative control strain of Msm that expresses LucA-F₃ and GCN4-F_{1,2}.

Table 2.2. Protein interaction constructs. +/- indicates robustness of growth on trimethoprim.

Construct	Plasmid	Protein Region	Length (AA)	mDHFR domain	mDHFR domain location	Trimethoprim IC ₅₀ when co-expressed with LucA(FL)-F3, μ M	Spotting assay when co-expressed with LucA(FL)-F3	Interacts with LucA
LucA(FL)-F3	pUAB200	LucA	1-254	F3	C terminus	-	-	-
Mam1A(TM)	pUAB300	Mam1A	1-84	F1,2	N terminus	92.54 \pm 38.42	-	-
Mam1C(TM)	pUAB300	Mam1C	1-50	F1,2	N terminus	902.2 \pm 40.16	++	Yes
Mam1C(FL)	pUAB300	Mam1C	1-185	F1,2	N terminus	29.12 \pm 2.376	+++	-
Mam1D(TM)	pUAB300	Mam1D	1-103	F1,2	N terminus	84.98 \pm 1.471	+	-
Mam4A(TM)	pUAB300	Mam4A	1-110	F1,2	N terminus	49.4 \pm 0.8415	-	-
Mam4A(FL)	pUAB300	Mam4A	1-243	F1,2	N terminus	39.44 \pm 2.192	-	-
Mam4B(TM)	pUAB300	Mam4B	1-30	F1,2	N terminus	430 \pm 21.22	++++	Yes
Mam4B(TR)	pUAB300	Mam4B	1-75	F1,2	N terminus	266.2 \pm 37.12	++++	Yes
Mam4B(FL)	pUAB300	Mam4B	1-161	F1,2	N terminus	47.67 \pm 1.739	-	-
OmamA(TM)	pUAB300	OmamA	1-66	F1,2	N terminus	92.08 \pm 8.224	++++	-
OmamA(FL)	pUAB300	OmamA	1-220	F1,2	N terminus	140.3 \pm 76.09	+++	Yes

	Trimethoprim IC ₅₀ when co-expressed with GCN4-F1,2, μ M
Positive control GCN4-F3	70.19 \pm 2.164
Negative control LucA(FL)-F3	764.8 \pm 51.83

Abbreviations:

FL- full length

TM - fragment containing transmembrane domain

TR - truncated

LucA stabilizes subunits of the Mce1 and Mce4 complexes.

Recently, it was demonstrated that Rv0199/OmamA is involved in cholesterol metabolism and stabilizes the Mce1 complex in Mtb (Perkowski et al., 2016). Given that LucA interacts with Rv0199/OmamA and the related homologs Rv3492c/Mam4B and Rv0177/Mam1C we hypothesized that both the Mce1 and Mce4 transporters may also be destabilized in the $\Delta lucA::hyg$ mutant. To test this, we generated whole cell lysates from Mtb grown under the conditions used in the lipid uptake experiments. Gene expression analysis by qPCR confirmed that the *mce1* genes are expressed in the $\Delta lucA::hyg$ mutant to equivalent levels relative to the wild type and complemented strains (Figure 2.9. A). In contrast, analysis of bacterial lysates revealed that, at the protein level, the putative subunits of the Mce1 complex (Mce1A, Mce1D, Mce1E) were completely degraded in the $\Delta lucA::hyg$ mutant (Figure 2.9. B,C). Unfortunately, thus far we have been unable to raise antibodies specific to the analogous Mce4 subunits.

It is thought that MceG/Rv0655 functions as a common ATPase to hydrolyze ATP and facilitate nutrient uptake through the Mce transporters in Mtb (Joshi et al., 2006). MceG is required for optimum growth of Mtb on cholesterol and a mutant lacking MceG displays a cholesterol import defect that is equivalent to the cholesterol import defect observed in a mutant lacking Mce4 (Pandey & Sassetti, 2008). Although the role of MceG in fatty acid uptake has not been confirmed, it has been previously established that the stability of MceG requires co-expression of the Mce1 and Mce4 permease

subunits in mycobacterial cells (Joshi et al., 2006). To further explore the cholesterol and fatty acid uptake defect in the $\Delta lucA::hyg$ mutant we hypothesized MceG may also be degraded or destabilized in this strain. Therefore we quantified MceG levels in the bacterial lysates and observed a ~30% decrease in amount of MceG in the whole cell lysates of the $\Delta lucA::hyg$ mutant (Figure 2.9. B). It has recently been reported that synthesis of Mce proteins can exceed the rates of degradation (Perkowski et al., 2016) and given that there is negligible difference in the expression of MceG at the RNA level across the strains we used chloramphenicol to suppress protein synthesis in the bacteria. Under this condition the relative amount of MceG protein decreased by ~75% in the $\Delta lucA::hyg$ mutant (Figure 2.9. B). These results demonstrate that, in the absence of LucA, not only subunits of the Mce1 transporter complex, but also shared MceG ATPase, are degraded, possibly due to activity of unknown specific proteases. These data provide an explanation for the linked defect in both fatty acid and cholesterol uptake observed in the $\Delta lucA::hyg$ mutant and that LucA serves to coordinate the uptake of these nutrients by protecting the Mce1 and Mce4 transporters from degradation (Figure 2.10).

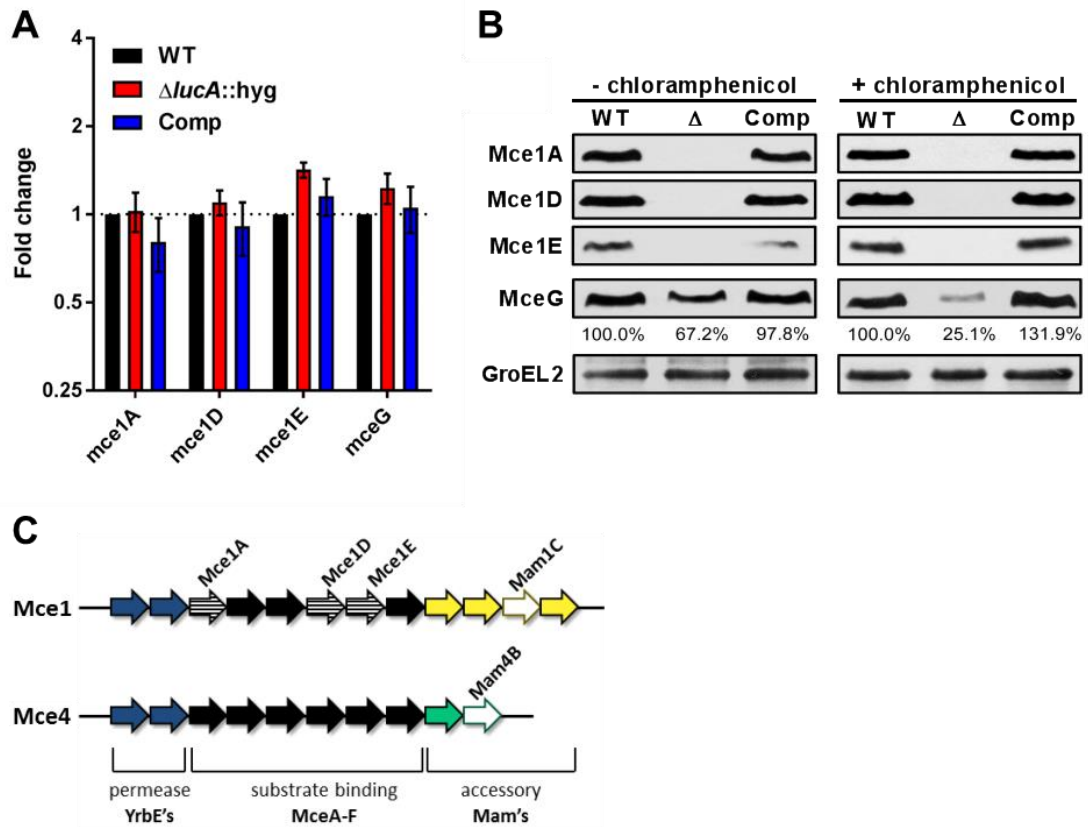


Figure 2.9. *LucA* is required for stability of *Mce1* and *Mce4* subunits. **A** Quantification of RNA transcripts by qPCR from untreated bacterial strains. Fold change values were determined by normalizing transcript levels to the *Mtb* housekeeping gene, *sigA*. Data are means \pm SD ($n = 6$). **B** Whole cell lysates probed by western blotting using antibodies specific for the indicated proteins. Chloramphenicol was added for 2 days before the lysate was prepared where indicated. Inset values indicate *MceG* protein levels that were quantified and expressed as a ratio relative to *MceG* in the wild type lysates. *GroEL2* is a loading control and blots are representative of two independent experiments. **C** Organization of genes that encode the *Mce1* and *Mce4* transporters. Striped arrows indicate genes encoding proteins that are degraded in the $\Delta lucA::hyg$ mutant. Empty arrows indicate genes encoding accessory proteins that interact with *LucA*.

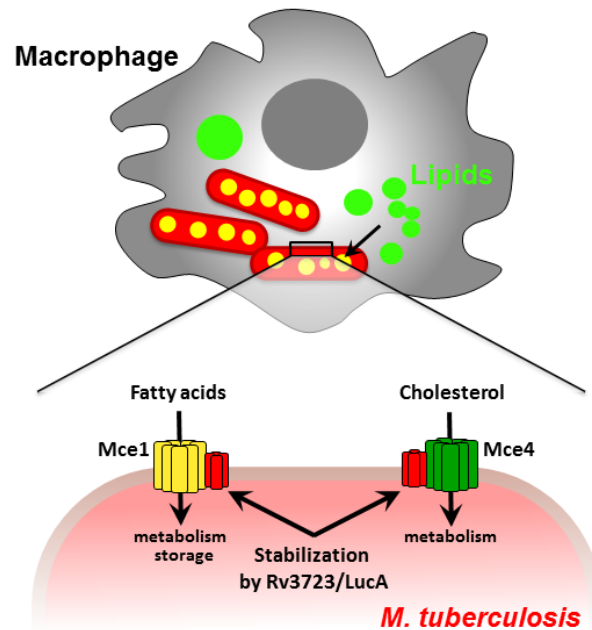


Figure 2.10. Schematic of LucA function in fatty acid and cholesterol uptake. Mtb scavenges lipids from macrophage during infection. Mce1 and Mce4 serve as fatty acid and cholesterol importers. LucA interacts with subunits of these protein complexes. Inactivation of LucA leads to degradation of Mce1 and Mce4 subunits and renders them nonfunctional.

LucA contributes to the *in vivo* fitness of Mtb.

These data indicate that LucA is involved in the utilization of two critical host-derived lipid substrates. It is known that deletion of one or both of the Mce1 and Mce4 transporters leads to decreased survival of the pathogen in mouse model infection (Joshi et al., 2006) and we predict that both of these transporters would be nonfunctional in the $\Delta lucA::hyg$ mutant. In human macrophages the $\Delta lucA::hyg$ mutant displayed a growth lag that culminates in a 10-fold difference in bacterial counts compared to wild type and complemented strains over a 7-day infection period (Figure 2.11. A). A similar phenotype was observed in the resting murine macrophages where the $\Delta lucA::hyg$ mutant replicated poorly over a 10-day infection period (Figure 2.11. B). In both human and murine macrophages the final CFU counts for the $\Delta lucA::hyg$ mutant remained close to initial inoculum levels. These data are consistent with the hypothesis that Mtb requires LucA to sustain maximal growth on cholesterol and/or fatty acid substrates in macrophages.

In the lung tissues of C57BL/6J mice, the $\Delta lucA::hyg$ mutant also demonstrated a fitness defect and did not attain levels of bacterial burden comparable to either the wild type or complemented strains. At day 14 post-infection 10-fold fewer CFU's of the $\Delta lucA::hyg$ mutant were recovered relative to wild type and the complemented strains. During the remainder of the 56-day infection period, growth of the $\Delta lucA::hyg$ mutant remained restricted, leading to 3- to 5-fold reduction in viable $\Delta lucA::hyg$ bacteria (Figure 2.11. C). The $\Delta lucA::hyg$ mutant also induced less pulmonary pathology throughout the

entire course of infection (Figure 2.11. D). Complementation almost completely restored pathogenicity and lung tissue pathology confirming the specificity of the mutant phenotype to the *lucA* gene.

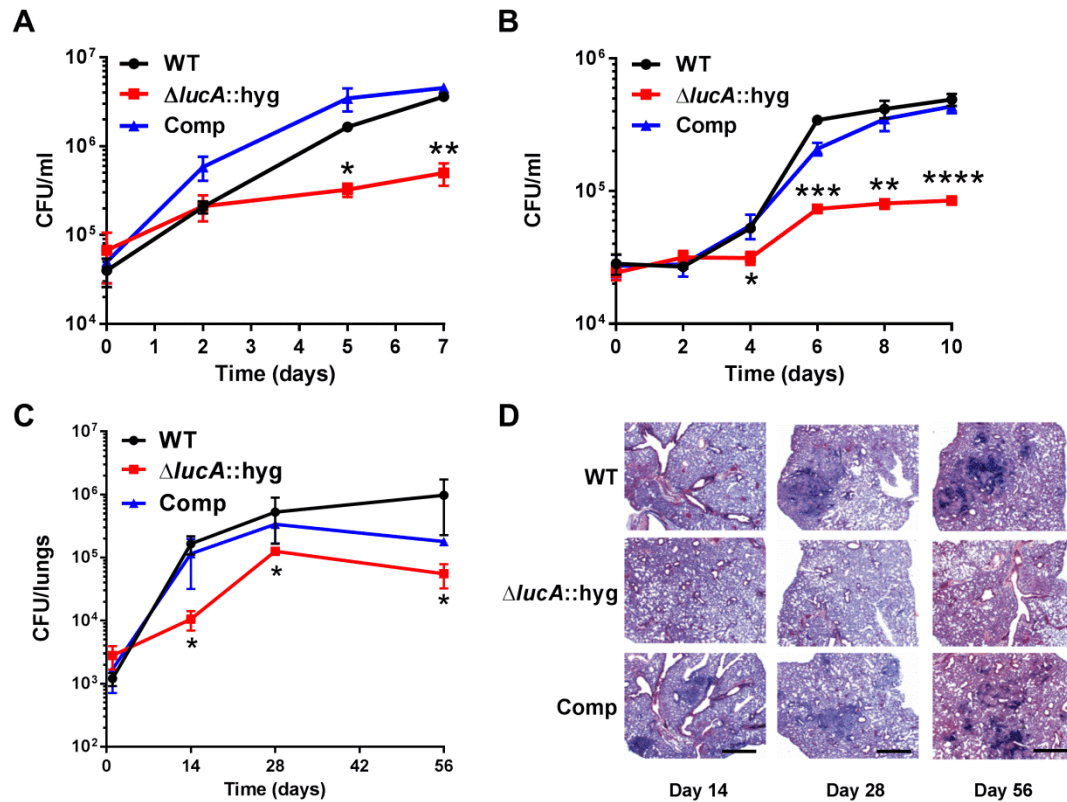


Figure 2.11. LucA is required for the full fitness of Mtb in macrophages and survival in mouse lungs. **A** Bacterial replication in resting human monocyte derived macrophages. Data are means \pm SD (n = 3). **B** Bacterial replication in resting murine bone marrow derived macrophages. Data are means \pm SD (n = 3). **C** Bacterial survival in mouse lung tissues. Data are means \pm SD (n = 5 per time point) **D** Lung pathology of infected mice collected at indicated time points and H&E stained. Scale bar 400 μ m.

*p < 0.05, **p < 0.005, ***p < 0.001, ****p < 0.0005 (Student's t test).

Discussion

While there is general agreement as to the role of Mce4 in cholesterol uptake in Mtb, the process of fatty acid assimilation by the bacterium has remained enigmatic. These data shed new light on the coordination of fatty acid and cholesterol import and reveal that a network of proteins associates with the Mce1 and Mce4 transporters to integrate the uptake of both fatty acids and cholesterol.

Using an unbiased forward genetic screen we discovered that transposon insertions in the *lucA* gene rescue cholesterol toxicity in an Mtb strain that lacks *Δicl1*. Subsequent analysis confirmed that mutation of *lucA* ($\Delta lucA::hyg$) has a profound impact on cholesterol uptake, and that this cholesterol uptake defect confers growth rescue in the $\Delta icl1 lucA::TnHimar$ double mutant.

Transcriptional profiling revealed that genes normally activated by cholesterol are down-regulated in the $\Delta lucA::hyg$ mutant during infection in macrophages. This is consistent with a defect in cholesterol uptake in this mutant. We were surprised to discover that the $\Delta lucA::hyg$ mutant also produces a gene expression signature indicative of a fatty acid metabolism defect. Although the functions for many of these “fatty acid-induced” genes are unknown, their expression pattern serves as a reliable indicator of a fatty acid uptake defect in Mtb. The majority of the 20 most highly-expressed genes in the $\Delta lucA::hyg$ during infection in macrophages map to the *mce1* locus. Up-regulation of genes encoding the Mce1 fatty acid transporter in the $\Delta lucA::hyg$

mutant during infection likely reflects an attempt by the bacterium to compensate for the absence of fatty acids that normally fuels Mtb's metabolism. The mechanism that controls expression of the *mce1* locus in response to fatty acid depletion is unknown but we hypothesize that Mtb has an ability to sense metabolite pools to control synthesis of the Mce1 fatty acid transporter complex.

The Mtb cell envelope constitutes a formidable barrier to the transport of any hydrophobic molecule. Actinomycetal bacteria with mycolic acid-containing cell walls that are capable of metabolizing cholesterol use the Mce4 complex to import the sterol (Mohn et al., 2008; Pandey & Sasseti, 2008; Perkowski et al., 2016) and this has led to the idea that all four of the Mce complexes transport hydrophobic molecules across the Mtb cell wall. Various studies have linked Mce1 to Mtb virulence (Shimono et al., 2003; Gioffre et al., 2005; Joshi et al., 2006) but the function of the Mce1 complex was hitherto unknown. It has been reported that inactivating Mce1 in Mtb induces a lipid homeostasis defect and the accumulation of free mycolic acids in the Mtb cell wall (Cantrell et al., 2013; Forrellad et al., 2014). Based on these observations it was hypothesized that the Mce1 may transport fatty acids and/or mycolic acids across the cell wall/membrane of Mtb but it was reported that Mce1 mutant in Mtb displayed a minor defect in fatty acid uptake (Forrellad et al., 2014). We used assays comparable to those previously described and detected major perturbations in fatty acid assimilation in our Mce1 mutants. We cannot fully explain the discrepancy between these findings but we have

noticed that spontaneous mutants of Mtb unable to produce phthiocerol dimycocerosate (PDIM) assimilate less fatty acids compared to PDIM positive strains. Our work was conducted in a PDIM positive strain of Mtb Erdman and we think this has allowed us to detect Mce1-mediated fatty acid transport.

Studies with *Mycobacterium leprae* (Mlep) are consistent with the interpretation that Mce1 functions as a mycobacterial fatty acid transporter. The Mlep genome contains a single *mce* locus which is most similar to the *mce1* operon found in Mtb and Mlep is fully capable of importing and metabolizing palmitate when the bacteria are recovered from animal tissues (Franzblau, 1988). The Mlep genome also encodes a homolog of *lucA* (ml2337) suggesting that LucA could be central for Mce1 function in this bacterium. Given that the Mlep genome does not conserve genes that encode proteins for cholesterol import/metabolism and this bacterium does not metabolize cholesterol, (Marques et al., 2015) it is likely that ml2337 has one role in Mlep. The finding that LucA facilitates fatty acid uptake and stabilizes components of the Mce1 transporter provides additional evidence that Mce1 functions as a fatty acid transporter. Therefore the fatty acid uptake defect in the Δ *lucA*::hyg mutant is most likely a consequence of the degradation of Mce1 components.

The *mce1-4* loci make up four separate operons in the Mtb genome and each operon encodes the putative protein subunits that likely comprise the individual substrate-specific Mce transporters. Although Mce1 and Mce4 are likely the main transporters of fatty acids and cholesterol, respectively, we can

detect a residual level of fatty acid and cholesterol uptake and metabolism in mutants lacking individual loci. It is very likely that compensatory systems function to import these lipids in the absence of Mce1 and Mce4 and we are currently testing this hypothesis.

Based on homology it is predicted that Mce operons encode 3 types of transporter subunits with discrete roles: i) two putative permease subunits (YrbE), ii) six cell wall associated proteins (Mce), and iii) two accessory/ mce associated membrane proteins (Mam). Function of the latter is the most elusive. The matter is also complicated by the presence of homologous mce associated proteins scattered throughout the Mtb genome. Recently it was reported that one such orphaned Mce associated protein Rv0199/OmamA facilitates cholesterol utilization in Msm and stabilizes the Mce1 complex in Mtb (Perkowski et al., 2016). This work demonstrates that LucA interacts with the Mce1 and Mce4 accessory subunits Rv0199/OmamA, Rv0177/Mam1C and Rv3492/Mam4A. And similarly to Rv0199/OmamA, we found that LucA is also required to stabilize subunits of the Mce1 transporter. Based on this we predict that LucA is recruited to the Mce1 and Mce4 complexes to stabilize or assemble the transporters via interactions with the accessory subunits. Given that MceG is required for cholesterol uptake and is thought to facilitate the import of additional nutrients in Mtb (Garcia-Fernandez et al., 2017; Joshi et al., 2006; Pandey & Sassetti, 2008) our finding that the MceG protein is also destabilized in the $\Delta lucA::hyg$ mutant may explain the various nutrient uptake defects in this mutant. Homology searches based on 3-dimensional structures

identified a putative protease inhibitor domain within the N-terminus of LucA (Kelley et al., 2015). We hypothesize that LucA may locally inactivate a protease to maintain the integrity of the transporter complexes. Regulating activity of the transport complexes through proteolysis could be a mechanism to rapidly halt nutrient uptake through the Mce transporters, however such a suggestion will require more research.

During growth in the presence of cholesterol, Mtb shunts cholesterol-derived methylmalonyl-CoA (originating from propionyl-CoA) towards the increased synthesis of methyl-branched, cell wall polyketide lipids (Griffin et al., 2012; Jain et al., 2007; Yang et al., 2009). This metabolic shunting requires that sufficient fatty acid derived acyl-AMP primers are available to support biosynthesis of polyketide lipids (Quadri, 2014). When excess fatty acids are supplied to infected macrophages, Mtb can enhance the flux of propionyl-CoA into polyketide lipids such as PDIM during infection (Lee et al., 2013). It would be advantageous for Mtb to regulate fatty acid assimilation to maintain the acyl-AMP pools required for efficient synthesis of methyl-branched lipids. Thus, coordination of cholesterol and fatty acid uptake by LucA could ensure that balanced levels of these nutrients are maintained for optimized metabolism.

The central carbon and lipid metabolic pathways of Mtb have emerged as potential drug targets (Rhee et al., 2011; VanderVen et al., 2015), therefore understanding the bottlenecks or weaknesses in these pathways will assist TB drug discovery. Additionally, the flux of fatty acids into TAG and central

metabolism contributes to drug tolerance in Mtb (Baek et al., 2011), a phenotype that is further enhanced by immune pressure during *in vivo* infection (Liu et al., 2016). Targeting the specialized lipid metabolic pathways in Mtb that are involved in fatty acid and cholesterol utilization could be a viable strategy for the development of new drugs that reduce Mtb drug tolerance and augment current TB drug regimens. Our data have defined new participants in the complex processes of fatty acid and cholesterol assimilation by Mtb. A better understanding of the functional integration of Mtb's specialized metabolic pathways is required to acquire a fuller appreciation of Mtb pathogenesis.

Acknowledgments

We thank Linda Bennett for excellent technical support, Robert Abramovitch, Shumin Tan, John Helmann, and Lu Huang for productive discussions, Maria Podinovskaia for assistance with imaging, Yancheng Liu for help with library construction for M-PFC. We also thank Adrie Steyn for the generous gift of the M-PFC vectors, Martin Pavelka for the *aacC4* apramycin resistance cassette, and Christopher Sasseti for the Mce1 antibodies. This work was supported by the NIH grants (AI099569 and AI119122) to BCV and (AI118582 and AI067027) to DGR.

Author Contributions

Conceptualization, E.V.N. and B.C.V.; Methodology, E.V.N., and B.C.V.; Formal Analysis, E.V.N. and B.C.V.; Investigation, E.V.N., C.R.M., T.L., N.S., W.L., S.C., K.M.W., B.C.V.; Writing – Original Draft, E.V.N. and B.C.V.; Writing – Review & Editing, E.V.N., B.C.V. and D.G.R.; Visualization, E.V.N. and B.C.V.; Funding Acquisition, D.G.R. and B.C.V.

References

Abramovitch, R.B., Rohde, K.H., Hsu, F.-F., and Russell, D.G. (2011). *aprABC*: a *Mycobacterium tuberculosis* complex-specific locus that modulates pH-driven adaptation to the macrophage phagosome. *Molecular microbiology* 80, 678-694.

Arruda, S., Bomfim, G., Knights, R., Huima-Byron, T., and Riley, L.W. (1993). Cloning of an *M. tuberculosis* DNA fragment associated with entry and survival inside cells. *Science* 261, 1454-1457.

Awai, K., Xu, C., Tamot, B., and Benning, C. (2006). A phosphatidic acid-binding protein of the chloroplast inner envelope membrane involved in lipid trafficking. *Proceedings of the National Academy of Sciences* 103, 10817-10822.

Baek, S.H., Li, A.H., and Sasseti, C.M. (2011). Metabolic regulation of mycobacterial growth and antibiotic sensitivity. *PLoS biology* 9, e1001065.

Black, P.N., Said, B., Ghosn, C.R., Beach, J.V., and Nunn, W.D. (1987). Purification and characterization of an outer membrane-bound protein involved in long-chain fatty acid transport in *Escherichia coli*. *The Journal of biological chemistry* 262, 1412-1419.

Bloch, H., and Segal, W. (1956). Biochemical differentiation of *Mycobacterium tuberculosis* grown *in vivo* and *in vitro*. *Journal of bacteriology* 72, 132-141.

Cantrell, S.A., Leavell, M.D., Marjanovic, O., Iavarone, A.T., Leary, J.A., and Riley, L.W. (2013). Free mycolic acid accumulation in the cell wall of the *mce1* operon mutant strain of *Mycobacterium tuberculosis*. *Journal of microbiology (Seoul, Korea)* 51, 619-626.

Capyk, J.K., Kalscheuer, R., Stewart, G.R., Liu, J., Kwon, H., Zhao, R., Okamoto, S., Jacobs, W.R., Jr., Eltis, L.D., and Mohn, W.W. (2009). Mycobacterial cytochrome p450 125 (Cyp125) catalyzes the terminal hydroxylation of C27 steroids. *The Journal of biological chemistry* 284, 35534-35542.

Casali, N., and Riley, L.W. (2007). A phylogenomic analysis of the *Actinomycetales mce* operons. *BMC genomics* 8, 60.

Chang, J.C., Harik, N.S., Liao, R.P., and Sherman, D.R. (2007). Identification of mycobacterial genes that alter growth and pathology in macrophages and in mice. *Journal of Infectious Diseases* 196, 788-795.

Cole, S.T., Brosch, R., Parkhill, J., Garnier, T., Churcher, C., Harris, D., Gordon, S.V., Eiglmeier, K., Gas, S., Barry, C.E., 3rd, *et al.* (1998). Deciphering the biology of *Mycobacterium tuberculosis* from the complete genome sequence. *Nature* 393, 537-544.

Costes, S.V., Daelemans, D., Cho, E.H., Dobbin, Z., Pavlakis, G., and Lockett, S. (2004). Automatic and quantitative measurement of protein-protein colocalization in live cells. *Biophysical journal* 86, 3993-4003.

Daniel, J., Maamar, H., Deb, C., Sirakova, T.D., and Kolattukudy, P.E. (2011). *Mycobacterium tuberculosis* uses host triacylglycerol to accumulate lipid droplets and acquires a dormancy-like phenotype in lipid-loaded macrophages. *PLoS pathogens* 7, e1002093.

de Carvalho, L.P., Fischer, S.M., Marrero, J., Nathan, C., Ehrt, S., and Rhee, K.Y. (2010). Metabolomics of *Mycobacterium tuberculosis* reveals compartmentalized co-catabolism of carbon substrates. *Chemistry & biology* 17, 1122-1131.

Dresen, C., Lin, L.Y., D'Angelo, I., Tocheva, E.I., Strynadka, N., and Eltis, L.D. (2010). A flavin-dependent monooxygenase from *Mycobacterium tuberculosis* involved in cholesterol catabolism. *The Journal of biological chemistry* 285, 22264-22275.

Edgar, R., Domrachev, M., and Lash, A.E. (2002). Gene Expression Omnibus: NCBI gene expression and hybridization array data repository. *Nucleic acids research* 30, 207-210.

Ekiert, D.C., Bhabha, G., Isom, G.L., Greenan, G., Ovchinnikov, S., Henderson, I.R., Cox, J.S., and Vale, R.D. (2017). Architectures of lipid transport systems for the bacterial outer membrane. *Cell* 169, 273-285.e217.

Eoh, H., and Rhee, K.Y. (2014). Methylcitrate cycle defines the bactericidal essentiality of isocitrate lyase for survival of *Mycobacterium tuberculosis* on fatty acids. *Proceedings of the National Academy of Sciences* 111, 4976-4981.

Feltcher, M.E., Gunawardena, H.P., Zulauf, K.E., Malik, S., Griffin, J.E., Sassetti, C.M., Chen, X., and Braunstein, M. (2015). Label-free Quantitative Proteomics Reveals a Role for the *Mycobacterium tuberculosis* SecA2 Pathway in Exporting Solute Binding Proteins and Mce Transporters to the Cell Wall. *Molecular & cellular proteomics : MCP* 14, 1501-1516.

Forrellad, M.A., McNeil, M., Santangelo Mde, L., Blanco, F.C., Garcia, E., Klepp, L.I., Huff, J., Niederweis, M., Jackson, M., and Bigi, F. (2014). Role of the Mce1 transporter in the lipid homeostasis of *Mycobacterium tuberculosis*. *Tuberculosis* 94, 170-177.

Franzblau, S.G. (1988). Oxidation of palmitic acid by *Mycobacterium leprae* in an axenic medium. *Journal of clinical microbiology* 26, 18-21.

Garcia-Fernandez, J., Papavinasasundaram, K., Galan, B., Sassetti, C.M., and Garcia, J.L. (2017). Unraveling the pleiotropic role of the MceG ATPase in *Mycobacterium smegmatis*. *Environmental microbiology*.

Gioffre, A., Infante, E., Aguilar, D., Santangelo, M.P., Klepp, L., Amadio, A., Meikle, V., Etchechoury, I., Romano, M.I., Cataldi, A., *et al.* (2005). Mutation in *mce* operons attenuates *Mycobacterium tuberculosis* virulence. *Microbes and infection* 7, 325-334.

Griffin, J.E., Gawronski, J.D., DeJesus, M.A., Ioerger, T.R., Akerley, B.J., and Sassetti, C.M. (2011). High-resolution phenotypic profiling defines genes essential for mycobacterial growth and cholesterol catabolism. *PLoS pathogens* 7, e1002251.

Griffin, J.E., Pandey, A.K., Gilmore, S.A., Mizrahi, V., McKinney, J.D., Bertozzi, C.R., and Sassetti, C.M. (2012). Cholesterol catabolism by *Mycobacterium tuberculosis* requires transcriptional and metabolic adaptations. *Chemistry & biology* 19, 218-227.

Ho, N.A., Dawes, S.S., Crowe, A.M., Casabon, I., Gao, C., Kendall, S.L., Baker, E.N., Eltis, L.D., and Lott, J.S. (2016). The structure of the transcriptional repressor KstR in complex with CoA thioester cholesterol metabolites sheds light on the regulation of cholesterol catabolism in *Mycobacterium tuberculosis*. *The Journal of biological chemistry* 291, 7256-7266.

Hu, Y., van der Geize, R., Besra, G.S., Gurcha, S.S., Liu, A., Rohde, M., Singh, M., and Coates, A. (2010). 3-Ketosteroid 9 α -hydroxylase is an essential factor in the pathogenesis of *Mycobacterium tuberculosis*. *Molecular microbiology* 75, 107-121.

Jain, M., Petzold, C.J., Schelle, M.W., Leavell, M.D., Mougous, J.D., Bertozzi, C.R., Leary, J.A., and Cox, J.S. (2007). Lipidomics reveals control of *Mycobacterium tuberculosis* virulence lipids via metabolic coupling. *Proceedings of the National Academy of Sciences* 104, 5133-5138.

Joshi, S.M., Pandey, A.K., Capite, N., Fortune, S.M., Rubin, E.J., and Sasseti, C.M. (2006). Characterization of mycobacterial virulence genes through genetic interaction mapping. *Proceedings of the National Academy of Sciences* 103, 11760-11765.

Kelley, L.A., Mezulis, S., Yates, C.M., Wass, M.N., and Sternberg, M.J. (2015). The Phyre2 web portal for protein modeling, prediction and analysis. *Nature Protocols* 10, 845-858.

Kendall, S.L., Withers, M., Soffair, C.N., Moreland, N.J., Gurcha, S., Sidders, B., Frita, R., Ten Bokum, A., Besra, G.S., Lott, J.S., *et al.* (2007). A highly conserved transcriptional repressor controls a large regulon involved in lipid degradation in *Mycobacterium smegmatis* and *Mycobacterium tuberculosis*. *Molecular microbiology* 65, 684-699.

Kim, M.J., Wainwright, H.C., Locketz, M., Bekker, L.G., Walther, G.B., Dittrich, C., Visser, A., Wang, W., Hsu, F.F., Wiehart, U., *et al.* (2010). Caseation of human tuberculosis granulomas correlates with elevated host lipid metabolism. *EMBO molecular medicine* 2, 258-274.

Lee, W., VanderVen, B.C., Fahey, R.J., and Russell, D.G. (2013). Intracellular *Mycobacterium tuberculosis* exploits host-derived fatty acids to limit metabolic stress. *The Journal of biological chemistry* 288, 6788-6800.

Listenberger, L.L., and Brown, D.A. (2007). Fluorescent detection of lipid droplets and associated proteins. *Current protocols in cell biology / editorial board, Juan S Bonifacino [et al] Chapter 24, Unit 24.22.*

Liu, Y., Tan, S., Huang, L., Abramovitch, R.B., Rohde, K.H., Zimmerman, M.D., Chen, C., Dartois, V., VanderVen, B.C., and Russell, D.G. (2016).

Immune activation of the host cell induces drug tolerance in *Mycobacterium tuberculosis* both *in vitro* and *in vivo*. *J Exp Med* 213, 809-825.

Malinverni, J.C., and Silhavy, T.J. (2009). An ABC transport system that maintains lipid asymmetry in the gram-negative outer membrane. *Proceedings of the National Academy of Sciences* 106, 8009-8014.

Mann, F.M., VanderVen, B.C., and Peters, R.J. (2011). Magnesium depletion triggers production of an immune modulating diterpenoid in *Mycobacterium tuberculosis*. *Molecular microbiology* 79, 1594-1601.

Marques, M.A., Berredo-Pinho, M., Rosa, T.L., Pujari, V., Lemes, R.M., Lery, L.M., Silva, C.A., Guimaraes, A.C., Atella, G.C., Wheat, W.H., *et al.* (2015). The essential role of cholesterol metabolism in the intracellular survival of *Mycobacterium leprae* is not coupled to central carbon metabolism and energy production. *Journal of bacteriology* 197, 3698-3707.

Marrero, J., Rhee, K.Y., Schnappinger, D., Pethe, K., and Ehrst, S. (2010). Gluconeogenic carbon flow of tricarboxylic acid cycle intermediates is critical for *Mycobacterium tuberculosis* to establish and maintain infection. *Proceedings of the National Academy of Sciences* 107, 9819-9824.

Masiewicz, P., Brzostek, A., Wolanski, M., Dziadek, J., and Zakrzewska-Czerwinska, J. (2012). A novel role of the PrpR as a transcription factor involved in the regulation of methylcitrate pathway in *Mycobacterium tuberculosis*. *PloS one* 7, e43651.

McKinney, J.D., zu Bentrup, K.H., Munoz-Elias, E.J., Miczak, A., Chen, B., Chan, W.-T., Swenson, D., Sacchettini, J.C., Jacobs, W.R., and Russell, D.G. (2000). Persistence of *Mycobacterium tuberculosis* in macrophages and mice requires the glyoxylate shunt enzyme isocitrate lyase. *Nature* 406, 735-738.

Mohn, W.W., van der Geize, R., Stewart, G.R., Okamoto, S., Liu, J., Dijkhuizen, L., and Eltis, L.D. (2008). The actinobacterial *mce4* locus encodes a steroid transporter. *The Journal of biological chemistry* 283, 35368-35374.

Muñoz-Elías, E.J., Upton, A.M., Cherian, J., and McKinney, J.D. (2006). Role of the methylcitrate cycle in *Mycobacterium tuberculosis* metabolism, intracellular growth, and virulence. *Molecular microbiology* 60, 1109-1122.

Nakayama, T., and Zhang-Akiyama, Q.M. (2017). *pqiABC* and *yebST*, Putative *mce* Operons of *Escherichia coli*, Encode Transport Pathways and Contribute to Membrane Integrity. *Journal of bacteriology*

Nesbitt, N.M., Yang, X., Fontan, P., Kolesnikova, I., Smith, I., Sampson, N.S., and Dubnau, E. (2010). A thiolase of *Mycobacterium tuberculosis* is required for virulence and production of androstenedione and androstadienedione from cholesterol. *Infect Immun* 78, 275-282.

Pandey, A.K., and Sasseti, C.M. (2008). Mycobacterial persistence requires the utilization of host cholesterol. *Proceedings of the National Academy of Sciences* 105, 4376-4380.

Perkowski, E.F., Miller, B.K., McCann, J.R., Sullivan, J.T., Malik, S., Allen, I.C., Godfrey, V., Hayden, J.D., and Braunstein, M. (2016). An orphaned Mce-associated membrane protein of *Mycobacterium tuberculosis* is a virulence factor that stabilizes Mce transporters. *Molecular microbiology* 100, 90-107.

Peyron, P., Vaubourgeix, J., Poquet, Y., Levillain, F., Botanch, C., Bardou, F., Daffe, M., Emile, J.F., Marchou, B., Cardona, P.J., *et al.* (2008). Foamy macrophages from tuberculous patients' granulomas constitute a nutrient-rich reservoir for *M. tuberculosis* persistence. *PLoS pathogens* 4, e1000204.

Podinovskaia, M., Lee, W., Caldwell, S., and Russell, D.G. (2013). Infection of macrophages with *Mycobacterium tuberculosis* induces global modifications to phagosomal function. *Cellular microbiology* 15, 843-859.

Prod'hom, G., Lagier, B., Pelicic, V., Hance, A.J., Gicquel, B., and Guilhot, C. (1998). A reliable amplification technique for the characterization of genomic DNA sequences flanking insertion sequences. *FEMS microbiology letters* 158, 75-81.

Quadri, L.E. (2014). Biosynthesis of mycobacterial lipids by polyketide synthases and beyond. *Critical reviews in biochemistry and molecular biology* 49, 179-211.

Rhee, K.Y., de Carvalho, L.P., Bryk, R., Ehrt, S., Marrero, J., Park, S.W., Schnappinger, D., Venugopal, A., and Nathan, C. (2011). Central carbon metabolism in *Mycobacterium tuberculosis*: an unexpected frontier. *Trends in microbiology* 19, 307-314.

Rohde, K.H., Abramovitch, R.B., and Russell, D.G. (2007). *Mycobacterium tuberculosis* invasion of macrophages: linking bacterial gene expression to environmental cues. *Cell Host & Microbe* 2, 352-364.

Roston, R., Gao, J., Xu, C., and Benning, C. (2011). Arabidopsis chloroplast lipid transport protein TGD2 disrupts membranes and is part of a large complex. *The Plant journal: for cell and molecular biology* 66, 759-769.

Russell, D.G., VanderVen, B.C., Lee, W., Abramovitch, R.B., Kim, M.-J., Homolka, S., Niemann, S., and Rohde, K.H. (2010). *Mycobacterium tuberculosis* wears what it eats. *Cell Host & Microbe* 8, 68-76.

Savvi, S., Warner, D.F., Kana, B.D., McKinney, J.D., Mizrahi, V., and Dawes, S.S. (2008). Functional characterization of a vitamin B12-dependent methylmalonyl pathway in *Mycobacterium tuberculosis*: Implications for propionate metabolism during growth on fatty acids. *J Bacteriol* 190, 3886-3895.

Schnappinger, D., Ehrt, S., Voskuil, M.I., Liu, Y., Mangan, J.A., Monahan, I.M., Dolganov, G., Efron, B., Butcher, P.D., Nathan, C., *et al.* (2003). Transcriptional adaptation of *Mycobacterium tuberculosis* within macrophages: Insights into the phagosomal environment. *The Journal of Experimental Medicine* 198, 693-704.

Shimono, N., Morici, L., Casali, N., Cantrell, S., Sidders, B., Ehrt, S., and Riley, L.W. (2003). Hypervirulent mutant of *Mycobacterium tuberculosis* resulting from disruption of the *mce1* operon. *Proceedings of the National Academy of Sciences* 100, 15918-15923.

Singh, A., Mai, D., Kumar, A., and Steyn, A.J. (2006). Dissecting virulence pathways of *Mycobacterium tuberculosis* through protein-protein association. *Proceedings of the National Academy of Sciences* 103, 11346-11351.

Sukumar, N., Tan, S., Aldridge, B.B., and Russell, D.G. (2014). Exploitation of *Mycobacterium tuberculosis* reporter strains to probe the impact of vaccination at sites of infection. *PLoS pathogens* 10, e1004394.

Sutterlin, H.A., Shi, H., May, K.L., Miguel, A., Khare, S., Huang, K.C., and Silhavy, T.J. (2016). Disruption of lipid homeostasis in the Gram-negative cell envelope activates a novel cell death pathway. *Proceedings of the National Academy of Sciences* 113, E1565-1574.

Theodoulou, F.L., Carrier, D.J., Schaedler, T.A., Baldwin, S.A., and Baker, A. (2016). How to move an amphipathic molecule across a lipid bilayer: different mechanisms for different ABC transporters? *Biochemical Society Transactions* 44, 774-782.

Thong, S., Ercan, B., Torta, F., Fong, Z.Y., Wong, H.Y., Wenk, M.R., and Chng, S.S. (2016). Defining key roles for auxiliary proteins in an ABC transporter that maintains bacterial outer membrane lipid asymmetry. *5*, e19042

van den Berg, B., Black, P.N., Clemons, W.M., Jr., and Rapoport, T.A. (2004). Crystal structure of the long-chain fatty acid transporter FadL. *Science* 304, 1506-1509.

Van der Geize, R., Yam, K., Heuser, T., Wilbrink, M.H., Hara, H., Anderton, M.C., Sim, E., Dijkhuizen, L., Davies, J.E., Mohn, W.W., *et al.* (2007). A gene cluster encoding cholesterol catabolism in a soil actinomycete provides insight into *Mycobacterium tuberculosis* survival in macrophages. *Proceedings of the National Academy of Sciences* 104, 1947-1952.

VanderVen, B.C., Fahey, R.J., Lee, W., Liu, Y., Abramovitch, R.B., Memmott, C., Crowe, A.M., Eltis, L.D., Perola, E., Deininger, D.D., *et al.* (2015). Novel inhibitors of cholesterol degradation in *Mycobacterium tuberculosis* reveal how the bacterium's metabolism is constrained by the intracellular environment. *PLoS pathogens* 11, e1004679.

Xu, C., Fan, J., Cornish, A.J., and Benning, C. (2008). Lipid trafficking between the endoplasmic reticulum and the plastid in *Arabidopsis* requires the extraplastidic TGD4 protein. *The Plant cell* 20, 2190-2204.

Yam, K.C., D'Angelo, I., Kalscheuer, R., Zhu, H., Wang, J.-X., Snieckus, V., Ly, L.H., Converse, P.J., Jacobs, W.R., Jr., Strynadka, N., *et al.* (2009). Studies of a ring-cleaving dioxygenase illuminate the role of cholesterol metabolism in the pathogenesis of *Mycobacterium tuberculosis*. *PLoS pathogens* 5, e1000344.

Yang, X., Nesbitt, N.M., Dubnau, E., Smith, I., and Sampson, N.S. (2009). Cholesterol metabolism increases the metabolic pool of propionate in *Mycobacterium tuberculosis*. *Biochemistry* 48, 3819-3821.

CHAPTER 3

**Insights into mechanisms of inter-regulation of cholesterol
and fatty acid transport in *Mycobacterium tuberculosis***

Abstract

M. tuberculosis has evolved to utilize fatty acids and cholesterol as the main carbon sources during infection, both at the level of the host cell and at the level of granuloma. Mtb requires strict regulation of metabolism of these carbon sources to maintain balance between supplying energy for survival and synthesis of lipids essential for virulence. Here we sought to identify the main mechanisms that the pathogen employs to balance import of fatty acids and cholesterol. We found that on one hand, catabolites of cholesterol negatively regulated the fatty acid transporter Mce1 at the transcriptional level. Conversely, long-chain fatty acids induced increased uptake of cholesterol. Additionally, we demonstrated that stability of the Mce1 transporter, and therefore fatty acid uptake was regulated at the protein level through protection from degradation by Zn²⁺ metalloprotease Zmp1. This protection was dependent on the Mce accessory subunit OmamA. While deletion of OmamA had no effect on cholesterol import, inactivation of both OmamA and Zmp1 led to a significant decrease in the amount of cholesterol catabolized. Therefore, we conclude that Mtb possesses mechanisms of inter-regulation of cholesterol and fatty acid assimilation, both at transcriptional and at protein levels through precise activity of specific proteases.

Introduction

Mtb can persist within its host for decades, therefore acquisition of nutrients available within the host is crucial to survival of the pathogen. Mtb is uniquely adapted to metabolize fatty acids and cholesterol (Russell et al., 2010; Lovewell et al., 2016), and most likely these processes are strictly regulated. Both of these lipids are degraded in Mtb with subsequent incorporation of catabolites into the TCA cycle to provide energy for bacterial survival. Metabolism of fatty acids and cholesterol rely on the same enzyme isocitrate lyase (Icl1) that performs dual function. It is an enzyme of the glyoxylate shunt that is used by Mtb during energy generation from fatty acids, and also functions in methylcitrate cycle that converts cholesterol breakdown products into succinate and pyruvate for incorporation into the TCA cycle (McKinney et al., 2000; Muñoz-Elías et al., 2006). Both fatty acids and cholesterol are required for synthesis of important virulence factors, such as phthiocerol dimycocerosates (PDIM), and various trehalose esters (sulfolipid-1 and polyacyltrehaloses) (Rainwater & Kolattukudy, 1982; Cox et al., 1999; Beatty et al., 2000; Jain et al., 2007; Kaur et al., 2009; Lee, et al., 2013). Additionally, excess of fatty acids can be esterified and stored within Mtb in the form of triacylglycerol (TAG) (Daniel et al., 2011). Induction of TAG synthesis is also triggered by stress conditions, suggesting that this pathway may be used to reduce bacterial growth by diverting fatty acids from the TCA cycle (Baek et al., 2011). Therefore, maintaining a balance of fatty acids and cholesterol within the bacterial cell would be crucial for mycobacterial growth

and adaptation to survival within the host. Here we sought to identify mechanisms employed by Mtb to regulate uptake of these lipids.

Mtb imports fatty acids through the Mce1 transporter, and cholesterol through the Mce4 transporter, which are encoded by the separate *mce1* and *mce4* loci in the Mtb genome. These complexes are comprised of two permease subunits (YrbE's), six cell wall associated Mce proteins, and accessory subunits (Mam).

Function of YrbE and Mce proteins in nutrient transport is predicted based on their homology, however the roles of accessory subunits Mam remain elusive. Mtb contains 5 additional homologues of the accessory proteins, encoded by genes scattered throughout its genome. Recently, it was shown that one of such Mce accessory proteins, OmamA, facilitates cholesterol utilization in Msm and stabilizes the Mce1 complex in Mtb (Perkowski et al., 2016). In the previous chapter we showed that LucA interacts with a number of accessory proteins (including orphaned OmamA and Mce4-associated Mam4B), and that LucA is required for stability of the Mce1 complex. Here we investigated further if these accessory proteins are involved in fatty acid and cholesterol uptake/metabolism. We determined that OmamA and Mam4B are required for certain steps in lipid import, and that they support transport of fatty acids and cholesterol, respectively. Moreover, we showed that inability to assimilate fatty acids in the absence of OmamA is achieved through activity of Zn²⁺ metalloprotease Zmp1. Targeted degradation

of specific transporters could serve as a rapid way to switch from intake of one nutrient to another in *Mtb*.

Finally, we investigated inter-regulation of lipid transport at the transcriptional level. Although downregulation of transcription of the *mce1* operon was shown during macrophage infection (Casali et al., 2006), the impact of lipid substrates on the control of transcription of this operon has not been studied. We found that cholesterol catabolites downregulate expression of *mce1* genes, representing another link between uptake of cholesterol and fatty acids.

Materials and Methods

Bacteria and growth conditions

M. tuberculosis strains were routinely grown at 37°C in 7H9 (broth) or 7H11 (agar) media supplemented with OAD enrichment (oleate-albumin-dextrose-NaCl), 0.05% glycerol and 0.05% tyloxapol (broth). AD enrichment consisted of fatty acid free albumin-dextrose-NaCl. Cholesterol (final concentration 100µM) and various fatty acids (final concentration 177µM) were added to the liquid media as tyloxapol:ethanol micelles as described (Lee et al., 2013). Propionate chloride and acetate chloride were added as water solution along with empty tyloxapol:ethanol micelles. Hygromycin 100 µg/ml, kanamycin 25 µg/ml, streptomycin 50 µg/ml, and apramycin 50 µg/ml were used for selection. For *E. coli* selection hygromycin was used at 150 µg/ml.

Strain construction

Mutant strains of Mtb were generated by allelic exchange (Mann et al., 2011) with hygromycin resistance cassette mutant. Allelic exchange was confirmed by sequencing. Strains used in the study are shown in Table 3.1.

qPCR

Mtb was cultured at an initial OD₆₀₀ of 0.1 in 7H9 AD medium in vented standing T-75 tissue culture flasks. After 5 days, cultures were normalized to OD₆₀₀ of 0.7 in 5-8ml using spent medium, and 1,000X stock of lipid was added for 3h. Compounds at concentration of 10X IC₅₀ were spiked in where indicated for 1 hour prior to addition of the lipid. The RNA was extracted and analyzed as previously described (Abramovitch et al., 2011). Housekeeping

gene *sigA* (*rv2703*) encoding sigma factor was used to normalize each sample.

Table 3.1. Strains used in the study

Strain	Location of hygromycin resistance cassette insertion	Background
<i>ΔlucA</i> ::hyg	(283-469 bp) of <i>rv3723</i>	<i>M. tuberculosis</i> Erdman
<i>Δmam4B</i> ::hyg	(1-483 bp) of <i>rv3492c</i>	<i>M. tuberculosis</i> Erdman
<i>Δomama</i> ::hyg	(1-660 bp) of <i>rv0199</i>	<i>M. tuberculosis</i> Erdman
<i>Δzmp1-omama</i> ::hyg	(starting at 1bp) of <i>rv0198c</i> - (ending at 660 bp) of <i>rv0199</i>	<i>M. tuberculosis</i> Erdman
Strain	Genetic features	Background
wild type	pMV306 <i>smyc'</i> :: <i>mCherry</i>	<i>M. tuberculosis</i> Erdman
<i>ΔlucA</i> ::hyg comp	pMV306 <i>hsp60'</i> :: <i>rv3723</i> and <i>smyc'</i> :: <i>mCherry</i>	<i>ΔlucA</i> ::hyg
<i>Δmam4B</i> ::hyg Comp	pMV306 <i>hsp60'</i> :: <i>rv3493c-rv3492c</i>	<i>Δmam4B</i> ::hyg
<i>Δomama</i> ::hyg Comp	pMV306 <i>hsp60'</i> :: <i>rv0199</i>	<i>Δomama</i> ::hyg
wild type (CDC1551, prpD reporter)	pDEA (hygromycin resistance) + <i>prpD'</i> :: <i>GFP</i> + <i>smyc'</i> :: <i>mCherry</i>	<i>M. tuberculosis</i> CDC1551
Tn:: <i>cyp125</i> (CDC1551, prpD reporter)	Mycomar transposon insertion in <i>rv3545c</i> (kanamycin resistance)	wild type (CDC1551, prpD reporter)
Tn:: <i>rv3542c</i> (CDC1551, prpD reporter)	Mycomar transposon insertion in <i>rv3542c</i> (kanamycin resistance)	wild type (CDC1551, prpD reporter)
Tn:: <i>itp2</i> (CDC1551, prpD reporter)	Mycomar transposon insertion in <i>rv3540c</i> (kanamycin resistance)	wild type (CDC1551, prpD reporter)
Tn:: <i>itp2</i> Comp (CDC1551, prpD reporter)	pVV16 + aacC4 (apramycin resistance) + <i>hsp60'</i> :: <i>itp2</i>	Tn:: <i>itp2</i> (CDC1551, prpD reporter)

Transcriptional profiling

Bacteria were cultured as described for qPCR. Bacterial RNA was isolated, amplified, dye labeled, and hybridized to the microarray as described (Rohde et al., 2007; Liu et al., 2016).

Lipid uptake assays

Mtb cultures were pre-grown in 7H9 AD for 5 days. Then, the cultures were normalized to OD₆₀₀ of 0.7 in 8ml using spent medium, and 1,000X stock of lipid was spiked in for 3 hours (where indicated). In case of itaconic acid treatment, bacteria were pre-incubated with 2mM of this Icl1 inhibitor 1 hour prior to lipid addition. Then 0.2 μCi of radiolabeled substrate ([4-¹⁴C]-cholesterol, [¹⁴C(U)]-palmitate, or [1-¹⁴C]-oleate) was added to bacteria. 1.5 ml

cultures were collected by centrifugation after 5, 30, 60 and 120 min of incubation at 37°C. Each bacterial pellet was washed thrice in 1 ml of ice-cold wash buffer (0.1% Fatty acid free-BSA and 0.1% Triton X-100 in PBS) and fixed in 0.2 ml of 4% PFA for 1h. The total amount of radioactive label associated with the fixed pellet was quantified by scintillation counting. The radioactive signal was normalized to the relative levels of bacterial growth, i.e. to the OD₆₀₀ of the bacterial cultures before addition of radioactive label. The uptake rate was calculated by applying linear regression to the normalized radioactive counts over time, and uptake efficiency was expressed as a ratio of uptake rate for each strain/treatment relative to the wild type control/no treatment.

Radiorespirometry assays

Lipid oxidation was monitored by quantifying the release of ¹⁴CO₂ from [4-¹⁴C]-cholesterol, and [1-¹⁴C]-oleate by radiorespirometry. Mtb cultures were pre-grown in 7H9 AD for 5 days. Then they were incubated at OD₆₀₀ of 0.7 in 5 ml 7H9 AD spent medium supplemented with 1.0 µCi of radiolabeled substrates in vented standing T-25 tissue culture flasks placed in a sealed air-tight vessel with an open vial containing 0.5 ml 1.0 M NaOH at 37°C. After 5 hours, the NaOH vial was recovered, neutralized with 0.5 ml 1.0 M HCl, and the amount of base soluble Na₂¹⁴CO₃ was quantified by scintillation counting. The radioactive signal was normalized to OD₆₀₀. % CO₂ release was expressed as a ratio of normalized radioactive signal for each strain relative to the wild type control.

Results

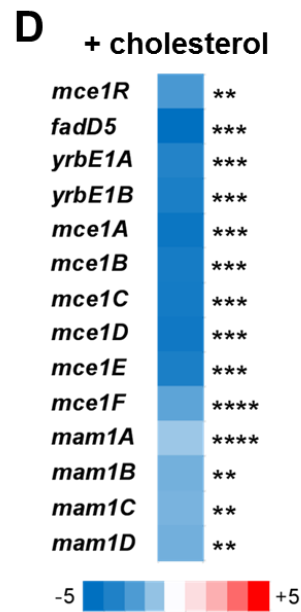
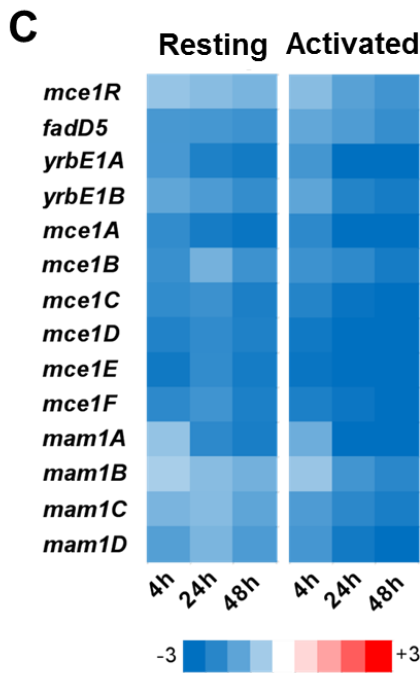
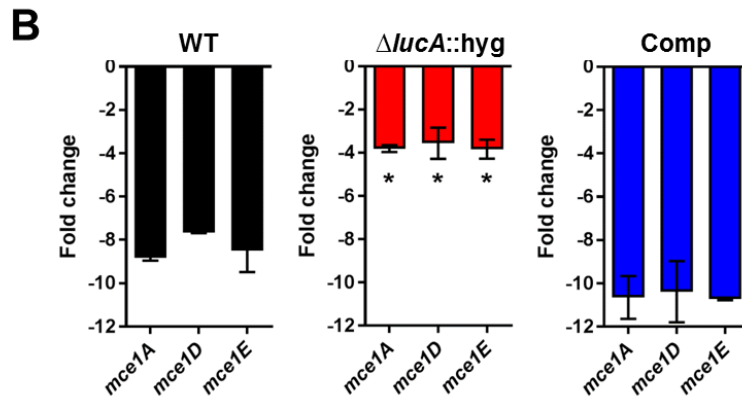
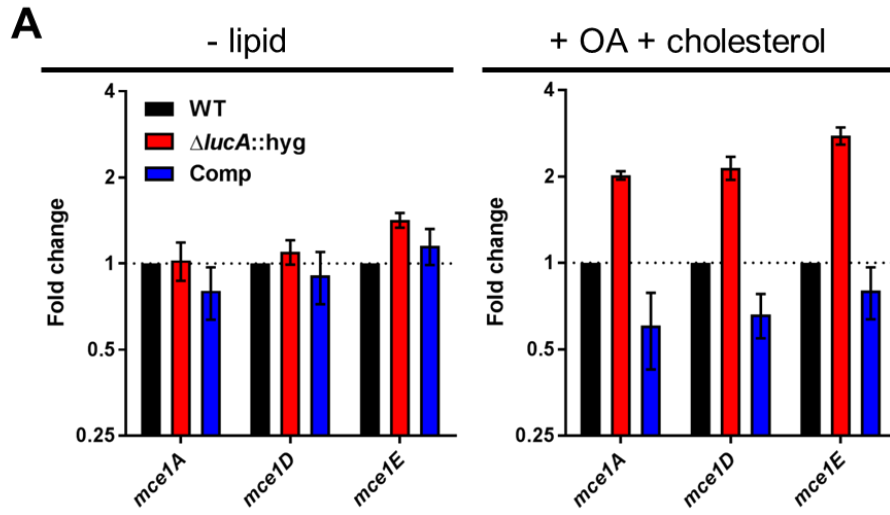
3.1. Cholesterol catabolites regulate transcription of the *mce1* locus.

Cholesterol downregulates transcription of the *mce1* locus.

In the previous chapter we provided evidence that the Mce1 complex functions as a fatty acid transporter. Although the expression profile of *mce1* genes has been studied during the different stages of growth in the regular axenic culture (Kumar et al., 2003), the potential impact of lipid substrates on the transcription of these genes was not investigated.

To address this question, we analyzed the transcriptional response of wild type and $\Delta lucA::hyg$ mutant strains to a mixture of oleate and cholesterol by qPCR. We used the $\Delta lucA::hyg$ mutant as a comparator because of its known defect in transport of these lipids. Relative to wild type and complemented strains, the $\Delta lucA::hyg$ mutant had upregulated levels of *mce1* genes during macrophage infection (Figure 2.2). Since it is believed that macrophages provide both fatty acids and cholesterol to Mtb, it was not surprising that addition of both of these lipids to axenic culture led to a similar phenotype (Figure 3.1. A).

Figure 3.1. Cholesterol negatively regulates expression of the *mce1* operon in wild type Mtb. **A** qPCR quantification of RNA transcripts from indicated bacterial strains pre-grown in 7H9 AD media for 5 days (left), and then incubated with addition of oleic acid (OA) and cholesterol (right) for 3 hours. Fold change was determined by normalizing to the wild type transcript levels. Data are means \pm SD (n = 6). **B** Transcriptional response quantified by qPCR in wild type, $\Delta lucA::hyg$ mutant and complemented strains to addition of oleic acid and cholesterol. Fold change was determined for each strain by normalizing to the transcript levels before addition of the lipids. Data are means \pm SD (n = 6). **C** Transcriptional response of *mce1* operon in wild type Mtb to resting (left) and activated (right) macrophage infection. Data are adapted from (Schnappinger et al., 2003). **D** Transcriptional response to addition of cholesterol quantified by microarray in wild type Mtb. Fold change was determined by normalizing to the transcript levels before addition of cholesterol. Data are means (n = 3).
*p < 0.05, **p < 5×10^{-5} , ***p < 1×10^{-6} , ****p < 0.01 (Student's t test).



When we looked at the transcriptional response of *mce1* genes to cholesterol and oleate for individual strains, we found that the wild type and complemented strains downregulated *mce1*, while the $\Delta lucA::hyg$ mutant was less efficient in this downregulation, consistent with the inability of this strain to import these lipids (Figure 3.1. B). Published data indicate that *mce1* genes are downregulated in wild type Mtb at least during early stages of macrophage infection (Figure 3.1. C) (Schnappinger et al., 2003; Casali, et al., 2006; Homolka, et al., 2010) mimicking response to cholesterol and fatty acids (Figure 3.1. A).

Next we tested if cholesterol alone can impact *mce1* expression. Microarray analysis revealed that all genes in the *mce1* locus were downregulated (up to 6.5 fold) in response to cholesterol (Figure 3.1. D). These results indicate that cholesterol can modulate expression of the Mce1 fatty acid transporter.

Early catabolites of cholesterol downregulate transcription of the *mce1* locus.

We proceeded to identify cholesterol catabolites responsible for regulation of the *mce1* operon. Catabolism of cholesterol in Mtb is an elaborate process that involves breakdown of the i) side chain, ii) A and B rings, and iii) C and D rings (Figure 3.2). The first two steps can happen concurrently (Capyk et al., 2011), but the third one does not begin until the second is complete (Casabon et al., 2013; Wipperman et al., 2014). Early metabolites are known to regulate expression of the core cholesterol metabolism enzymes in the KstR regulon through direct binding to KstR repressor (Figure 3.2). We hypothesized that these early metabolites could also regulate *mce1* expression. To test this hypothesis we analyzed transcription of *mce1* genes (*mce1A*, *mce1D*, *mce1E*) in response to cholesterol in transposon mutants defective in early steps of cholesterol catabolism, i.e. side chain breakdown: Tn::*cyp125*, Tn::*rv3542c* and Tn::*ltp2* (Figure 3.3. A). Cyp125 is a cholest-4-en-3-one 26-monooxygenase, and it catalyzes the very first reaction of side chain metabolism: oxidation to the carboxylic acid. Although exact function of Rv3542c and Ltp2 is not yet assigned, they are believed to be involved in the subsequent steps of the side chain breakdown, which produce one acetate and two propionate molecules (Figure 3.2).

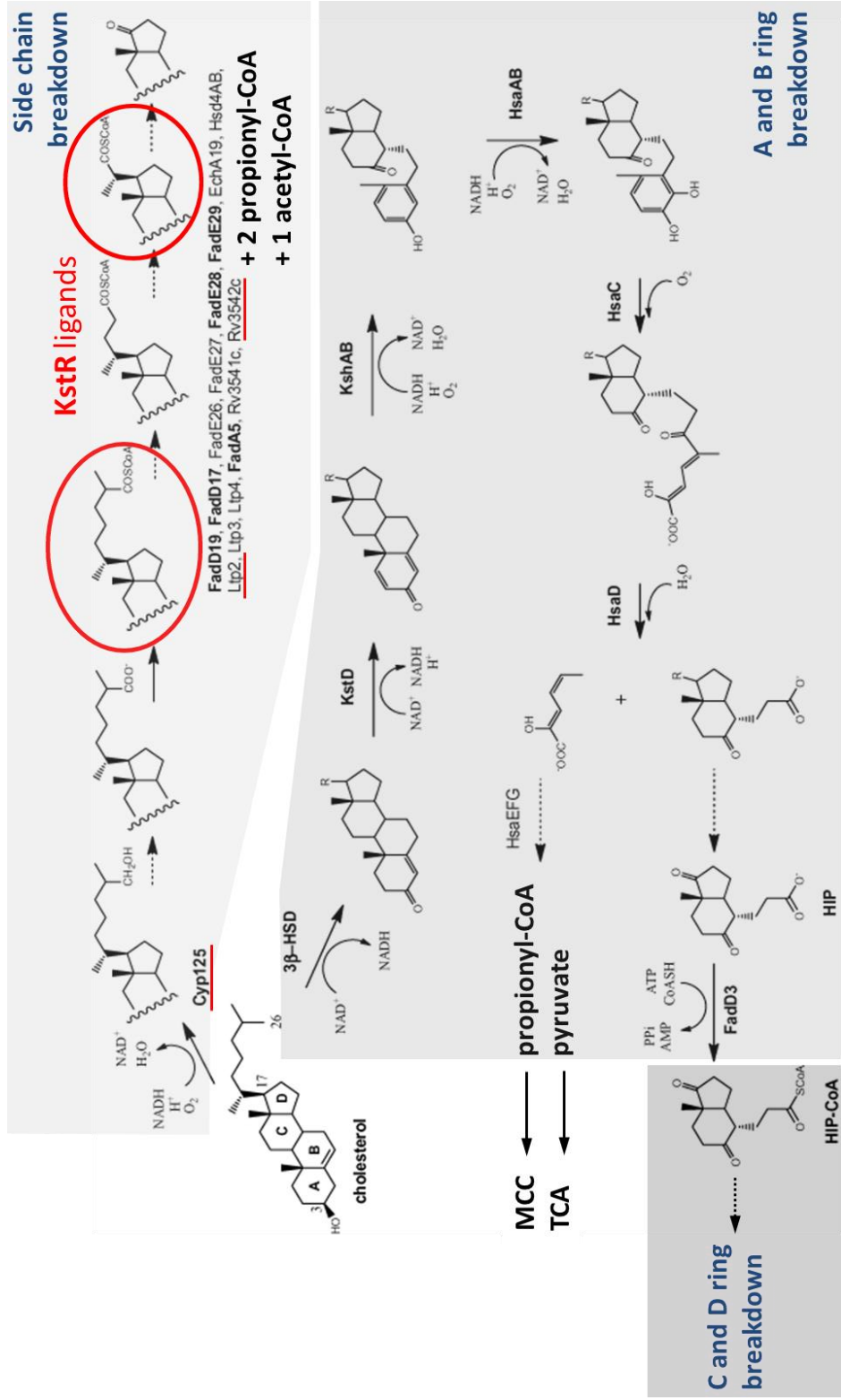


Figure 3.2. Cholesterol catabolic pathway in *Mtb*. Adapted from (Casabon, et al., 2013). Known KstR ligands are circled in red. Genes which inactivation was tested here are underlined in red.

The Tn::*cyp125* mutant did not downregulate *mce1* genes in response to cholesterol (Figure 3.3. A), which demonstrates that the cholesterol metabolite(s) responsible for *mce1* regulation is/are not produced in this mutant. Both Tn::*rv3542c* and Tn::*ltp2* mutants downregulated *mce1* genes to the same extent as the wild type strain. These results indicate that the *mce1*-regulating molecule is produced downstream of Cyp125 but upstream of Rv3542c and Ltp2. Overexpression of Ltp2 in Tn::*ltp2* mutant (Tn::*ltp2* Comp) significantly abolished downregulation of *mce1*, demonstrating that Ltp2 catalyzes reaction that diminishes amounts of the *mce1*-regulating cholesterol metabolite, which is likely to be the cholesterol side chain CoA thioester. Although propionate and acetate are also produced as the result of cholesterol side chain catabolism, only the cholesterol side chain CoA thioester would be used by Ltp2 as a substrate, and not these short chain fatty acids. These results indicate that early cholesterol metabolites such as side chain CoA thioesters are likely candidates in the regulation of the *mce1* gene expression.

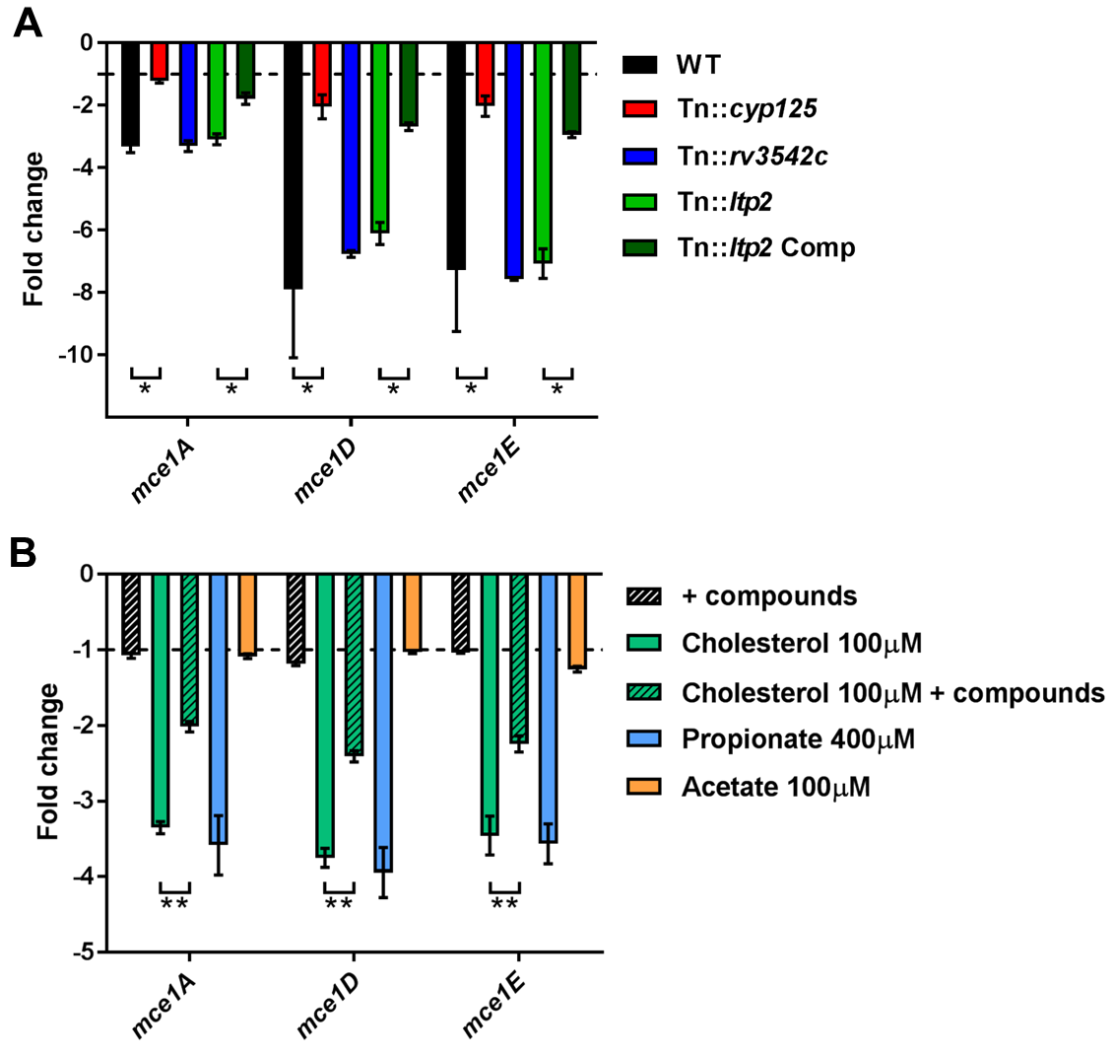


Figure 3.3. Cholesterol metabolites regulate expression of the *mce1* genes. **A** qPCR quantification of RNA transcripts from indicated bacterial strains pre-grown in 7H9 AD media for 5 days, and then incubated with addition of cholesterol, 100 μ M for 3 hours. Transcriptional response to cholesterol (fold change) was determined for each strain by normalizing to the transcript levels before addition of cholesterol. Data are means \pm SEM (n = 4). **B** qPCR quantification of RNA transcripts from wild type Mtb pre-grown in 7H9 AD media for 5 days, and then incubated with addition of indicated carbon sources for 3 hours. Compounds (inhibitors of cholesterol catabolism blocking release of propionate) were added where indicated 1 hour prior to carbon sources. Fold change was determined by normalizing to the transcript levels before addition of compounds or carbon sources. Data are means \pm SEM (n = 4).

*p < 0.05, **p < 0.005 (Student's t test).

Cholesterol breakdown product propionate downregulates transcription of the *mce1* locus.

We showed that a cholesterol side chain CoA thioester but not propionate is most likely responsible for downregulation of *mce1* in Tn::*ltp2* mutant. However Tn::*ltp2* mutant produced only 1 molecule of propionyl-CoA from the side chain, which is substantially lower than the total amount that wild type bacteria experiences if cholesterol metabolism goes to completion. Breakdown of 1 molecule of cholesterol releases 3-5 molecules of propionate: 2 – from the side chain, 1 – from the A and B rings, and up to 2 - from the C and D rings (predicted). To test if propionate derived from cholesterol affects *mce1* transcription, we analyzed *mce1* expression in response to cholesterol when inhibitors of propionate release were added (Figure 3.3. B). These compounds were identified in Dr. VanderVen laboratory to block production of propionate from catabolism of both cholesterol side chain and rings (data not shown). Without cholesterol these propionate release inhibitors did not change *mce1* transcription. However, they did partially abolish *mce1* downregulation in response to cholesterol, suggesting importance of propionate in *mce1* transcription regulation. In support of this, propionate amounts comparable to the ones produced as the result of full cholesterol breakdown, downregulated *mce1* as efficiently as cholesterol (Figure 3.3. B). Acetate had no effect on *mce1* expression. Based on these results we conclude that the cholesterol breakdown product propionate downregulates *mce1* transcription.

3.2. Long chain fatty acids induce an increase in cholesterol uptake by Mtb.

Given that cholesterol metabolites regulate expression of *mce1* genes encoding a fatty acid transporter, we sought to determine if cholesterol can affect fatty acid uptake. We quantified uptake of [1-¹⁴C]-oleic acid and [U-¹⁴C]-palmitic acid by Mtb pre-incubated with cholesterol for 3 hours. Uptake of fatty acids decreased only by ~20% (Figure 3.4. A). This indicates that despite downregulation of *mce1* gene expression, Mtb still imports fatty acids, either by using Mce1 that was produced prior to cholesterol addition or by using a different fatty acid transporter. Surprisingly, when we tested if there is a reverse correlation between cholesterol and fatty acid uptake, we found that oleic acid induced a significant increase in [4-¹⁴C]-cholesterol uptake (Figure 3.4. A).

Fatty acids undergo β -oxidation to release acetyl-CoA that is fed into the TCA and glyoxylate cycles. To distinguish if fatty acid itself or its metabolites impact cholesterol import, we used a known inhibitor of isocitrate lyase (*icl1*) – itaconic acid (Eoh & Rhee, 2014). Itaconic acid did not affect cholesterol uptake (Figure 3.4. B). Additionally, acetate did not induce an increase in cholesterol uptake. It is important to point out that for acetate we used a 9X molar concentration of oleic acid, considering that 1 mole of oleic acid produces 9 moles of acetate. Our results indicate that the signal for cholesterol import is mediated directly by intact fatty acid.

Finally, we wanted to evaluate the structural characteristics of fatty acids that enabled them to regulate cholesterol uptake. For saturated even chain fatty acid, we used palmitate (C16:0); for saturated odd chain fatty acid - margaric acid (C17:0); and for unsaturated even chain fatty acid - oleate (C18:1). All of the fatty acids tested induced a comparable increase in cholesterol uptake (Figure 3.4. C), indicating that saturation and evenness/oddness of fatty acid length are not determining factors in this process.

Overall we can conclude that long chain fatty acids induce an increase in cholesterol uptake.

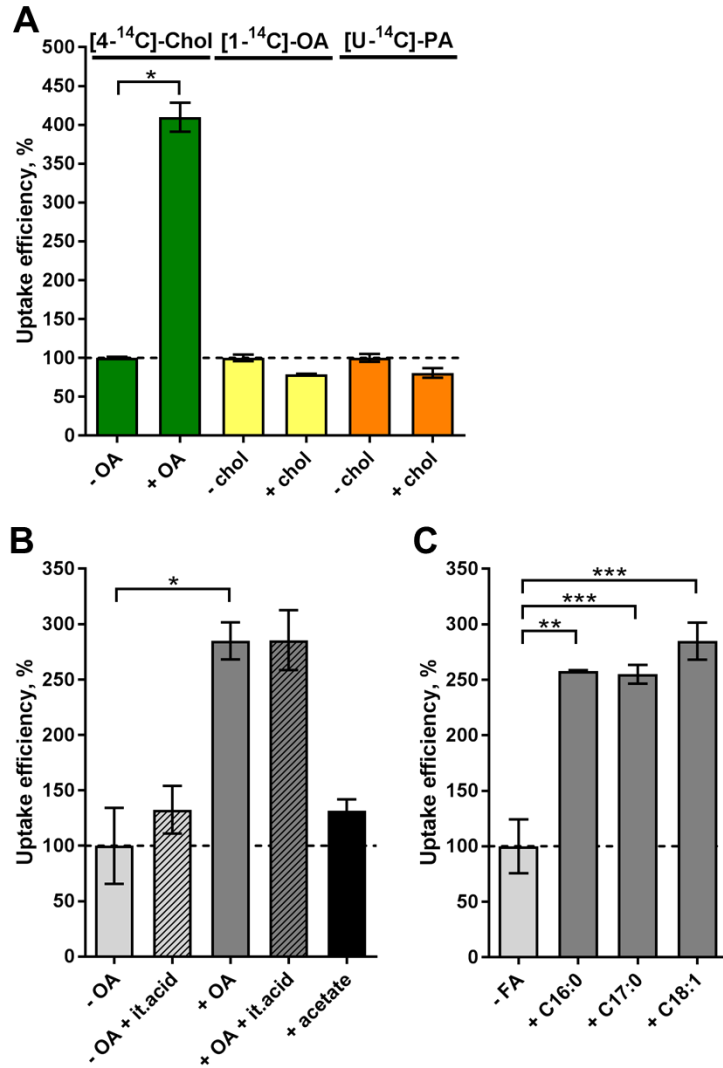


Figure 3.4. Fatty acids induce an increase in cholesterol uptake in Mtb. A

Uptake of [4-¹⁴C]-cholesterol (chol), [1-¹⁴C]-oleic acid (OA), or [U-¹⁴C]-palmitic acid (PA) by wild type Mtb in 7H9 AD 3 hours after addition of indicated lipid (oleic acid, or cholesterol). **B** Uptake of [4-¹⁴C]-cholesterol by wild type Mtb in 7H9 AD pre-incubated with or without itaconic acid 3 hours after addition of indicated lipid (oleic acid, or acetate). **C** Uptake of [4-¹⁴C]-cholesterol by wild type Mtb in 7H9 AD 3 hours after addition of indicated fatty acid (FA) (palmitic acid (C16:0), margaric acid (C17:0), or oleic acid (C18:1)).

Data are means \pm SD ($n \geq 2$).

* $p < 0.05$, ** $p < 0.01$, *** $p < 0.005$ (Student's t test).

3.3. Mce accessory proteins are essential for lipid import in Mtb, likely through protection from activity of specialized proteases.

Our results indicate that despite the ability of cholesterol to downregulate expression of *mce1*, which encodes a fatty acid transporter, uptake of fatty acids was not significantly affected by cholesterol. Alternatively, fatty acids modulate cholesterol uptake, but transcription of the cholesterol transporter-encoding *mce4* was not affected (data not shown). These observations led us to believe that regulation of transporters being used by Mtb might happen post-transcriptionally, even post-translationally. Such hypothesis was supported by the role LucA played in providing stability to subunits of the Mce1 and Mce4 transporters (Chapter 2). Therefore, we performed additional experiments to identify possible mechanisms regulating activity of transporters through their stability.

Mam4B facilitates internalization of cholesterol but not its binding to the bacterial surface.

We showed in a previous chapter that LucA interacts with Mce1 and Mce4-accessory proteins Rv3492c/Mam4B, Rv0177/Mam1C, and Rv0199/OmamA. Perkowski and colleagues reported that deletion of Rv0199/OmamA leads to a marginal defect in cholesterol uptake in Msm (Perkowski et al., 2016), but the role of these accessory proteins in lipid assimilation in Mtb is unknown. To test if Mce4-associated Rv3492c/Mam4B is required for cholesterol import, we inactivated this protein by allelic exchange ($\Delta mam4B::hyg$) and quantified the rate of [4-¹⁴C]-cholesterol uptake in this mutant. We found that relative to the wild type and complemented strains the $\Delta mam4B::hyg$ mutant is still capable of importing [4-¹⁴C]-cholesterol (Figure 3.5. A). Importantly, the $\Delta mam4B::hyg$ mutant has an obvious cholesterol metabolism defect resulting in an ~80% reduction in the mutant's ability to metabolize [4-¹⁴C]-cholesterol (Figure 3.5. B). The phenotype of the $\Delta mam4B::hyg$ strain is specific to cholesterol given that the mutant has no defect in the uptake or metabolism of [1-¹⁴C]-oleate (Figure 3.5. C,D). Our interpretation of these observations is that the Rv3492c/Mam4B mutant binds and/or partly imports cholesterol across the Mtb cell envelope which accounts for the uptake activity that we detect with this strain. Given that cholesterol is likely not metabolized by Mtb until the substrate reaches the bacterial cytosol, we predict that the final translocation of cholesterol across the bacterial cytoplasmic membrane is defective in the $\Delta mam4B::hyg$ mutant and a

blockade at this step prevents subsequent degradation of cholesterol in this strain. Together these data indicate that Rv3492c/Mam4B is required to complete the process of Mce4-mediated cholesterol internalization by Mtb.

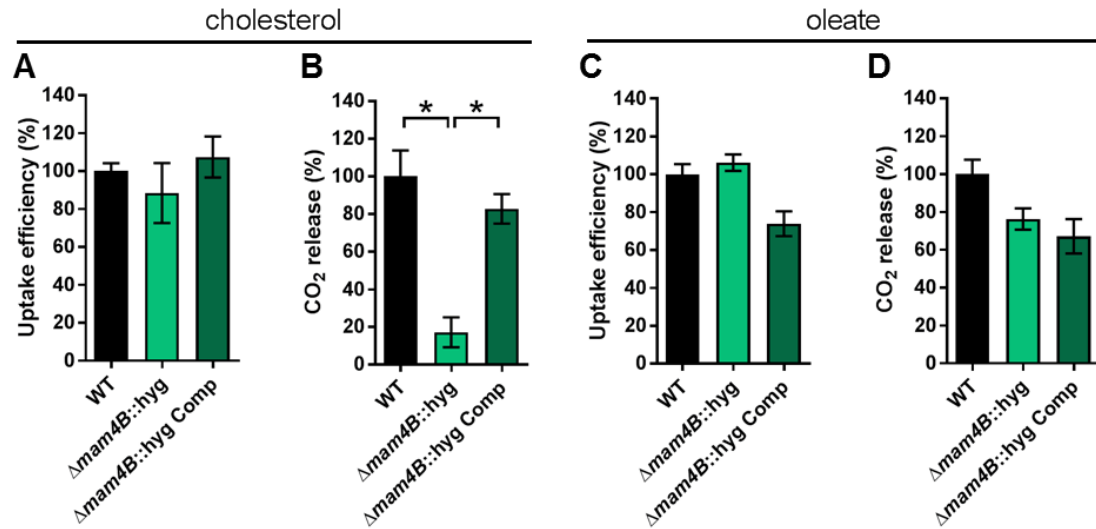


Figure 3.5. Deletion of the Mam4B leads to cholesterol metabolism defect but does not affect cholesterol uptake. A and B Cholesterol import and metabolism by the $\Delta mam4B::hyg$ mutant. Data are means \pm SD (n = 4). **C and D** Oleate import and metabolism by the $\Delta mam4B::hyg$ mutant. Data are means \pm SD (n = 4).

* $p < 0.0001$ (Student's t test).

OmamA facilitates import of fatty acids.

Next we decided to determine the role in lipid assimilation for another Mce accessory protein that interacted with LucA, Rv0199/OmamA. We inactivated Rv0199/OmamA by allelic exchange ($\Delta omamA::hyg$) and quantified the [1- ^{14}C]-oleate uptake rate and metabolism levels in this mutant. We found that relative to the wild type and complemented strains, the $\Delta omamA::hyg$ mutant decreased [1- ^{14}C]-oleate import by ~65%, and metabolism by ~85% (Figure 3.6. A,B). The $\Delta omamA::hyg$ mutant had no significant defect in [4- ^{14}C]-cholesterol uptake or metabolism indicating that Rv0199/OmamA is involved solely in the uptake of fatty acids (Figure 3.6. C,D). Our results demonstrate that OmamA facilitates both initial binding and downstream translocation of oleic acid. This is in contrast to Mam4B, which is required only for the internalization step. We conclude that despite sharing homology, Mce associated proteins perform distinct functions in Mtb, both in terms of substrate specificity, and in terms of steps of import they support.

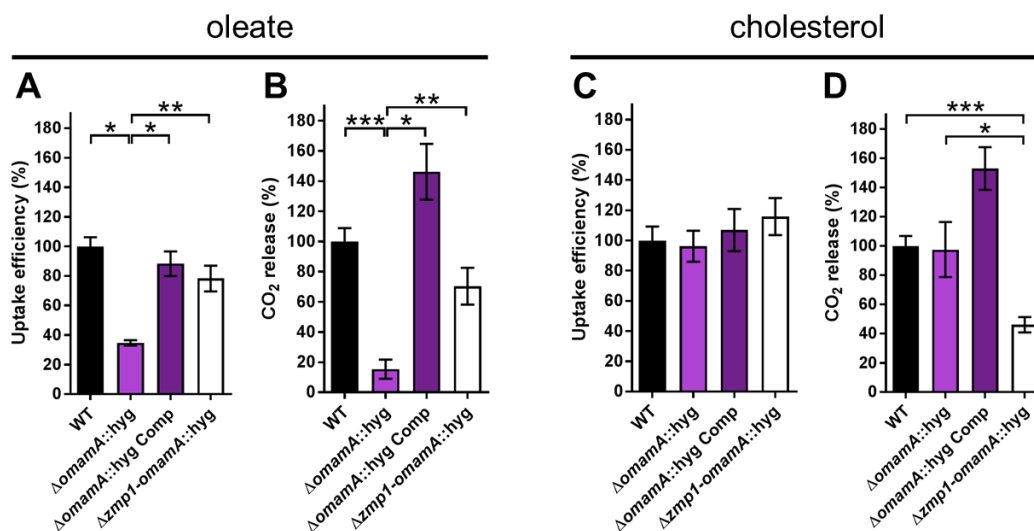


Figure 3.6. Deletion of Zmp1 reverses lipid uptake/metabolism in $\Delta omamA::hyg$. **A** and **B** Oleate import and metabolism by the $\Delta omamA::hyg$ and $\Delta zmp1-omamA::hyg$ mutants. Data are means \pm SD (n \geq 4). **C** and **D** Cholesterol import and metabolism by the $\Delta omamA::hyg$ and $\Delta zmp1-omamA::hyg$ mutants. Data are means \pm SD (n \geq 4).

*p < 0.001, **p < 0.002, ***p < 0.0001 (Student's t test).

Deletion of Zmp1/Rv0198c restores fatty acid uptake in $\Delta omamA::hyg$.

Deletion of Rv0199/OmamA leads to degradation of the putative subunits of the Mce1 complex (Mce1A, Mce1D, Mce1E) despite no change in their transcript levels (Perkowski et al., 2016). Given that Rv0199/OmamA is required for uptake of fatty acids and that Mce1 is a fatty acid transporter, we can attribute inability of $\Delta omamA::hyg$ to import fatty acids to degradation of Mce1 transporter. But we still do not understand the exact function of accessory proteins in this process. There are three possible roles that accessory proteins might play:

- 1) They are involved in transport and assembly of the Mce protein complex;
- 2) They provide support to the complex to maintain its integrity;
- 3) They protect the Mce complex from protease activity (jointly with LucA).

To distinguish the third possibility from the rest, we decided to inactivate the protease that we suspected was responsible for the degradation of the Mce complex in the absence of an accessory protein. If accessory proteins are involved in protection from protease degradation, inactivation of this enzyme has the potential to rescue lipid uptake in the mutant lacking an accessory protein.

To test this hypothesis we focused our attention on the protease encoded by *rv0198c/zmp1*, adjacent to *rv0199/omamA*. Zmp1 is a Zn²⁺ metalloprotease that was shown to be involved in modulation of phagosome

maturation and IL-1 β processing in macrophages (Master et al., 2008; Ferraris et al., 2011; Petrera et al., 2012). We inactivated both Rv0198c/Zmp1 and Rv0199/OmamA by allelic exchange ($\Delta zmp1-omamA::hyg$), and measured uptake and metabolism of [1- ^{14}C]-oleate. Uptake and metabolism of oleic acid was restored in the $\Delta zmp1-omamA::hyg$ mutant to ~70-80% of the wild type (Figure 3.6. A,B). These results indicate that the defect in fatty acid metabolism in the $\Delta omamA::hyg$ mutant resulted from active degradation by the specific protease, Zmp1. If OmamA was involved in transport/assembly of the Mce1 complex or in maintaining integrity of the Mce1 through stabilization of subunit complexes, then inactivation of Zmp1 would not restore uptake, since the transporter would still be nonfunctional. We have preliminary data showing that stability of Mce1 subunits (Mce1A, Mce1D, Mce1E) is restored in the $\Delta zmp1-omamA::hyg$ mutant (data not shown), in support of the proposed role of OmamA as protector from Zmp1 protease activity.

Similarly to the $\Delta omamA::hyg$ mutant, uptake of [4- ^{14}C]-cholesterol was not affected in the $\Delta zmp1-omamA::hyg$ mutant (Figure 3.6. C). However, we detected a ~55% reduction in the $\Delta zmp1-omamA::hyg$ mutant's ability to metabolize [4- ^{14}C]-cholesterol relative to the wild type and $\Delta omamA::hyg$ mutant (Figure 3.6. D). Although we cannot fully explain these results, it is possible that specific proteases (Zmp1) function in combination with accessory proteins (OmamA) to regulate the balance in uptake of these essential lipids in Mtb.

Discussion

While there is a body of evidence suggesting co-regulation of cholesterol and fatty acid metabolism in *Mtb*, data on the mechanisms that link uptake of these lipids are absent. Our current data provides evidence that these lipid substrates can cross-regulate their uptake by modulation of transporter transcription and stability.

We found that intermediates of early cholesterol catabolism (likely cholesterol side chain CoA thioesters) downregulate expression of *mce1* genes, encoding a fatty acid transporter complex Mce1. Propionyl-CoA that is produced when cholesterol is fully catabolized also negatively regulates these genes. We speculate that early cholesterol metabolites modulate *mce1* expression as soon as cholesterol is inside of the bacterial cell, however as metabolism proceeds, propionyl-CoA may also assume this function. We believe that cholesterol might serve as a signal molecule for the lipid-rich environment experienced within the host cell. Downregulation of *mce1* could be used to reduce fatty acid transporter activity to avoid overloading of the bacterial cell with fatty acids, which could have a knock-on effect on bacterial replication and drug tolerance (Garton et al., 2008; Baek et al., 2011; Daniel et al., 2011; Caire-Brändli et al., 2014; Rodríguez et al., 2014). Alternatively, downregulation of *mce1* could coincide with a switch to an unknown alternative transporter to balance fatty acids/cholesterol levels.

The *mce1* operon is transcribed as a 13 gene polycistronic RNA, and it is preceded by *rv0165c/mce1R*, which encodes a transcription factor homologous to the fatty acid metabolism regulating repressor FadR of the

GntR family. In *E coli* binding of a long-chain fatty acid (>14 carbons) CoA thioester to FadR leads to its de-repression (Fujita et al., 2007). In Mtb Mce1R functions as a repressor of the *mce1* operon (Casali et al., 2006), however its effectors are unknown. Our findings indicate that cholesterol metabolites modulate function of this operon, suggesting that they could serve as ligands for Mce1R. It is also possible that other transcription factors capable of binding cholesterol metabolites are involved in regulation of *mce1* (Zeng et al., 2012).

While significant changes in *mce1* transcription were observed, only a slight decrease in fatty acid uptake was caused by cholesterol. However, fatty acids increased cholesterol uptake greatly (3-4 fold) within just 3-5 hours, despite negligible changes in *mce4* transcription. By inhibiting protein synthesis (Chapter 2), we demonstrated that subunits of Mce transporters are stable in wild type Mtb (Figure 2.9. B), therefore effect of *mce* transcription shutdown on uptake of lipids most likely is delayed. Transport activity can be regulated through the activity of proteases, such as the Zn²⁺ metalloprotease Zmp1, to specifically degrade undesirable transport complexes. Function of the Zmp1 protease is dependent on the orphaned Mce accessory protein OmamA. Given the key role of LucA in preserving subunits of Mce transporters, we conclude that LucA interacts with accessory proteins to protect Mce transporters from degradation (Figure 3.7).

Defect in cholesterol metabolism in the mutant lacking both OmamA and Zmp1 suggests the significant role of such proteases in maintaining balance in fatty acid and cholesterol import. In support of the idea that regulation of the lipid import is important for Mtb's pathogenesis, Zmp1 was shown to be required for Mtb infection of macrophages and for survival in mice (Master et al., 2008).

Finally, we found that certain accessory subunits of Mce1 and Mce4 transporters are specific to their substrates, i.e. Mam4B – for cholesterol, and OmamA – for fatty acids. More importantly, these accessory subunits regulate different steps of lipid import. These studies allowed us to determine that transport of cholesterol consists of at least two dissociable events: substrate binding/shuttling across the cell wall followed by the final translocation through the cytoplasmic membrane delivering cholesterol into the cytosol. The accessory subunit of Mce4 likely participates in the final translocation of cholesterol across the cytoplasmic membrane, while orphaned accessory protein OmamA appears to be involved in the binding/shuttling of fatty acids across the Mtb cell envelope.

Overall our data demonstrate that fatty acids and cholesterol inter-regulate import of each other. Metabolites of both of these lipids (acyl-AMP for fatty acids, and propionyl-CoA derived methylmalonyl-CoA for cholesterol) serve as required precursors for synthesis of sulfolipids and PDIM, methyl-branched virulence lipids of Mtb (Jain et al., 2007; Singh et al., 2009; Yang et al., 2009; Griffin et al., 2012; Quadri, 2014). These anabolic pathways are

essential for adaptation of the pathogen to the intracellular environment, where fatty acids derived from macrophages relieve toxicity caused by cholesterol derived propionyl-CoA metabolites (Lee et al., 2013). Regulation of a balance in intracellular levels of cholesterol and fatty acids would ensure optimal metabolism and therefore survival of Mtb during infection. Here we have begun to unravel the mechanisms of this co-regulation. Deeper knowledge of inner-workings of balanced lipid assimilation in Mtb will expand our understanding on how Mtb adapts to the host environment.

Acknowledgments

We thank Brian VanderVen for guidance throughout this project, and also his lab members Christine R Montague, Thuy La for generation of Mtb strains and western blot analysis, and Naman Shah for sharing inhibitors of propionate release from cholesterol. We thank Linda Bennett for excellent technical support and Lu Huang for productive discussions. We also thank Martin Pavelka for the aacC4 apramycin resistance cassette, and Christopher Sassetti for the Mce1 antibodies.

References

- Abramovitch, R. B., Rohde, K. H., Hsu, F. F., & Russell, D. G. (2011). *aprABC*: A *Mycobacterium tuberculosis* complex-specific locus that modulates pH-driven adaptation to the macrophage phagosome. *Molecular Microbiology*, 80, 678–694.
- Baek, S. H., Li, A. H., & Sassetti, C. M. (2011). Metabolic regulation of mycobacterial growth and antibiotic sensitivity. *PLoS Biology*, 9, e1001065.
- Beatty, W. L., Rhoades, E. R., Ullrich, H.-J., Chatterjee, D., Heuser, J. E., & Russell, D. G. (2000). Trafficking and release of mycobacterial lipids from infected macrophages. *Traffic*, 1, 235–247.
- Caire-Brändli, I. B., Papadopoulos, A., Malaga, W., Marais, D., Canaan, S., Thilo, L., & De Chastelliera, C. (2014). Reversible lipid accumulation and associated division arrest of *Mycobacterium avium* in lipoprotein-induced foamy macrophages may resemble key events during latency and reactivation of tuberculosis. *Infection and Immunity*, 82, 476–490.
- Capyk, J. K., Casabon, I., Gruninger, R., Strynadka, N. C., & Eltis, L. D. (2011). Activity of 3-ketosteroid 9 α -hydroxylase (KshAB) indicates cholesterol side chain and ring degradation occur simultaneously in *Mycobacterium tuberculosis*. *Journal of Biological Chemistry*, 286, 40717–40724.
- Casabon, I., Crowe, A. M., Liu, J., & Eltis, L. D. (2013). FadD3 is an acyl-CoA synthetase that initiates catabolism of cholesterol rings C and D in actinobacteria. *Molecular Microbiology*, 87, 269–283.
- Casali, N., White, A. M., & Riley, L. W. (2006). Regulation of the *Mycobacterium tuberculosis mce1* operon. *Journal of Bacteriology*, 188, 441–449.
- Cox, J. S., Chen, B., McNeil, M., & Jacobs, W. R. (1999). Complex lipid determines tissue-specific replication of *Mycobacterium tuberculosis* in mice. *Nature*, 402, 79–83.
- Daniel, J., Maamar, H., Deb, C., Sirakova, T. D., & Kolattukudy, P. E. (2011). *Mycobacterium tuberculosis* uses host triacylglycerol to accumulate lipid droplets and acquires a dormancy-like phenotype in lipid-loaded

macrophages. PLoS Pathogens, 7, e1002093.

Eoh, H., & Rhee, K. Y. (2014). Methylcitrate cycle defines the bactericidal essentiality of isocitrate lyase for survival of *Mycobacterium tuberculosis* on fatty acids. PNAS, 111, 4976–4981.

Ferraris, D. M., Sbardella, D., Petrera, A., Marini, S., Amstutz, B., Coletta, M., ... Rizzi, M. (2011). Crystal structure of mycobacterium tuberculosis zinc-dependent metalloprotease-1 (Zmp1), a metalloprotease involved in pathogenicity. Journal of Biological Chemistry, 286, 32475–32482.

Fujita, Y., Matsuoka, H., & Hirooka, K. (2007). Regulation of fatty acid metabolism in bacteria. Molecular Microbiology, 66, 829-839.

Garton, N. J., Waddell, S. J., Sherratt, A. L., Lee, S. M., Smith, R. J., Senner, C., ... Barer, M. R. (2008). Cytological and transcript analyses reveal fat and lazy persister-like bacilli in tuberculous sputum. PLoS Medicine, 5, 0634–0645.

Griffin, J. E., Pandey, A. K., Gilmore, S. A., Mizrahi, V., McKinney, J. D., Bertozzi, C. R., & Sasseti, C. M. (2012). Cholesterol catabolism by *Mycobacterium tuberculosis* requires transcriptional and metabolic adaptations. Chemistry and Biology, 19, 218–227.

Homolka, S., Niemann, S., Russell, D. G., & Rohde, K. H. (2010). Functional genetic diversity among *Mycobacterium tuberculosis* complex clinical isolates: Delineation of conserved core and lineage-specific transcriptomes during intracellular survival. PLoS Pathogens, 6, 1–17.

Jain, M., Petzold, C. J., Schelle, M. W., Leavell, M. D., Mougous, J. D., Bertozzi, C. R., ... Cox, J. S. (2007). Lipidomics reveals control of *Mycobacterium tuberculosis* virulence lipids via metabolic coupling. Proceedings of the National Academy of Sciences, 104, 5133–5138.

Kaur, D., Guerin, M. E., Skovierová, H., Brennan, P. J., & Jackson, M. (2009). Chapter 2 Biogenesis of the cell wall and other glycoconjugates of *Mycobacterium tuberculosis*. Advances in Applied Microbiology, 69, 23-78.

Kumar, A., Bose, M., & Brahmachari, V. (2003). Analysis of expression profile of mammalian cell entry (*mce*) operons of *Mycobacterium tuberculosis*. Infect Immun, 71, 6083–6087.

Lee, W., VanderVen, B. C., Fahey, R. J., & Russell, D. G. (2013). Intracellular *Mycobacterium tuberculosis* exploits host-derived fatty acids to limit metabolic stress. *Journal of Biological Chemistry*, 288, 6788–6800.

Liu, Y., Tan, S., Huang, L., Abramovitch, R. B., Rohde, K. H., Zimmerman, M. D., ... Russell, D. G. (2016). Immune activation of the host cell induces drug tolerance in *Mycobacterium tuberculosis* both *in vitro* and *in vivo*. *The Journal of Experimental Medicine*, 213, 809–825.

Lovewell, R. R., Sasseti, C. M., & VanderVen, B. C. (2016). Chewing the fat: Lipid metabolism and homeostasis during *M. tuberculosis* infection. *Current Opinion in Microbiology*, 29, 30–36.

Master, S. S., Rampini, S. K., Davis, A. S., Keller, C., Ehlers, S., Springer, B., ... Deretic, V. (2008). *Mycobacterium tuberculosis* prevents inflammasome activation. *Cell Host and Microbe*, 3, 224–232.

McKinney, J. D., Höner zu Bentrup, K., Muñoz-Elías, E. J., Miczak, a, Chen, B., Chan, W. T., ... Russell, D. G. (2000). Persistence of *Mycobacterium tuberculosis* in macrophages and mice requires the glyoxylate shunt enzyme isocitrate lyase. *Nature*, 406, 735–738.

Muñoz-Elías, E. J., Upton, A. M., Cherian, J., & McKinney, J. D. (2006). Role of the methylcitrate cycle in *Mycobacterium tuberculosis* metabolism, intracellular growth, and virulence. *Molecular Microbiology*, 60, 1109–1122.

Perkowski, E. F., Miller, B. K., Mccann, J. R., Sullivan, J. T., Malik, S., Allen, I. C., ... Braunstein, M. (2016). An orphaned Mce-associated membrane protein of *Mycobacterium tuberculosis* is a virulence factor that stabilizes Mce transporters. *Molecular Microbiology*, 100, 90–107.

Petrera, A., Amstutz, B., Gioia, M., Hähnlein, J., Baici, A., Selchow, P., ... Sander, P. (2012). Functional characterization of the *Mycobacterium tuberculosis* zinc metallopeptidase Zmp1 and identification of potential substrates. *Biological Chemistry*, 393, 631–640.

Quadri, L. E. N. (2014). Biosynthesis of mycobacterial lipids by polyketide synthases and beyond. *Critical Reviews in Biochemistry and Molecular Biology*, 49, 179–211.

Rainwater, D. L., & Kolattukudy, P. E. (1982). Isolation and characterization of acyl coenzyme A carboxylases from *Mycobacterium tuberculosis* and *Mycobacterium bovis*, which produce multiple ethyl-branched mycocerosic acids. *Journal of Bacteriology*, 151, 905–911.

Rodríguez, J. G., Hernández, A. C., Helguera-Repetto, C., Ayala, D. A., Guadarrama-Medina, R., Anzóla, J. M., ... Portillo, P. Del. (2014). Global adaptation to a lipid environment triggers the dormancy-related phenotype of *Mycobacterium tuberculosis*. *mBio*, 5, e01125-14.

Rohde, K. H., Abramovitch, R. B., & Russell, D. G. (2007). *Mycobacterium tuberculosis* invasion of macrophages: Linking bacterial gene expression to environmental cues. *Cell Host and Microbe*, 2, 352–364.

Russell, D. G., VanderVen, B. C., Lee, W., Abramovitch, R. B., Kim, M. J., Homolka, S., ... Rohde, K. H. (2010). *Mycobacterium tuberculosis* wears what it eats. *Cell Host and Microbe*, 8, 68-76.

Schnappinger, D., Ehrt, S., Voskuil, M. I., Liu, Y., Mangan, J. A., Monahan, I. M., ... Schoolnik, G. K. (2003). Transcriptional adaptation of *Mycobacterium tuberculosis* within macrophages: Insights into the phagosomal environment. *The Journal of Experimental Medicine*, 198, 693–704.

Singh, A., Crossman, D. K., Mai, D., Guidry, L., Voskuil, M. I., Renfrow, M. B., & Steyn, A. J. C. (2009). *Mycobacterium tuberculosis* WhiB3 maintains redox homeostasis by regulating virulence lipid anabolism to modulate macrophage response. *PLoS Pathogens*, 5, e1000545.

Wipperman, M. F., Sampson, N. S., & Thomas, S. T. (2014). Pathogen roid rage: Cholesterol utilization by *Mycobacterium tuberculosis*. *Critical Reviews in Biochemistry and Molecular Biology*, 49, 269–293.

Yang, X., Nesbitt, N. M., Dubnau, E., Smith, I., & Sampson, N. S. (2009). Cholesterol metabolism increases the metabolic pool of propionate in *Mycobacterium tuberculosis*. *Biochemistry*, 48, 3819–3821.

Zeng, J., Cui, T., & He, Z. G. (2012). A genome-wide regulator-DNA interaction network in the human pathogen *Mycobacterium tuberculosis* H37Rv. *J Proteome Res*, 11, 4682–4692.

CHAPTER 4

**Identification of genes required for fatty acid assimilation by
Mycobacterium tuberculosis during macrophage infection**

Abstract

M. tuberculosis acquires fatty acids and cholesterol from its host during infection. Although assimilation of cholesterol was studied extensively, yet the machinery required for fatty acid intake by mycobacteria has remained enigmatic. In the Chapters 2 and 3 we demonstrated that Mce1 is a fatty acid transporter, and examined regulation of this protein complex. However genetic requirements for assimilation of fatty acids during infection have not yet been studied in an unbiased manner, mostly because the experimental approaches required to address this question had not been developed. Here we describe a novel unbiased approach using fluorescent substrates for the metabolic labeling of a transposon mutant library during macrophage infection. Mutants defective in accumulation of the fluorescent label are sorted and sequenced prior to further characterization of their phenotype through their ability to metabolize lipids in axenic culture. This approach allowed us to isolate mutants unable to assimilate fatty acids in both macrophages and in axenic culture, as well as mutants that were only defective within the host cell environment. This screen identified a number of proteins, including Mce1 subunits and MceG that are essential for fatty acid uptake by Mtb inside of the host.

Introduction

It is believed that one of the key nutrients utilized by Mtb within the host is fatty acids.

First, this pathogen has access to this lipid. Mtb infection results in induction of a foamy phenotype in macrophages (Almeida et al., 2012; Singh et al., 2012), the hallmark of which is accumulation of lipid bodies most likely comprised of triacylglycerols and cholesterol esters. Mtb can acquire fatty acids directly from the macrophage (Lee et al., 2013) or as products of triacylglycerol breakdown (Daniel et al., 2011). Mycobacteria-containing vacuoles can be found fused with these lipid bodies as revealed by electron microscopy, suggesting lipid bodies as a possible route of fatty acid delivery to the pathogen (Peyron et al., 2008; Podinovskaia et al., 2013; Caire-Brändli et al., 2014). In the lungs, Mtb resides in foamy macrophages of granulomas (Hunter et al., 2007; Cáceres et al., 2009) or in the midst of lipids in caseating granulomas (Kim et al., 2010), all of which comprise an excellent source of fatty acids. Importantly, Mtb isolated from mouse lungs had higher preference for metabolism of fatty acids compared to bacteria grown in axenic culture, indicating a metabolic shift towards fatty acids in Mtb *in vivo* (Segal & Bloch, 1956).

Second, Mtb upregulates fatty acid β -oxidation and fatty acid metabolism-related genes in the macrophage, in a mouse model of infection, and in human lung tissue (Schnappinger et al., 2003; Rachman et al., 2006;

Rohde et al., 2007; Fontán et al., 2008; Tailleux et al., 2008; Homolka et al., 2010; Rohde et al., 2012).

Despite all these data supporting utilization of fatty acids by Mtb during infection, very little is known on how Mtb actually imports and degrades fatty acids. As the genome of Mtb is highly enriched for genes predicted to be devoted to β -oxidation (~100) (Cole et al., 1998), assigning of their function absent direct demonstration of phenotype, is problematic. Only recently we started to gain information on specific details relating to enzymes of this pathway (Taylor et al., 2010; Venkatesan & Wierenga, 2013; Srivastava et al., 2015). We described Mce1 as a fatty acid transporter for the first time, and it has been shown that inactivation of Mce1 leads to defect in bacterial growth in mouse infection (Joshi et al., 2006). Here we sought to identify genes involved in the complex processes associated with the uptake and downstream assimilation of carbon from lipid substrates in context of the host.

We developed a forward genetic screen to identify Mtb mutants defective in assimilation of fatty acids during macrophage infection. We metabolically labeled macrophages infected with transposon mutants using fluorescently-tagged palmitate, and flow-sorted bacterial mutants unable to acquire this fatty acid from macrophage. We subsequently analyzed selected mutants for their ability to metabolize fatty acids and cholesterol in axenic culture. This unbiased approach allowed us to identify genes encoding the fatty acid transporter Mce1, Mce accessory subunit OmamB, ATPase MceG,

GTP pyrophosphokinase RelA, Rv2799 and Rv0966c to be required for assimilation of fatty acids inside of the host.

Materials and Methods

Bacteria and growth conditions

M. tuberculosis strains were routinely grown at 37°C in 7H9 (broth) or 7H11 (agar) media supplemented with OAD enrichment (oleate-albumin-dextrose-NaCl), 0.05% glycerol and 0.05% tyloxapol (broth). AD enrichment consisted of fatty acid free albumin-dextrose-NaCl. Hygromycin 100 µg/ml, kanamycin 25 µg/ml, and streptomycin 50 µg/ml were used for selection. For *E. coli* selection hygromycin was used at 150 µg/ml.

Strain construction and transposon screen

Generation of wild type and $\Delta lucA::hyg$ strains constitutively expressing mCherry is described in Chapter 2.

Transposon HiMar (kan^R) mutant library (~2X10⁴ independent mutants) was generated as described (Lee et al., 2013) in a wild type Mtb Erdman with integrated plasmid pDEA43n *smyc::mCherry* (hyg^R). Sorting was performed as described below. Sorted material was plated onto 7H11 OAD agar. Pooled mutants were frozen in 15% glycerol and re-grown in 7H9 OAD before re-infection. Individual mutants were recovered in culture. Chromosomal DNA was isolated and the transposon insertion sites were PCR amplified and sequenced according to (Prod'hom et al., 1998).

Macrophage isolation and culturing

Macrophages were differentiated using bone marrow cells from BALB/c mice (Jackson Laboratories, USA) and maintained in DMEM supplemented with 10% heat inactivated fetal calf serum, 2.0 mM L-glutamine, 1.0 mM

sodium pyruvate, 10% L-cell-conditioned media and antibiotics (100 U/ml penicillin and 100 mg/ml streptomycin) at 37°C and 7.0% CO₂ for 10 days before infection. Media without antibiotics was used for infections with Mtb.

Flow cytometry and sorting.

Bacteria (Tn mutant library or selected strains) were pre-grown in 7H9 OAD media till mid log phase. Murine bone marrow-derived macrophages were seeded into T-75 tissue culture flasks (2×10^7 cells per flask) and infected with Mtb at a MOI of 4:1. 4 flasks were infected with Tn mutant library for the screens. Where indicated, 7958 compound was added at concentration of 10 μ M at the time of infection and left in media for 3 days. After 3 days of infection Bodipy-palmitate (final concentration 9 μ M) conjugated to de-fatted 1% BSA was added to the cells for 1 hour pulse and then chased with cell media for another hour. The infected macrophages were scraped into 15 ml of homogenization buffer (250 mM sucrose, 0.5 mM EGTA, 20 mM HEPES, 0.05% gelatin, pH 7.0) and pelleted by centrifugation at 514xG (1,500 rpm, Beckman Allegra 6KR centrifuge, GH-3.8 rotor), followed by cell lysis by 70 passages through a 25 gauge needle. 5 ml of cell lysate was centrifuged at 146xG (800 rpm) for 10 minutes, supernatant (suspensions of phagosomes) was retained and treated with 0.1% Tween-80 at 4°C for 15 minutes to break-open Mtb containing vacuoles. Isolated bacteria were washed twice in PBS+0.05% tyloxapol, and then in PBS+0.1% Triton X-100+0.1% fatty acid-free BSA. Bacterial suspensions were resuspended in PBS+0.05% tyloxapol and passed through a 25 gauge needle 20 times. Aliquots of these

suspensions were diluted in Basal uptake buffer (Nazarova & Russell, 2017) for flow cytometry analysis or sorting performed on S3™ sorter (Bio-Rad). Data were analyzed using FlowJo (Tree Star, Inc).

Imaging of intracellular lipid inclusions

Confluent monolayers of macrophages in Ibidi eight-well glass-bottom chambers were infected with bacteria at a MOI of 4:1. Extracellular bacteria were removed after 4 hours of infection. Where indicated, 7958 compound was added at concentration of 10 μ M at this time and left in media for 3 days. Infected macrophages were maintained in cell culture medium at 37°C and 7% CO₂ for 3 days. For metabolic labeling Bodipy-palmitate (final concentration 20 μ M) conjugated to 1.0% de-fatted bovine serum albumin (BSA) was pulsed for 30 minutes and chased for a 1-2 hour with fresh media. Live-cell images were acquired as described (Podinovskaia et al., 2013). Post-acquisition, images were analyzed using Volocity (PerkinElmer Life Sciences).

Lipid uptake assays

Mtb was cultured at an initial OD₆₀₀ of 0.1 in 7H9 AD medium in vented standing T-75 tissue culture flasks. After 5 days, cultures were normalized to OD₆₀₀ of 0.7 in 8ml using spent medium, and 0.2 μ Ci of radiolabeled substrates ([4-¹⁴C]-cholesterol, [¹⁴C(U)]-palmitate, or [1-¹⁴C]-oleate) was added to bacteria. After 5, 30, 60 and 120 min of incubation at 37°C 1.5 ml of the bacterial cultures were collected by centrifugation. Each bacterial pellet was washed thrice in 1 ml of ice-cold wash buffer (0.1% Fatty acid free-BSA and 0.1% Triton X-100 in PBS) and fixed in 0.2 ml of 4% PFA for 1h. The total

amount of radioactive label associated with the fixed pellet was quantified by scintillation counting. The radioactive signal was normalized to the relative levels of bacterial growth, i.e. to the OD₆₀₀ of the bacterial cultures before addition of radioactive label. The uptake rate was calculated by applying linear regression to the normalized radioactive counts over time, and uptake efficiency was expressed as a ratio of uptake rate for each strain relative to the wild type control.

Radiorespirometry assays

Mtb cultures were pre-grown in 7H9 AD for 5 days. Then they were incubated at OD₆₀₀ of 0.7 in 5 ml 7H9 AD spent medium supplemented with 1.0 µCi of radiolabeled substrates ([4-¹⁴C]-cholesterol, [¹⁴C(U)]-palmitate, or [1-¹⁴C]-oleate) in vented standing T-25 tissue culture flasks placed in a sealed air-tight vessel with an open vial containing 0.5 ml 1.0 M NaOH at 37°C. After 5 hours, the NaOH vial was recovered, neutralized with 0.5 ml 1.0 M HCl, and the amount of base soluble Na₂¹⁴CO₃ was quantified by scintillation counting. The radioactive signal was normalized to the relative levels of bacterial growth by determining the OD₆₀₀ for the bacterial cultures. % CO₂ release was expressed as a ratio of normalized radioactive signal for each strain relative to the wild type control.

Results

Validation of the proposed genetic screen

To determine which genes are required for Mtb to accumulate fatty acids during macrophage infection, we exploited metabolic labeling with fluorescent Bodipy-palmitate as described in Chapter 2. We have shown that the $\Delta lucA::hyg$ mutant has a significant defect in importation of fatty acids during macrophage infection. To find mutations that would generate defects similar to the $\Delta lucA::hyg$, we infected macrophages with a transposon mutant library constitutively expressing mCherry for three days, pulse labeled with Bodipy-palmitate, isolated bacteria, and sorted mutants with low Bodipy fluorescence.

To validate our experimental platform we infected two sets of macrophages, one with wild type Mtb and another one with the $\Delta lucA::hyg$ mutant, both constitutively expressing mCherry and analyzed them after metabolic labeling and isolation. We gated on the mCherry-positive singlet bacterial population (Figure 4.1. A and B). As expected, the $\Delta lucA::hyg$ mutant had a lower level of Bodipy signal than the wild type strain (Figure 4.1. C). Then we combined these two populations at the ratio of 1:1, and flow-sorted bacteria with low Bodipy signal (Figure 4.1. D). The gates for sorting were drawn so that there would be minimum “contamination” by wild type bacteria (based on Figure 4.1. C). The sorted bacterial population demonstrated ~90% purity (Figure 4.1. E). Equal aliquots of the sorted population were grown on plates with or without hygromycin. The $\Delta lucA::hyg$ mutant is hygromycin-

resistant while the wild type strain is not, which allows us to quantify the specificity of the sort. 98.68% of the colonies were hygromycin-resistant, i.e. represented the $\Delta lucA::hyg$ mutant population. These results demonstrate that the experimental protocol for sorting bacteria unable to take up fluorescent fatty acids during macrophage infection has validity.

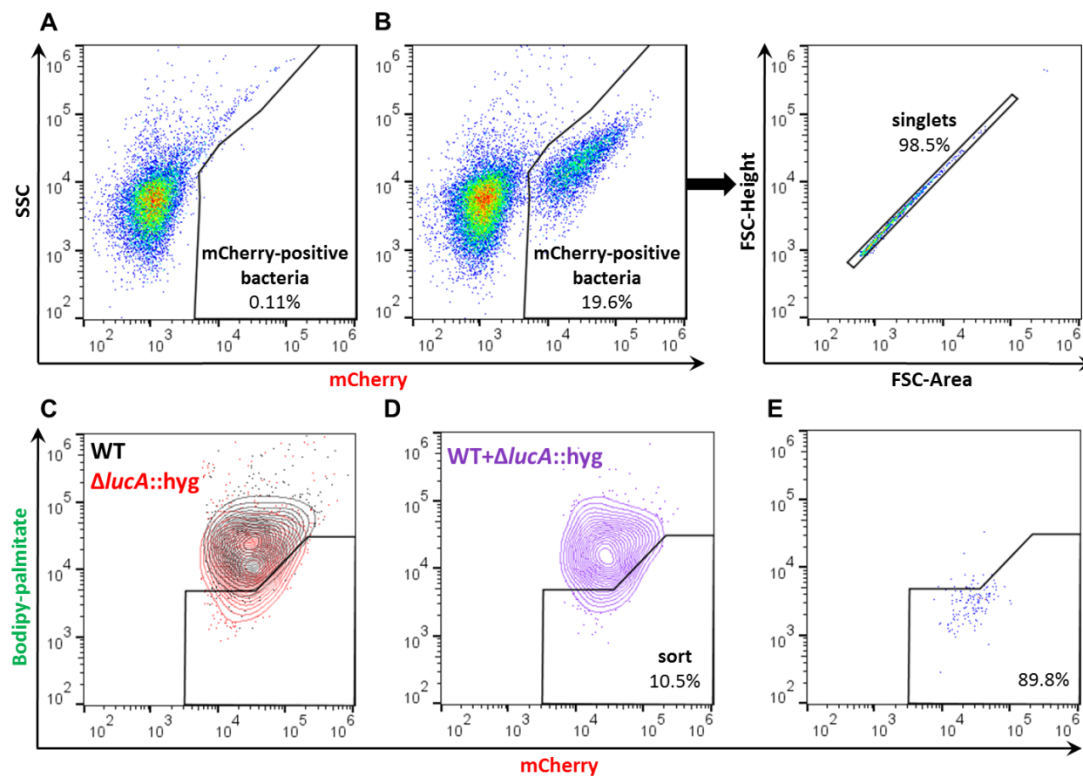


Figure 4.1. Bacterial populations with low Bodipy-palmitate uptake during macrophage infection can be sorted out with high level of purity. Bacteria were isolated from macrophages on the third day of infection after pulse-labeling with Bodipy-palmitate. **A** Flow cytometry analysis of mock bacterial isolate from uninfected macrophages. **B** Gating strategy for sorting out mCherry-positive bacterial population. **C** Flow cytometry analysis of Bodipy-palmitate incorporation by wild type and $\Delta lucA::hyg$ mutant isolated from pulse labeled macrophages. **D** Flow cytometry of combined wild type and $\Delta lucA::hyg$ mutant (1:1) used for sorting of population with low Bodipy-palmitate signal. **E** Purity of sorted low Bodipy-palmitate population.

Two rounds of genetic screen to identify mutants deficient in uptake of fatty acids during macrophage infection

To perform the genetic screen we used a transposon mutant library generated in the wild type Erdman strain, constitutively expressing mCherry from an integrated plasmid. Additionally, we isolated wild type and the $\Delta lucA::hyg$ mutant from labeled macrophages to determine the gate for sorting out bacteria with low Bodipy-palmitate signal (Figure 4.2. A). 10^5 clones were sorted out and plated, however, only $\sim 1.28 \times 10^4$ gave rise to colonies. 9 randomly selected clones were tested by microscopy to assess the exhibited defect in uptake of Bodipy-palmitate during macrophage infection. One clone with a transposon insertion in the *cpsA* gene was strongly negative (Table 4.1, Figure 4.2. C), and this phenotype was also verified by flow cytometry (Figure 4.2. B). CpsA (capsular polysaccharide biosynthesis) belongs to LytR-CpsA-Psr family of proteins that play an important role in bacterial cell wall/capsule synthesis. In *Mycobacterium marinum* CpsA participates in cell wall assembly, and inactivation of CpsA leads to a decrease in the content of mycobacterial cell wall polysaccharide arabinogalactan (Wang et al., 2015). CpsA and Lcp1, another member of this protein family are required for ligation of arabinogalactan to peptidoglycan in Mtb (Grzegorzewicz et al., 2016; Harrison et al., 2016). Therefore, we concluded that inability to take up fatty acids by this mutant during macrophage infection is most likely caused by perturbed integrity of the mycobacterial cell wall and is not directly linked to the fatty acid uptake machinery or its regulation.

In support of these observations with randomly selected mutants, we found that pooled sorted material were heterogeneous with respect to Bodipy-palmitate uptake (Figure 4.2. C), suggesting that only a fraction of this population had a specific defect in fatty acid uptake during macrophage infection. Thus, we decided to perform the second round of mutant selection (Figure 4.2. D). We again used wild type and $\Delta lucA::hyg$ mutant strains as controls for drawing the sorting gate. We also compared mutants pooled in the first round with the original input mutant library, and noted an enrichment for mutants with low Bodipy-palmitate signal (Figure 4.2. D). From the second round of enrichment, we collected 10^5 clones, and $\sim 5.3 \times 10^4$ of them were able to grow on the agar plates. We noted a significant decrease in the Bodipy-palmitate signal with each step of the sort, indicating increasing purity of the sorted pools (Figure 4.3).

Figure 4.2. Two rounds of genetic screen to identify mutants deficient in uptake of fatty acids during macrophage infection. **A** Left, Flow cytometry of Bodipy-palmitate incorporation by wild type and $\Delta lucA::hyg$ mutant isolated from pulse labeled macrophages. These data were used to determine the gate for the sorting. Right, Flow cytometry of transposon mutant library for sorting of population with low Bodipy-palmitate signal. **B** Flow cytometry analysis of Bodipy-palmitate incorporation by Tn::*cpsA* mutant isolated from the first round of screen. **C** Substantial fraction of mutants isolated in the 1st round of the screen is still capable of accumulating Bodipy-palmitate during macrophage infection. Bodipy-palmitate does not accumulate in Tn::*cpsA* mutant as cytosolic lipid inclusions. Representative confocal images of infected macrophages (red = mCherry Mtb, green = Bodipy-palmitate). Scale bar 5.0 μm . **D** Left, Flow cytometry of Bodipy-palmitate incorporation by wild type and $\Delta lucA::hyg$ mutant isolated from pulse labeled macrophages. These data were used to determine the gate for the second round of sorting. Middle, Flow cytometry of original unsorted transposon mutant library. Right, Flow cytometry of transposon mutant library isolated after first round of screen used for the second round of sorting of population with low Bodipy-palmitate signal.

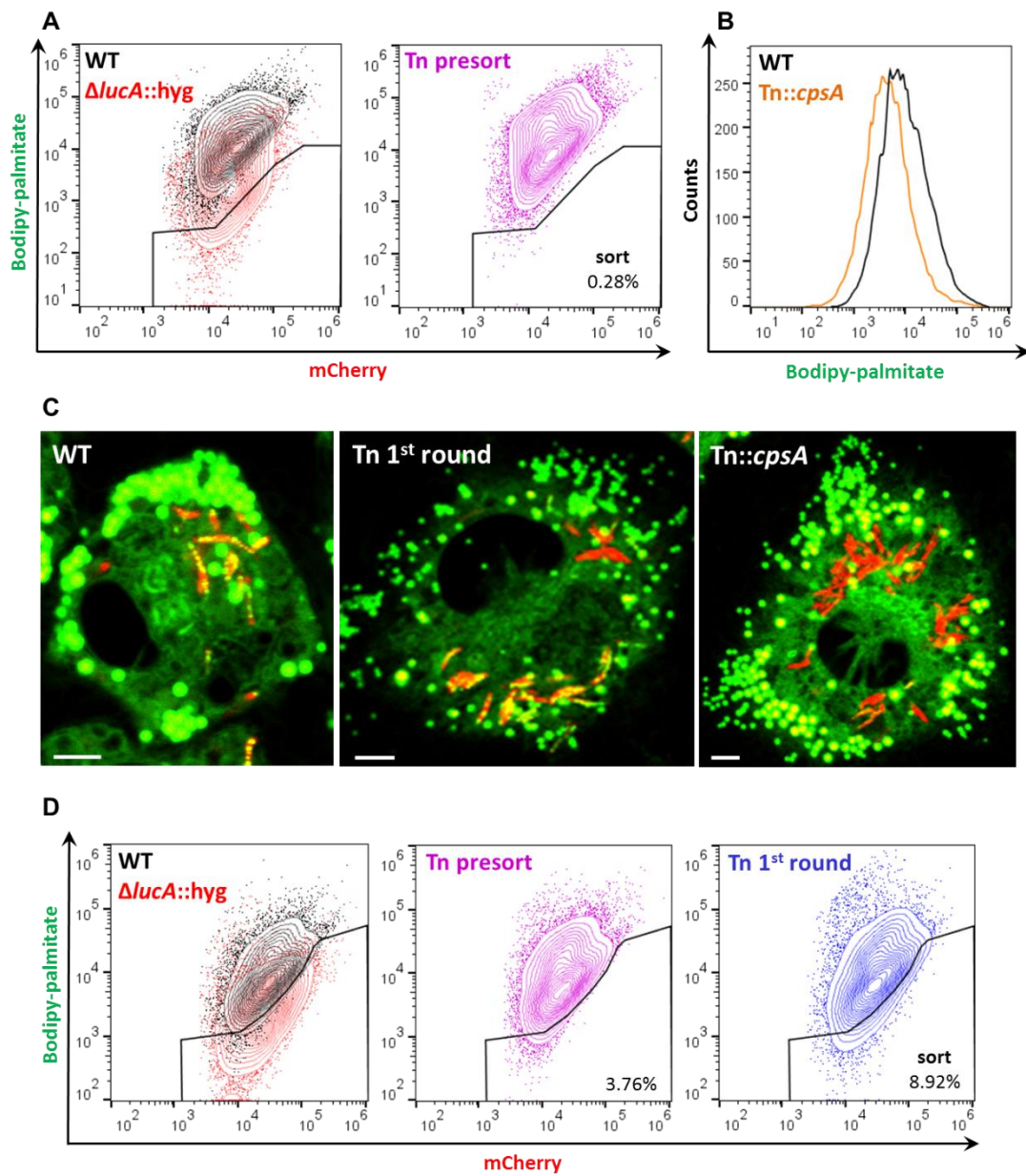


Table 4.1. Randomly selected mutants from the first round of the screen tested for their ability to assimilate Bodipy-palmitate during macrophage infection

Rv name	Common name	Description	Number of mutants *	Positive for Bodipy-palmitate puncta
<i>rv1564c</i>	<i>treX</i>	trehalose biosynthesis	1(1)	Yes
<i>rv1829</i>		Unknown	2(1)	Yes
<i>rv1910c</i>		Unknown	1(1)	Yes
<i>rv2958c</i>		glycosyl transferase, required for resistance to killing by human macrophages	1(1)	Yes
<i>rv3045c</i>	<i>adhC</i>	probable alcohol dehydrogenase, adjacent to <i>fecB</i> - import of Fe ³⁺	1(1)	Yes
<i>rv3329</i>		possibly in promoter of <i>rv3330-dacB1</i> - peptidoglycan synthesis	1(1)	Yes
<i>rv3484</i>	<i>cpsA</i>	bacterial cell wall/capsule synthesis; likely arabinogalactan and peptidoglycan assembly in mycobacteria	2(1)	No
<i>rv3573c</i>	<i>fadE34</i>	adjacent to <i>kstR</i>	1(1)	Yes
<i>rv3865</i>	<i>espF</i>	ESX-1	1(1)	Yes

Highlighted in yellow – mutant negative for Bodipy-palmitate puncta

* the number of independent insertions found in the specific gene is shown in parenthesis

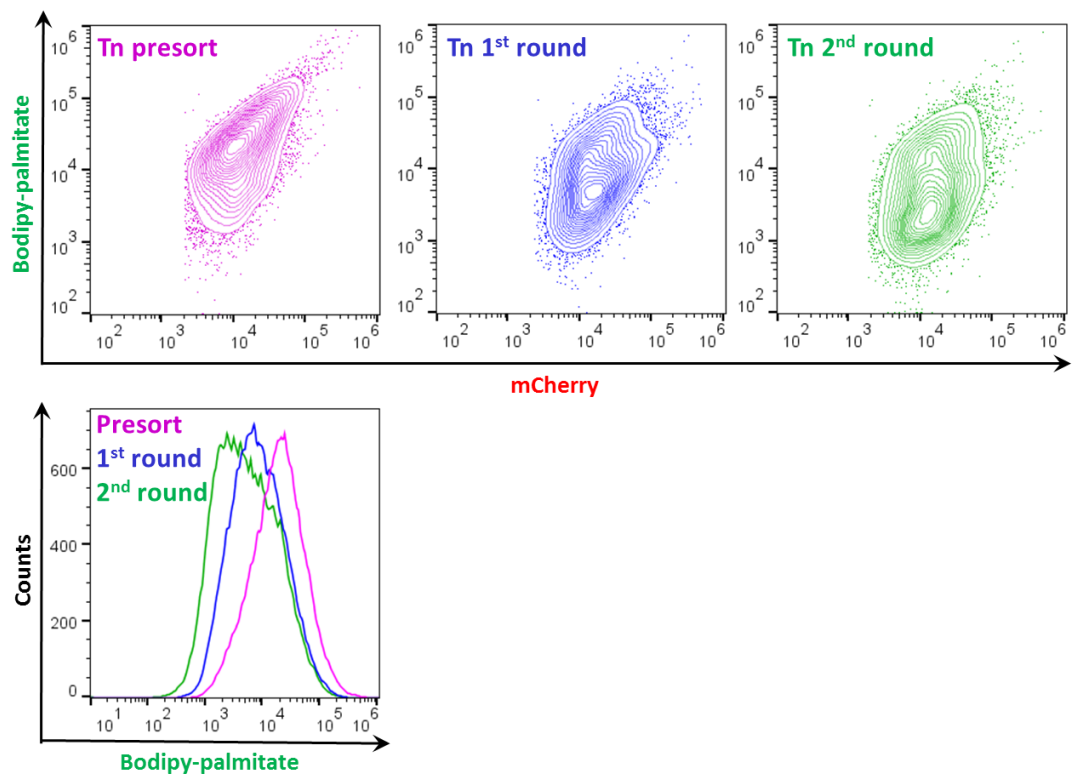


Figure 4.3. Flow cytometry analysis of Bodipy-palmitate incorporation by original unsorted transposon mutant library, transposon mutants purified in the first round of screen, and transposon mutants purified in the second round of screen.

38 and 46 independent clones were sequenced from the first and the second rounds of selection, respectively. The first round library contained only one or two copies of the mutants with the transposon insertion in the same gene, while the second round had multiple copies (Table 4.2). This is another indication of increasing specificity of the mutants with subsequent rounds of selection. Some mutants that were found in the second round were absent from the first one (Table 4.3), which could be explained by low frequency of them in the first round. Most importantly, there were 7 mutants that were found in both rounds, suggesting that the selection process had specificity (Table 4.4).

Table 4.2. Mutants identified in the first round of screen.

Blue font denotes lipid metabolism-related genes. Red font denotes genes of potential interest. % of lipid assimilation are color coded based on their value, where 0% is red, and 100% is blue. * the number of independent insertions found in the specific gene is shown in parenthesis.

Rv name	Common name	Description	Number of mutants *	Microscopy (MΦ): Bodipy-palmitate-positive, %	FACS (MΦ): Bodipy-palmitate signal, %	CO ₂ release (media): [1- ¹⁴ C]-oleate, %	CO ₂ release (media): [4- ¹⁴ C]-cholesterol, %
<i>rv1176c</i>		adjacent to <i>fadH</i> , <i>fxC</i> (<i>rv1177</i>) - ferredoxin	1(1)	50		99.28±12.77	
<i>rv1552</i>	<i>frdA</i>	fumarate reductase	1(1)	50		118.85±22.83	
<i>rv1847</i>		adjacent to transcriptional regulator <i>bla/R</i>	1(1)	50	67.09	121.55±17.48	
<i>rv3865</i>	<i>espF</i>	ESX-1	1(1)	50	82.26	121.33±18.46	
<i>rv0611c</i>		MT-specific island. <i>rv0613c</i> - similar to pre-protein translocases (<i>secA</i>)	1(1)	67		98.62±3.09	
<i>rv1318c</i>		adenylate cyclase	1(1)	67		89.77±13.43	
<i>rv2390c</i>	<i>omameE</i>	adjacent to <i>rfpD</i> ; orphaned accessory protein for <i>mce</i>	1(1)	67		114.68±19.03	88.04±6.12
before <i>rv2524</i>	<i>fas</i>	fatty acid synthesis	1(1)	67		88.28±11.37	
before <i>rv3860/rv3859c</i>	<i>gltB</i>	before <i>gltB</i> - glutamate synthesis; adjacent to <i>whiB6</i> - transcriptional regulator	1(1)	67		105.51±16.91	
<i>rv0612</i>		MT-specific island. <i>rv0613c</i> - similar to pre-protein translocases (<i>secA</i>)	1(1)	75		93.65±4.75	
<i>rv0688</i>		ferredoxin reductase	1(1)	75		105.57±9.40	
<i>rv2933</i>	<i>ppsC</i>	PDIM biosynthesis	1(1)	75		99.80±16.48	
<i>rv1646</i>		adjacent to <i>rv1647</i> - adenylate cyclase	1(1)	100		117.29±23.16	
<i>rv1724c</i>		adjacent to <i>rv1725</i> - possible transcriptional regulator	1(1)	100		112.77±17.41	
<i>rv1829</i>		unknown	2(1)	100		72.65±13.20	
<i>rv3447c</i>	<i>eccC4</i>	membrane <i>eccC4</i> - hydrolyzes ATP/GTP (ESX-4 type VII SS)	1(1)	100		114.18±14.41	
<i>rv3573c</i>	<i>fadE34</i>	adjacent to <i>kstR</i>	1(1)	100		95.24±12.55	

Table 4.2. (Continued)

Rv name	Common name	Description	Number of mutants *	Microscopy (MΦ): Bodipy-palmitate positive, %	FACS (MΦ): Bodipy-palmitate signal, %	CO ₂ release (media): [1- ¹⁴ C]-oleate, %	CO ₂ release (media): [4- ¹⁴ C]-cholesterol, %
<i>rv0101</i>	<i>nrp</i>	peptide/mycobactin synthesis	1(1)				
<i>rv0171</i>	<i>mce1C</i>	Fatty acid transport, <i>mce1</i> subunit	1(1)				
<i>rv0233</i>	<i>nrdB</i>	DNA replication	1(1)				
before <i>rv0500B</i>		unknown	1(1)				
<i>rv1564c</i>	<i>treX</i>	trehalose biosynthesis	1(1)				
<i>rv1910c</i>		Unknown	1(1)				
before <i>rv2190c/rv2191</i>		Unknown	1(1)				
<i>rv2531c</i>		aminoacid synthesis	1(1)				
<i>rv2958c</i>		glycosyl transferase, required for resistance to killing by human macrophages	1(1)				
<i>rv3045c</i>	<i>adhC</i>	probable alcohol dehydrogenase, adjacent to <i>fecB</i> - import of Fe ³⁺	1(1)				
<i>rv3099c</i>		Unknown	1(1)				
<i>rv3329</i>		possibly in promoter of <i>rv3330</i> -(<i>dacB1</i>) - peptidoglycan synthesis	1(1)				

Table 4.3. Mutants identified in the second round of screen.

Blue font denotes lipid metabolism-related genes. Red font denotes genes of potential interest. % of lipid assimilation are color coded based on their value, where 0% is red, and 100% is blue. * the number of independent insertions found in the specific gene is shown in parenthesis.

Rv name	Common name	Description	Number of mutants *	Microscopy (MΦ): Bodipy-palmitate-positive, %	FACS (MΦ): Bodipy-palmitate signal, %	CO ₂ release (media): [1- ¹⁴ C]-oleate, %	CO ₂ release (media): [4- ¹⁴ C]-cholesterol, %
<i>rv0966c</i>		adjacent to <i>cspR</i> - copper sensitive operon repressor	2(2)	0	20.23	41.03±6.23	68.42±2.81
<i>rv1339</i>		adjacent to <i>murI</i> - peptidoglycan synthesis	8(5)	20		100.93±14.91	
before <i>rv1127c</i>	<i>ppdK</i>	pyruvate di-kinase (pyruvate to gluconeogenesis)	1(1)	33		120.49±19.81	80.93±9.48
<i>rv2585c</i>		lipoprotein, close to <i>relA</i> ((PPGPP)-stringent response - close to Sec proteins. apt (AMP), <i>ppjB</i>)	1(1)	33	69.70	83.92±11.68	73.20±8.25
<i>rv3018c</i>		adjacent to <i>esxQ</i> - ESAT-6-like protein	1(1)	33	66.87	79.71±9.02	95.54±4.14
<i>rv0175</i>	<i>mam1A</i>	accessory protein for <i>mce1</i>	1(1)	75	78.98	2.47±0.35	61.63±2.04
before <i>rv3520c/rv3521</i>		KstR-regulon (cholesterol A & B ring degradation)	1(1)	75		71.97±7.74	
<i>rv3867</i>	<i>espH</i>	ESX-1, possibly in promoter of <i>rv3868/ecca1</i>	1(1)	75		117.07±18.07	
<i>rv3500c</i>	<i>yrbE4B</i>	cholesterol transport, <i>mce4</i> permease	1(1)	100	68.98	89.63±22.28	
<i>rv0989c</i>	<i>grcC2</i>	polyprenyl-diphosphate synthase	1(1)				
<i>rv1336</i>	<i>cysM</i>	Cystein synthase B - possibly in promoter of <i>rv1337</i>	1(1)				
before <i>rv1340</i>	<i>rphA</i>	tRNA modification	1(1)				
before <i>rv2699c/rv2700</i>		unknown	1(1)				
<i>rv2803</i>		close to <i>rv2799</i>	1(1)				
<i>rv3496c</i>	<i>mce4D</i>	cholesterol transport, <i>mce4</i> subunit	2(2)				

Table 4.4. Mutants identified in both first and second rounds of screen
Blue font denotes lipid metabolism-related genes. % of lipid assimilation are color coded based on their value, where 0% is red, and 100% is blue. * the number of independent insertions found in the specific gene is shown in parenthesis.

Rv name	Common name	Description	Number of mutants*			Microscopy (MΦ): Bodipy-palmitate positive, %	FACS (MΦ): Bodipy-palmitate signal, %	CO ₂ release (media): [1- ¹⁴ C]-Oleate, %	CO ₂ release (media): [4- ¹⁴ C]-Cholesterol, %
			1 st round	2 nd round	Total				
<i>rv0655</i>	<i>mceG</i>	ATPase, predicted fatty acid and cholesterol transport	1(1)	5(3)	6(3)	0	4.94	2.69±1.07	7.50±2.71
<i>rv3484</i>	<i>cpsA</i>	bacterial cell wall/capsule synthesis; likely arabinogalactan and peptidoglycan assembly in mycobacteria	2(1)	7(4)	9(4)	0		78.81±7.82	
<i>rv2799</i>		membrane protein, adjacent to <i>rv2800</i> - hydrolase	1(1)	1(1)	2(1)	25	47.95	133.02±21.78	74.64±5.10
<i>rv0172</i>	<i>mce1D</i>	Fatty acid transport, <i>mce1</i> subunit	1(1)	1(1)	2(2)	33	46.32	8.18±2.26	86.23±11.10
<i>rv0200</i>	<i>OmamB</i>	orphaned accessory protein for <i>mce</i>	1(1)	2(1)	3(1)	33	45.84	17.54±0.46	71.71±6.94
<i>rv3497c</i>	<i>mce4C</i>	cholesterol transport, <i>mce4</i> subunit	1(1)	1(1)	2(2)	33	55.66	116.06±18.09	10.39±1.07
<i>rv2583c</i>	<i>relA</i>	(PPGPP)-stringent response - close to Sec proteins, apt (AMP), <i>ppiB</i>	1(1)	5(1)	6(2)	75	32.66	227.09±28.93	109.88±3.27

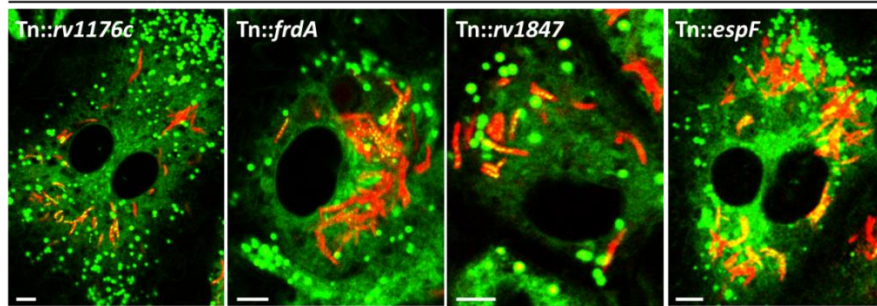
Characterization of lipid metabolism defect in selected mutants

Although there was an obvious enrichment in mutants with low uptake of Bodipy-palmitate with each round of the screen, we still anticipated to find off-target or trivial mutants in each of the pools. To help reduce their number, we selected 38 mutants to test with microscopy (Figure 4.4). We compared amounts of bacteria with Bodipy puncta for each of the mutants to the wild type. We assigned 100% if the amount of bacteria with Bodipy puncta was equal to that of the wild type, and 0% if we couldn't find a single bacterium with Bodipy-puncta. We estimated that 75% of the mutants identified only in the first round of the screen had over half of bacteria positive for Bodipy-palmitate (Table 4.2). For the second round there were 45% of such mutants (Table 4.3), and only 15% - for the mutants identified in both rounds (Table 4.4).

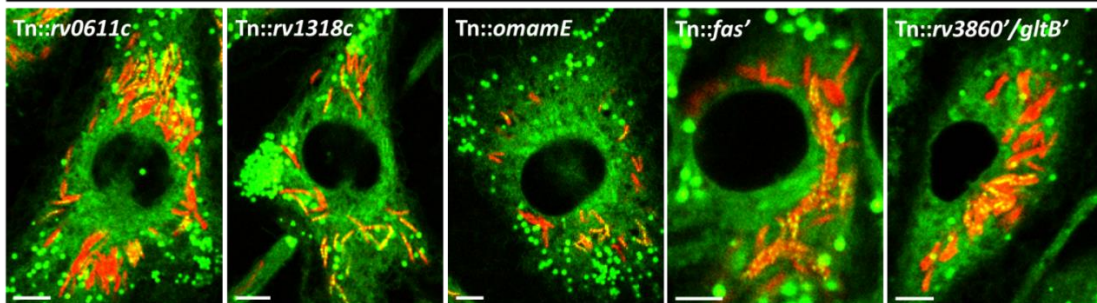
Figure 4.4. Pulse labeling of transposon mutants with Bodipy-palmitate on third day of macrophage infection. Representative confocal images are shown (red = mCherry Mtb, green = Bodipy-palmitate). Scale bar 5.0 μm .

1st round of screen

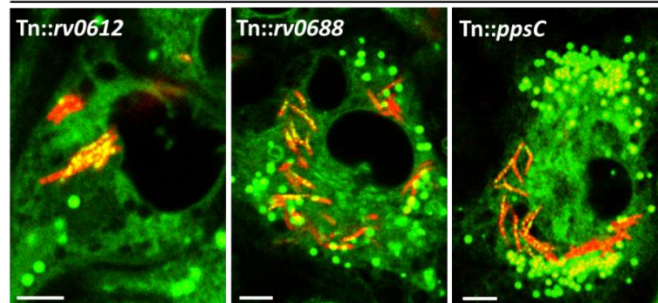
50% BC16-positive



67% BC16-positive



75% BC16-positive



100% BC16-positive

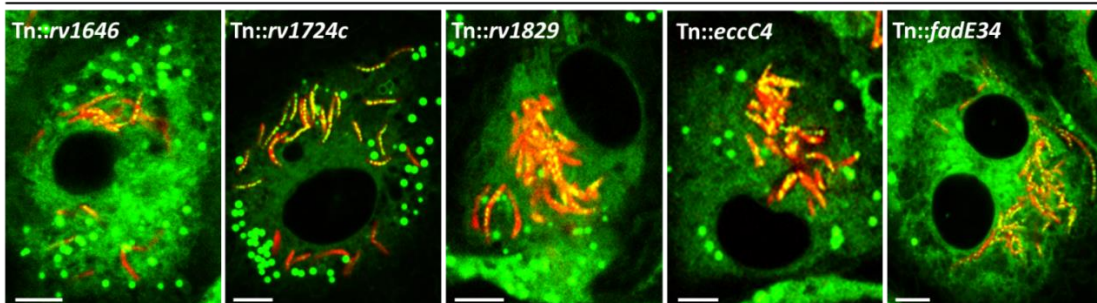
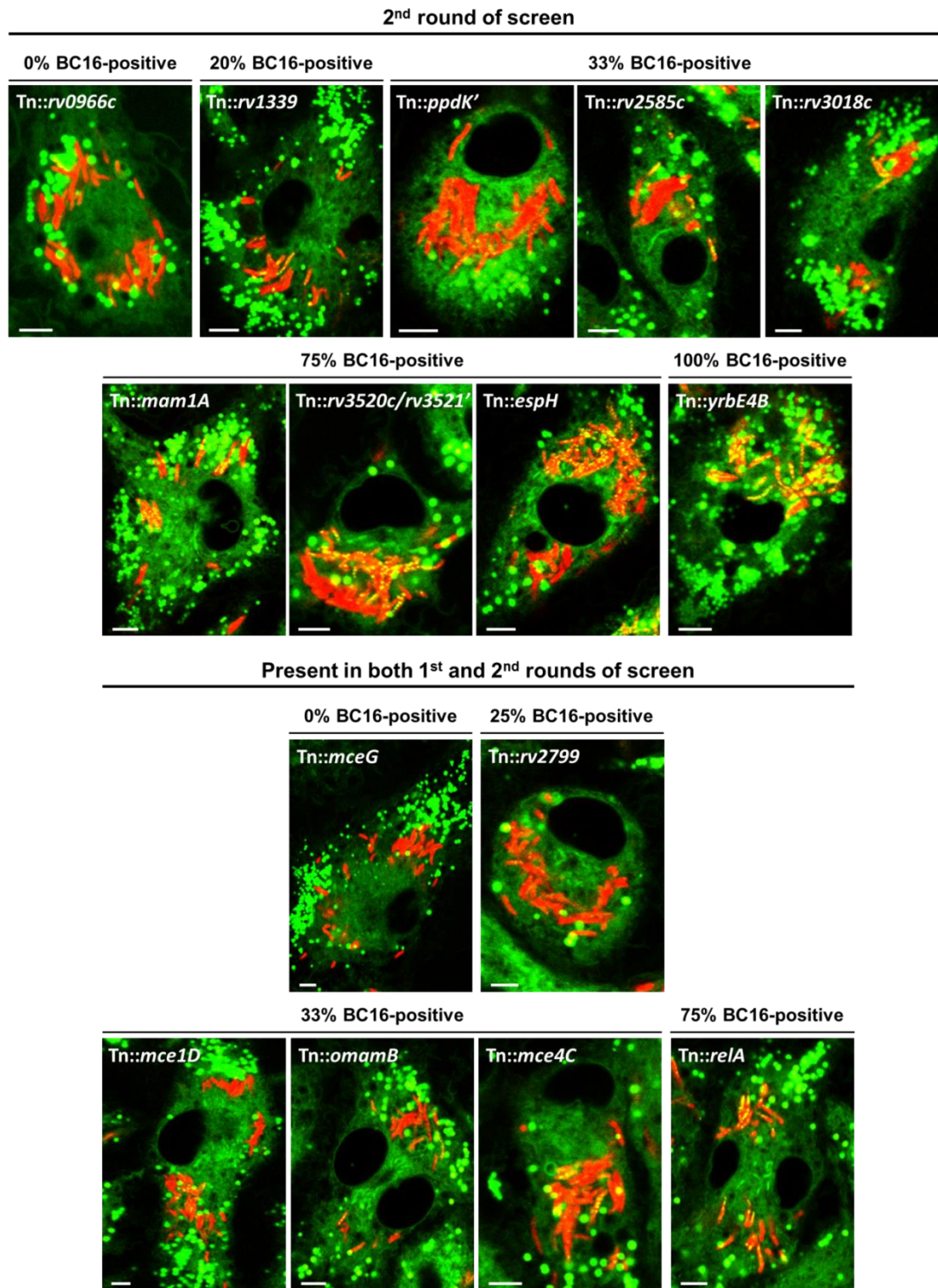


Figure 4.4. (Continued)



To quantify these observations we performed flow cytometry on selected mutants. We used treatment with the 7958 compound as the negative control, since it demonstrated the lowest amount of Bodipy-palmitate uptake compared to the wild type and the $\Delta lucA::hyg$ strains (Figure 4.5 A-B). This 7958 compound is a recently described small molecule that inhibits Mtb growth in macrophages and in media containing cholesterol (Johnson et al., 2017; VanderVen et al., 2015). 7958 also blocks uptake of fatty acids in Mtb when grown in axenic culture (Figure 4.5 C). We quantified mean Bodipy fluorescence for each of the 13 individual mutants tested and normalized it assigning 100% to no treatment and 0% to 7958 treatment (Figure 4.5 D).

Mutants that demonstrated the strongest defect in assimilation of fluorescent fatty acid during macrophage infection can be split in four categories:

- 1) The ones required for maintenance of cell wall integrity (*cpsA*, *rv1339*)
- 2) The ones involved in regulation of metabolism during starvation (*relA*, *ppdK*).
- 3) The ones linked to lipid uptake machinery (*mceG*, *omamB*, *mce1D*, *mce4C*)
- 4) The ones with unknown link to lipid metabolism (*rv0966c*, *rv3018c*, *rv2799*).

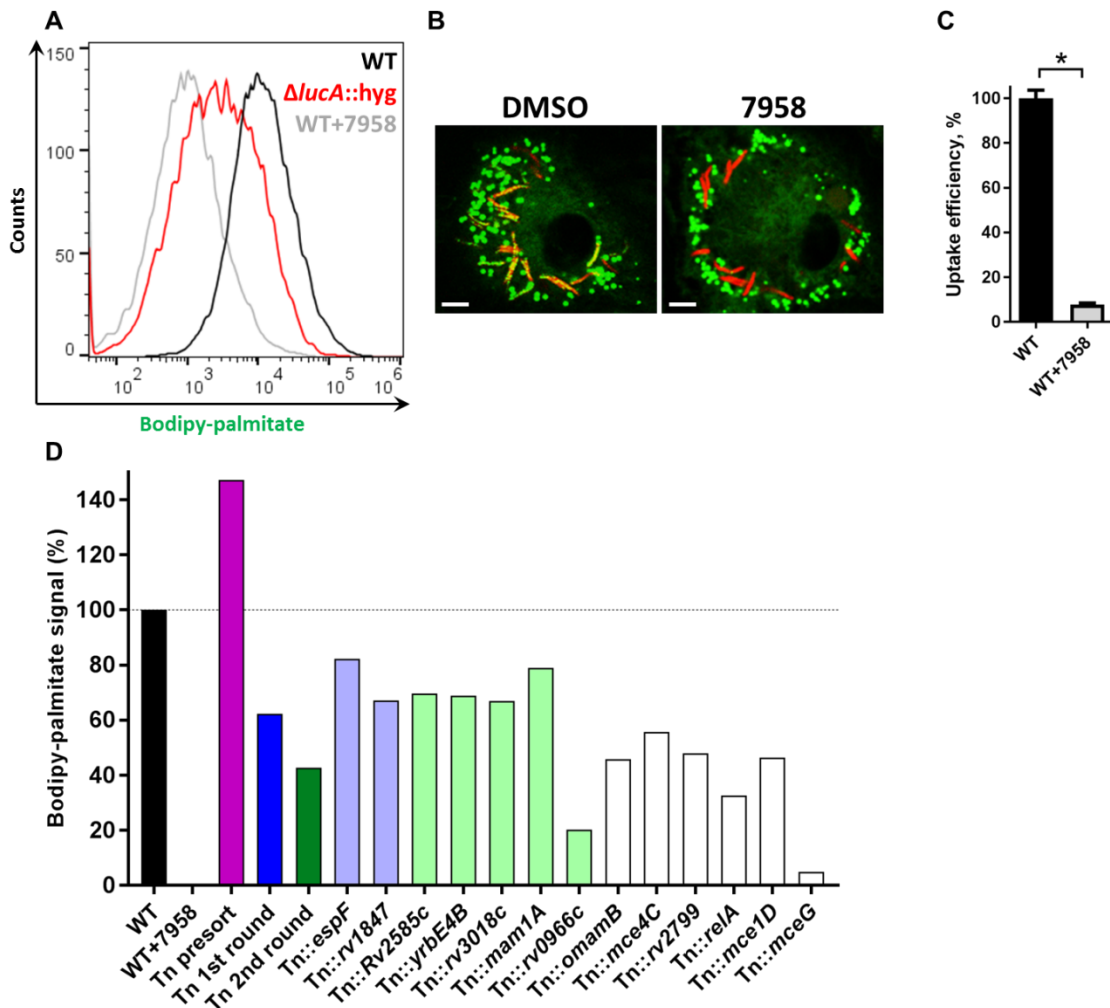


Figure 4.5. Quantification of Bodipy-palmitate uptake by transposon mutants on third day of macrophage infection. **A** Flow cytometry analysis of Bodipy-palmitate incorporation by wild type, $\Delta lucA::hyg$ mutant, and wild type treated with 7958 compound isolated from pulse labeled macrophages. **B** Treatment with 7958 compound abolished Bodipy-palmitate uptake by wild type Mtb during macrophage infection. Representative confocal images are shown (red = mCherry Mtb, green = Bodipy-palmitate). Scale bar 5.0 μ m. **C** Treatment with 7958 compound abolished [$1-^{14}C$]-oleate uptake by wild type Mtb in axenic culture. **D** Flow cytometry quantification of Bodipy-palmitate incorporation by transposon mutants isolated from pulse labeled macrophages. Wild type was taken for 100%, and 7958 treatment for 0%. Tn presort – original transposon library used for the screen; Tn 1st round – pooled mutants identified after the first round of screen; Tn 2nd round – pooled mutants identified after the second round of screen. Pale blue bars – mutants only found in the first round; pale green bars – mutants only found in the second round; white bars – mutants identified in both rounds.

To further characterize the defect in fatty acid uptake in these mutants, we measured fatty acid metabolism in axenic culture by quantifying the catabolic release of $^{14}\text{C-CO}_2$ from [1- ^{14}C]-oleate (Table 4.2-4). This assay allowed us to identify mutants in which a fatty acid uptake defect is not triggered by macrophage environment (Figure 4.6. A). Mutants that had significant defect in fatty acid metabolism even in axenic culture either had transposon insertions in *mce1* operon (*mam1A* and *mce1D*) or in genes encoding proteins possibly linked to it (*omamB* – accessory Mce protein, adjacent to *omamA* – accessory protein stabilizing Mce1 protein complex, *mceG* – shown to be linked to *mce1* in epistasis study (Joshi et al., 2006)). The only exception from this rule was a mutation in *rv0966c*, encoding a protein of unknown function but adjacent to *cspR* – which encodes a copper sensitive operon repressor, which could possibly link copper sensing with fatty acid uptake.

As we have shown earlier a link between cholesterol and fatty acid metabolism, we tested selected mutants with a fatty acid assimilation defect in macrophages (highlighted in two shades of red in Figure 4.6. A) for their ability to metabolize [4- ^{14}C]-cholesterol. We excluded Tn::*cpsA* mutants from this experiment, since its fatty acid intake defect was most likely caused by perturbed integrity of the mycobacterial cell wall. The only mutant impaired in cholesterol metabolism was found to be Tn::*mceG* (Figure 4.6. B).

Overall, we can conclude that the defect of Tn::*mce1D*, Tn::*omamB* and Tn::*rv0966c* mutants in fatty acid acquisition during macrophage infection is

caused by an intrinsic inability to assimilate fatty acids, and the defect of Tn::*mceG* mutant – by inability to assimilate both fatty acids and cholesterol. Contrary, the fatty acid uptake defect in Tn::*rv2799* and Tn::*relA* mutants is triggered by the macrophage environment (Figure 4.6. A).

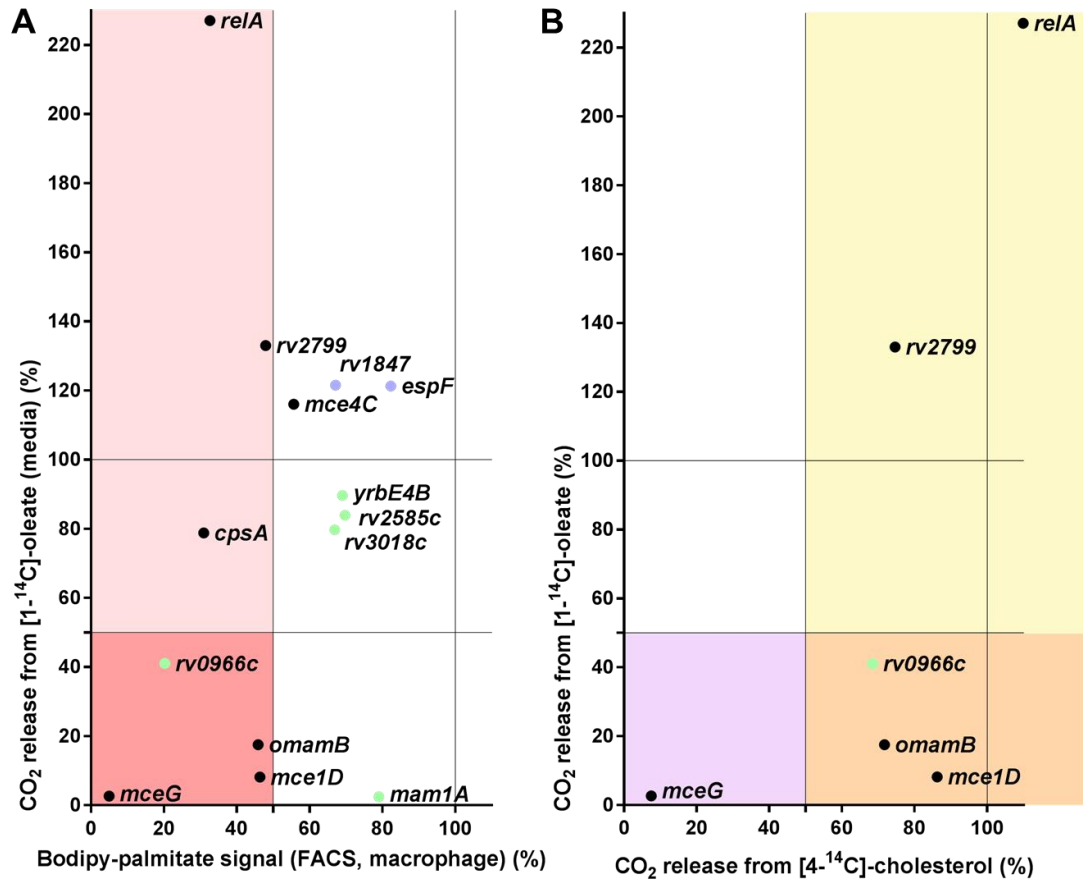


Figure 4.6. Analysis of selected mutants for their ability to metabolize fatty acids and cholesterol. **A** Analysis of selected mutants based on their ability to import Bodipy-palmitate during macrophage infection (quantified by flow cytometry, X axis) and to metabolize [1-¹⁴C]-oleic acid in axenic culture (Y axis). Red shading (both light and dark) – mutants with defect in fatty acid assimilation during macrophage infection. Darker red shading – mutants defective in fatty acid assimilation in macrophages and in fatty acid metabolism in axenic culture. **B** Analysis of mutants (highlighted in two shades of red in panel A) based on their ability to metabolize [4-¹⁴C]-cholesterol (X axis) and [1-¹⁴C]-oleic acid (Y axis) in axenic culture. Yellow and orange shading – mutants with no substantial defect in cholesterol metabolism in axenic culture; where yellow – mutants with no defect, and orange – with defect in fatty acid metabolism in axenic culture. Purple shading – mutants defective in metabolism of both fatty acids and cholesterol in axenic culture. Tables 4.2-4.4 were used to create this figure. Pale blue dots – mutants only found in the first round; pale green dots – mutants only found in the second round; black dots – mutants identified in both rounds.

MceG is required for both fatty acid and cholesterol uptake.

MceG is predicted to be an ATPase that functions in conjunction with both the Mce1 and Mce4 transporters (Joshi et al., 2006). Inactivation of *mceG* leads to a growth defect in media with cholesterol as a single carbon source, similar to *mce4* inactivation. Additionally, MceG was shown to be required for cholesterol metabolism in *Mtb* (Pandey & Sasseti, 2008), and cholesterol uptake in *Msm* (García-Fernández et al., 2017), however the role of MceG in fatty acid assimilation had not been described previously. According to results of our screen, among all the mutants tested *Tn::mceG* demonstrated the strongest defect in fatty acid uptake during macrophage infection. Therefore we decided to test directly if MceG is required for uptake of fatty acids in axenic culture. In parallel with metabolism measurements, we quantified uptake efficiency for this mutant and compared it to the wild type strain. We detected $\geq 90\%$ decrease in fatty acid uptake/metabolism, 75% decrease in cholesterol uptake, and 90% in cholesterol metabolism (Figure 4.7).

Based on these results we conclude that MceG is required for import of both fatty acids and cholesterol. Mce4 is a known cholesterol transporter, and Mce1 was just revealed to be responsible for fatty acid transport. Consistent with genetic interaction of *mceG* with *mce1* and *mce4* loci (Joshi et al., 2006), our results support an idea that MceG functions as an ATPase providing energy for transport of these lipids via Mce1 and Mce4 transporters.

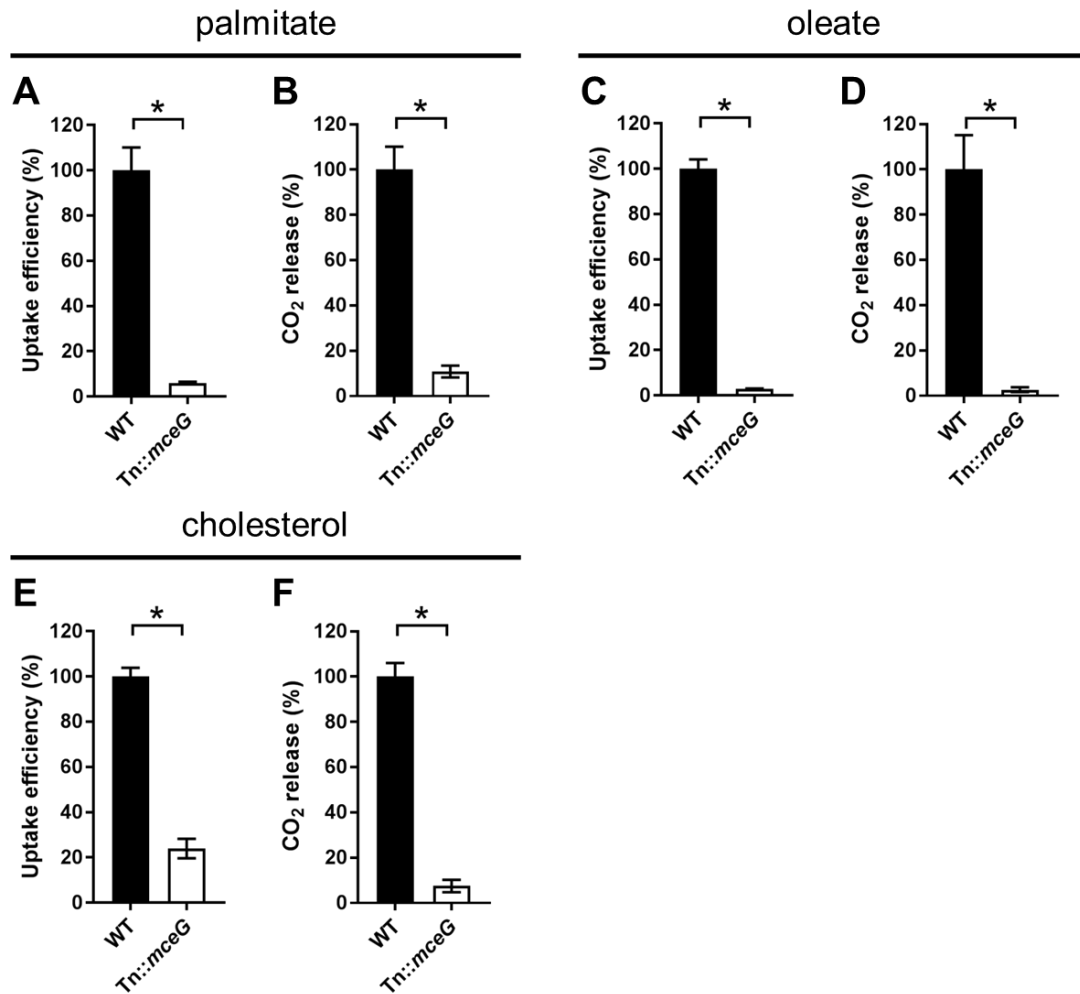


Figure 4.7. Tn::mceG mutant has a significant defect in uptake and metabolism of fatty acids and cholesterol. A and B Palmitate import and metabolism by the Tn::mceG mutant. C and D Oleate import and metabolism by the Tn::mceG mutant. E and F Cholesterol import and metabolism by the Tn::mceG mutant.

Data are means \pm SD (n = 4). *p < 0.0001 (Student's t test)

Discussion

While a substantial body of evidence suggests that Mtb relies on the utilization of fatty acids inside its host, the genetic requirements for this process remain largely uncharacterized. We used an unbiased genetic screen to identify some of the key players in this process.

We employed metabolic labeling of a transposon mutant library during macrophage infection using fluorescently labeled fatty acid – Bodipy-palmitate. To assess if any fatty acid uptake defect is host-dependent we also quantified fatty acid metabolism of individual mutants in axenic culture. We found that Tn::*mceG*, Tn::*mce1D*, Tn::*omamB* and Tn::*rv0966c* are deficient in fatty acid assimilation regardless of their surroundings, while fatty acid uptake defect in Tn::*rv2799* and Tn::*relA* mutants is triggered by the intra-macrophage environment.

We show for the first time that MceG is required for fatty acid assimilation during macrophage infection and in axenic culture, which supports the proposed function for this protein as a putative ATPase providing energy for both Mce1 and Mce4 transporter function. Tn::*mceG* mutant was among the most abundant in our screen, and it had one of the strongest defects in lipid uptake and metabolism, supporting its essential role in these processes.

We did determine earlier that Mce1 is a fatty acid transporter in Mtb, but we did not know if it performs this function inside of the host. Our results indicate that a subunit of Mce1 complex, Mce1D, is required for fatty acid transport in Mtb during macrophage infection. Another Mce-related protein

identified in our screen, OmamB, is an orphaned Mce accessory subunit encoded by a gene adjacent to *omamA*. OmamA is a Mce accessory subunit, required for protection of Mce1 from degradation by the protease Zmp1. It is highly likely that OmamB and OmamA are working jointly to stabilize Mce1, and therefore deletion of OmamB results in inactivation of fatty acid transport. We conclude that Mce1 is the main fatty acid transporter for Mtb at the early stage of macrophage infection.

We found that Rv0966c, previously unlinked to lipid metabolism, is required for assimilation of fatty acids in Mtb both in macrophages and in axenic culture. The *rv0966c* is adjacent to *cspR* encoding a copper sensitive operon repressor, inferring a possible link between copper sensing and fatty acid uptake. Importance of this gene is supported by high expression of the locus including *cspR* and *rv0966c* in Mtb in the mouse infection model (Talaat et al., 2007). Interestingly, a locus containing putative fatty acid metabolism genes *rv0971c-rv0975c* is located adjacently downstream, and EchA7 encoded by *rv0971c* is required for mouse infection (Ward et al., 2010).

The Tn::*rv2799* and Tn::*relA* mutants in which fatty acid uptake defect is only triggered by macrophage infection are also of an interest. Unfortunately there is not much known about *rv2799* except that it is adjacent to *rv2800* encoding putative hydrolase. RelA mediates the stringent response to nutrient deprivation by regulating levels of (p)ppGpp (Avarbock et al., 1999). In Mtb it is required for long term survival *in vitro* and *in vivo*, however deletion of RelA has no effect on Mtb growth during short term macrophage infections (Primm

et al., 2000; Dahl et al., 2003; Klinkenberg et al., 2010; Weiss & Stallings, 2013). Additionally, inactivation of RelA causes downregulation of *mce1*, *mce3* and *mce4* loci in response to starvation (Dahl et al., 2003), indicating that RelA might be implicated in the control of lipid import. Interestingly, our data indicates that inactivation of RelA doubles fatty acid uptake in axenic culture. Obviously, more work needs to be done to determine if RelA regulates lipid transport in the hostile environment of a macrophage.

This screen allowed us to identify numerous genes required for fatty acid acquisition by Mtb during macrophage infection, however, it did have some limitations. We had to validate the phenotype for each of the mutants individually, because of the false Bodipy-palmitate negative clones in our screened pools. This could be explained by the heterogeneous response of Mtb to macrophage infection, which is observed even in the wild type strain.

Although we did recover a few mutants that likely had defects in their cell wall integrity, making them vulnerable to infection, we believe that the majority of clones with mutations in genes essential for infection were eliminated due to their inability to grow on the agar plates after recovery from macrophages. At the same time, it is possible that inactivation of lipid uptake might result in a severe survival defect for Mtb in macrophages, and we missed such mutants. To identify such essential genes, inducible mutants, where genes could be inactivated after bacteria have entered the host, could be used in the future.

This work is the first one addressing a long standing question of how Mtb assimilates fatty acids from the host. Identification of MceG and Mce1 in this screen indicates the prevalent role of these proteins in fatty acid import. It is of interest to learn which transport systems Mtb employs in different cell types, in cells with altered immune status, or at later stages of infection. We believe that the experimental platform developed here can be applied to answer these questions to further evaluate the role of fatty acids in Mtb infection *in vivo*.

Acknowledgments

We thank Brian VanderVen for help with the screen development and for guidance throughout this project, Thuy La for generation of Mtb transposon mutant library, Lu Huang for help with experiments validating phenotypes of the mutants, Christine R Montague for her help with initial development of the screen, and Linda Bennett for excellent technical support.

References

- Almeida, P. E., Carneiro, A. B., Silva, A. R., & Bozza, P. T. (2012). PPAR-gamma expression and function in mycobacterial infection: Roles in lipid metabolism, immunity, and bacterial killing. *PPAR Research.*, 2012, 383829.
- Avarbock, D., Salem, J., Li, L. S., Wang, Z. M., & Rubin, H. (1999). Cloning and characterization of a bifunctional RelA/SpoT homologue from *Mycobacterium tuberculosis*. *Gene*, 233, 261–269.
- Cáceres, N., Tapia, G., Ojanguren, I., Altare, F., Gil, O., Pinto, S., ... Cardona, P. J. (2009). Evolution of foamy macrophages in the pulmonary granulomas of experimental tuberculosis models. *Tuberculosis*, 89, 175–182.
- Caire-Brändli, I. B., Papadopoulos, A., Malaga, W., Marais, D., Canaan, S., Thilo, L., & De Chastelliera, C. (2014). Reversible lipid accumulation and associated division arrest of *Mycobacterium avium* in lipoprotein-induced foamy macrophages may resemble key events during latency and reactivation of tuberculosis. *Infection and Immunity*, 82, 476–490.
- Cole, S. T., Brosch, R., Parkhill, J., Garnier, T., Churcher, C., Harris, D., ... Barrell, B. G. (1998). Deciphering the biology of *Mycobacterium tuberculosis* from the complete genome sequence. *Nature*, 393, 537–544.
- Dahl, J. L., Kraus, C. N., Boshoff, H. I. M., Doan, B., Foley, K., Avarbock, D., ... Barry, C. E. (2003). The role of Rel_{Mtb}-mediated adaptation to stationary phase in long-term persistence of *Mycobacterium tuberculosis* in mice. *Proceedings of the National Academy of Sciences*, 100, 10026–31.
- Daniel, J., Maamar, H., Deb, C., Sirakova, T. D., & Kolattukudy, P. E. (2011). *Mycobacterium tuberculosis* uses host triacylglycerol to accumulate lipid droplets and acquires a dormancy-like phenotype in lipid-loaded macrophages. *PLoS Pathogens*, 7, e1002093.
- Fontán, P., Aris, V., Ghanny, S., Soteropoulos, P., & Smith, I. (2008). Global transcriptional profile of *Mycobacterium tuberculosis* during THP-1 human macrophage infection. *Infection and Immunity*, 76, 717–725.

García-Fernández, J., Papavinasasundaram, K., Galán, B., Sasseti, C. M., & García, J. L. (2017). Unravelling the pleiotropic role of the MceG ATPase in *Mycobacterium smegmatis*. *Environmental Microbiology*, 0, 1–13.

Grzegorzewicz, A. E., De Sousa-D’Auria, C., McNeil, M. R., Huc-Claustre, E., Jones, V., Petit, C., ... Jackson, M. (2016). Assembling of the *Mycobacterium tuberculosis* cell wall core. *Journal of Biological Chemistry*, 291, 18867–18879.

Harrison, J., Lloyd, G., Joe, M., Lowary, T. L., Reynolds, E., Walters-Morgan, H., ... Alderwick, L. J. (2016). Lcp1 is a phosphotransferase responsible for ligating arabinogalactan to peptidoglycan in *Mycobacterium tuberculosis*. *mBio*, 7, e00972-16.

Homolka, S., Niemann, S., Russell, D. G., & Rohde, K. H. (2010). Functional genetic diversity among *Mycobacterium tuberculosis* complex clinical isolates: Delineation of conserved core and lineage-specific transcriptomes during intracellular survival. *PLoS Pathogens*, 6, 1–17.

Hunter, R. L., Jagannath, C., & Actor, J. K. (2007). Pathology of postprimary tuberculosis in humans and mice: Contradiction of long-held beliefs. *Tuberculosis*, 87, 267–278.

Johnson, R. M., Bai, G., DeMott, C. M., Banavali, N. K., Montague, C. R., Moon, C., ... McDonough, K. A. (2017). Chemical activation of adenylyl cyclase Rv1625c inhibits growth of *Mycobacterium tuberculosis* on cholesterol and modulates intramacrophage signaling. *Molecular Microbiology*, 0, 1–15.

Joshi, S. M., Pandey, A. K., Capite, N., Fortune, S. M., Rubin, E. J., & Sasseti, C. M. (2006). Characterization of mycobacterial virulence genes through genetic interaction mapping. *Proceedings of the National Academy of Sciences*, 103, 11760–11765.

Kim, M. J., Wainwright, H. C., Locketz, M., Bekker, L. G., Walther, G. B., Dittrich, C., ... Russell, D. G. (2010). Caseation of human tuberculosis granulomas correlates with elevated host lipid metabolism. *EMBO Molecular Medicine*, 2, 258–274.

Klinkenberg, L. G., Lee, J.-H., Bishai, W. R., & Karakousis, P. C. (2010). The stringent response is required for full virulence of *Mycobacterium tuberculosis* in guinea pigs. *The Journal of Infectious Diseases*, 202, 1397–1404.

Lee, W., VanderVen, B. C., Fahey, R. J., & Russell, D. G. (2013). Intracellular *Mycobacterium tuberculosis* exploits host-derived fatty acids to limit metabolic stress. *Journal of Biological Chemistry*, 288, 6788–6800.

Nazarova, E. V., & Russell, D. G. (2017). Growing and handling of *Mycobacterium tuberculosis* for macrophage infection assays. In *Methods in Molecular Biology*, 1519, 325–331.

Pandey, A. K., & Sasseti, C. M. (2008). Mycobacterial persistence requires the utilization of host cholesterol. *Proceedings of the National Academy of Sciences*, 105, 4376–4380.

Peyron, P., Vaubourgeix, J., Poquet, Y., Levillain, F., Botanch, C., Bardou, F., ... Altare, F. (2008). Foamy macrophages from tuberculous patients' granulomas constitute a nutrient-rich reservoir for *M. tuberculosis* persistence. *PLoS Pathogens*, 4, e1000204.

Podinovskaia, M., Lee, W., Caldwell, S., & Russell, D. G. (2013). Infection of macrophages with *Mycobacterium tuberculosis* induces global modifications to phagosomal function. *Cellular Microbiology*, 15, 843–859.

Primm, T. P., Andersen, S. J., Mizrahi, V., Avarbock, D., Rubin, H., & Barry III, C. E. (2000). The stringent response of *Mycobacterium tuberculosis* is required for long-term survival. *Journal of Bacteriology*, 182, 4889–4898.

Prod'hom, G., Lagier, B., Pelicic, V., Hance, A. J., Gicquel, B., & Guilhot, C. (1998). A reliable amplification technique for the characterization of genomic DNA sequences flanking insertion sequences. *FEMS Microbiol Lett*, 158, 75–81.

Rachman, H., Strong, M., Ulrichs, T., Grode, L., Schuchhardt, J., Mollenkopf, H., ... Kaufmann, S. H. E. (2006). Unique transcriptome signature of *Mycobacterium tuberculosis* in pulmonary tuberculosis. *Infection and Immunity*, 74, 1233–1242.

Rohde, K. H., Abramovitch, R. B., & Russell, D. G. (2007). *Mycobacterium tuberculosis* invasion of macrophages: Linking bacterial gene expression to environmental cues. *Cell Host and Microbe*, 2, 352–364.

Rohde, K. H., Veiga, D. F. T., Caldwell, S., Balázsi, G., & Russell, D. G. (2012). Linking the transcriptional profiles and the physiological states of *Mycobacterium tuberculosis* during an extended intracellular infection. *PLoS Pathogens*, 8, e1002769.

Schnappinger, D., Ehrt, S., Voskuil, M. I., Liu, Y., Mangan, J. A., Monahan, I. M., ... Schoolnik, G. K. (2003). Transcriptional adaptation of *Mycobacterium tuberculosis* within macrophages: Insights into the phagosomal environment. *The Journal of Experimental Medicine*, 198, 693–704.

Segal, W., Bloch, H. (1956). Biochemical differentiation of *Mycobacterium tuberculosis* grown *in vivo* and *in vitro*. *Journal of Bacteriology*, 72, 132–141.

Singh, V., Jamwal, S., Jain, R., Verma, P., Gokhale, R., & Rao, K. V. S. (2012). *Mycobacterium tuberculosis*-driven targeted recalibration of macrophage lipid homeostasis promotes the foamy phenotype. *Cell Host and Microbe*, 12, 669–681.

Srivastava, S., Chaudhary, S., Thukral, L., Shi, C., Gupta, R. D., Gupta, R., ... Gokhale, R. S. (2015). Unsaturated lipid assimilation by mycobacteria requires auxiliary cis-trans enoyl CoA isomerase. *Chemistry and Biology*, 22, 1577–1587.

Tailleux, L., Waddell, S. J., Pelizzola, M., Mortellaro, A., Withers, M., Tanne, A., ... Neyrolles, O. (2008). Probing host pathogen cross-talk by transcriptional profiling of both *Mycobacterium tuberculosis* and infected human dendritic cells and macrophages. *PLoS ONE*, 3, e1403.

Talaat, A. M., Ward, S. K., Wu, C. W., Rondon, E., Tavano, C., Bannantine, J. P., ... Johnston, S. A. (2007). Mycobacterial bacilli are metabolically active during chronic tuberculosis in murine lungs: Insights from genome-wide transcriptional profiling. *Journal of Bacteriology*, 189, 4265–4274.

Taylor, R. C., Brown, A. K., Singh, A., Bhatt, A., & Besra, G. S. (2010). Characterization of a beta-hydroxybutyryl-CoA dehydrogenase from *Mycobacterium tuberculosis*. *Microbiology*, 156, 1975–1982.

VanderVen, B. C., Fahey, R. J., Lee, W., Liu, Y., Abramovitch, R. B., Memmott, C., ... Russell, D. G. (2015). Novel inhibitors of cholesterol degradation in *Mycobacterium tuberculosis* reveal how the bacterium's

metabolism is constrained by the intracellular environment. PLoS Pathogens, 11, e1004679.

Venkatesan, R., & Wierenga, R. K. (2013). Structure of mycobacterial beta-oxidation trifunctional enzyme reveals its altered assembly and putative substrate channeling pathway. ACS Chemical Biology, 8, 1063–1073.

Wang, Q., Zhu, L., Jones, V., Wang, C., Hua, Y., Shi, X., ... Gao, Q. (2015). CpsA, a LytR-CpsA-Psr family protein in *Mycobacterium marinum*, is required for cell wall integrity and virulence. Infection and Immunity, 83, 2844-2854.

Ward, S. K., Abomoelak, B., Marcus, S. A., & Talaat, A. M. (2010). Transcriptional profiling of *Mycobacterium tuberculosis* during infection: Lessons learned. Frontiers in Microbiology, 1, 121.

Weiss, L. A., & Stallings, C. L. (2013). Essential roles for *Mycobacterium tuberculosis* Rel beyond the production of (p)ppGpp. Journal of Bacteriology, 195, 5629–5638.

CHAPTER 5

Summary and further directions

Despite strong belief in the field that fatty acids are acquired and metabolized by Mtb inside of the host, little was known how fatty acid assimilation happens. Here we revealed a few key players in this process and possible mechanisms of its regulation.

We have expanded our understanding of a role Mce transporters play in lipid transport and shed new light on their organization and regulation. The *mce1-4* loci make up four separate operons in the Mtb genome and each operon encodes the putative protein subunits (2 permeases YrbEA and YrbEB, 6 Mce proteins and variable number of accessory subunits of unknown function) that likely comprise the individual Mce transporters. It is thought that each Mce transporter is substrate-specific: Mce4 designated to cholesterol import (Pandey & Sassetti, 2008) and Mce1 is described here to import fatty acids. Based on cholesterol assimilation studies with Mce4 accessory subunit Mam4B mutant, we propose that Mce4 imports cholesterol via a two-step process that involves cholesterol binding/shuttling across the cell wall followed by the final translocation through the cytoplasmic membrane delivering cholesterol into the cytosol (Figure 5.1). The permease subunits may participate in the final translocation of cholesterol across the cytoplasmic membrane while the Mce proteins likely participate in the binding/shuttling of cholesterol across the Mtb cell envelope. Although Mtb is considered a gram-positive bacteria, its outer layer of lipids makes its cell wall more similar to that of gram-negative bacteria, and therefore binding/shuttling of lipids across the Mtb cell envelope may be analogous to what has been proposed for lipid

trafficking by Mce proteins across the periplasm of gram-negative bacteria (Malinverni & Silhavy, 2009; Thong et al., 2016; Nakayama & Zhang-Akiyama, 2017). This two-step mechanism of nutrient uptake may be a generalizable mechanism for all Mce transporters.

We found that the LucA protein is required for intake of both fatty acids and cholesterol, and inactivation of LucA leads to degradation of Mce1 subunits and MceG, an ATPase predicted to supply energy for Mce transporters. Homology searches based on 3-dimensional structures identified a putative protease inhibitor domain within the N-terminus of LucA (Kelly et al., 2015). We hypothesize that LucA may locally inactivate a protease to maintain the integrity of the transporter complexes. Based on our data showing interaction between LucA and accessory subunits of Mce1 and Mce4, we suggest that these accessory subunits recruit LucA to inhibit protease activity (Figure 5.1). This hypothesis is partially supported by degradation of Mce1 proteins and subsequent defect in fatty acid uptake in the absence of OmamA. We verified that the Mce1 protein disappearance in OmamA mutant resulted from protease activity, by inactivation of Zn²⁺ metalloprotease Zmp1 in this mutant. This degradation of Mce subunits could be a mechanism to rapidly halt nutrient uptake through the specific Mce transporters and possibly switch to a different route of nutrient assimilation.

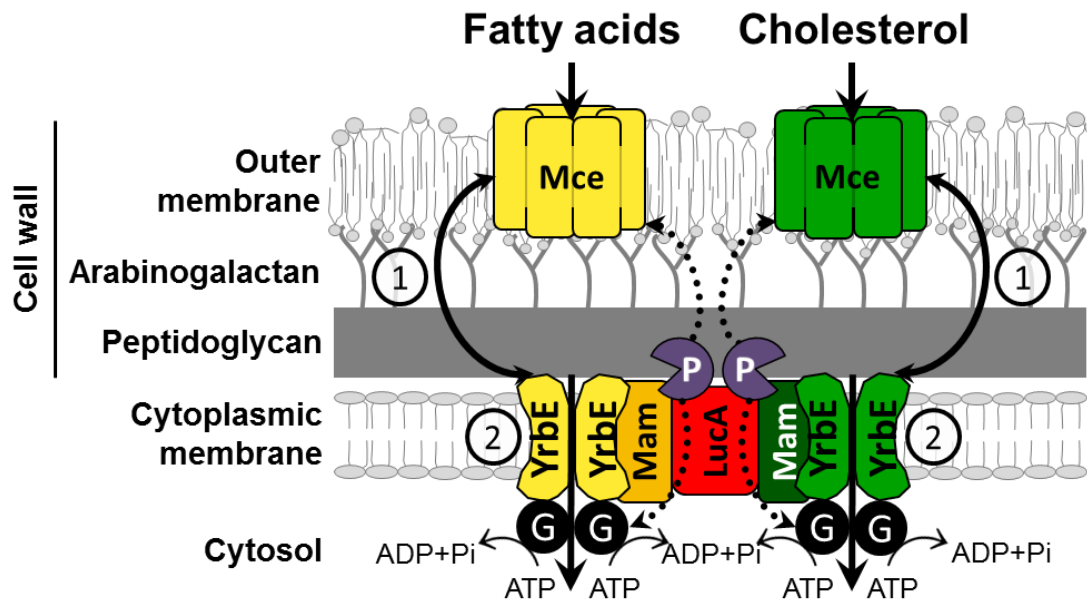


Figure 5.1. Model for Mce mediated transport of lipids in *Mtb*. The MceA-F proteins bind and shuttle nutrients across the outer lipid layer and “pseudo-periplasmic space” of the *Mtb* cell wall (step 1). The cytoplasmic membrane permeases YrbE’s translocate nutrients across the membrane using energy provided by ATPase MceG (G) (step 2). The accessory subunits Mam’s likely act as adapters to recruit additional proteins to the complex such as LucA. Each transporter is specific for its lipid substrate, and coordination of their function is performed by LucA and accessory proteins Mam’s through protection from degradation by protease (P). In the absence of accessory proteins Mam’s or LucA protease degrades Mce and MceG proteins, rendering transporters nonfunctional.

We believe that these efficient means to regulate lipid import in Mtb should be investigated further. It is very likely that proteases other than Zmp1 are involved in regulation of Mce function. To find proteases inhibited by LucA we propose to genetically screen for mutations that will restore lipid uptake in the $\Delta lucA::hyg$ mutant strain. Metabolic labeling with fluorescent fatty acids and *prpD*::GFP reporter could be employed for such screen to distinguish proteases regulating fatty acid and cholesterol assimilation, respectively. Among other unanswered questions about Mce transporter organization are specificity of proteases towards specific Mce subunits (Mce, YrbE or MceG), and identification of interacting partners within Mce complexes. Besides Mce1 and Mce4, Mtb likely uses alternative lipid transporters which still need to be identified. This prediction comes from observation of residual level of fatty acid and cholesterol uptake and metabolism in mutants lacking Mce1 and Mce4, respectively. Mce2 and Mce3 could be possible candidates, considering that their function has not been determined yet.

As co-metabolism of fatty acids and cholesterol in Mtb is predicted (Lee et al., 2013), we have explored possible co-regulation of these lipids. We found that cholesterol metabolites downregulate transcription of the *mce1* locus, with no substantial effect on fatty acid uptake in the short term. These results suggest that posttranscriptional regulation is used by Mtb to rapidly respond to the changing environment. We also discovered that fatty acids induce higher levels of cholesterol uptake. We propose further investigation of

the mechanisms involved in this enhancement of cholesterol accumulation by performing a genetic screen with fluorescently-labeled cholesterol.

Finally, we conducted a forward genetic screen to identify requirements for Mtb to assimilate fatty acids at an early stage of macrophage infection. We identified a group of proteins that are required for uptake of fatty acids both in macrophages and in axenic culture, as well as a group of proteins which function in fatty acid uptake is triggered only inside of the host cell. This work needs to be followed up with an in-depth investigation of roles played by these proteins. Interestingly, Mce1D, OmamB and MceG were found to be required for fatty acid assimilation in macrophage, reinforcing significance of the Mce1 complex, Mce accessory subunits, and the ATPase MceG, despite high redundancy in lipid metabolism in Mtb.

It is important to remember that the majority of the work described here was done in resting murine bone marrow-derived macrophages, which does not fully reflect all the nuances of *in vivo* infection. Inside of an infected individual, Mtb experiences a spectrum of immune responses associated with changes in available nutrients (Olive & Sasseti, 2016; Huang et al., 2017; Mishra et al., 2017). For example, cholesterol-responsive KstR regulon is equally expressed in Mtb during infection of both resting and activated macrophages (Schnappinger et al., 2003; Homolka et al., 2010). However, the ability to import cholesterol through Mce4 is required for survival of the pathogen only in activated macrophages or at the later stages of mouse infection when T cells produce IFN- γ to activate these immune cells (Joshi et

al., 2006; Pandey & Sasseti, 2008). These observations suggest that i) cholesterol is available to Mtb independently of the activation status of the host cell, however ii) nutrients that can be imported independently of Mce4 are used by Mtb for growth in resting macrophages. Importantly, Mce1 was shown to be required for Mtb survival in mice in the first two weeks of mouse infection (Sasseti & Rubin, 2003). Additionally, the LucA mutant with inactivated subunits of multiple Mce transporters demonstrates a growth defect in resting macrophages, supporting an idea that transporters other than Mce4 are used by Mtb in macrophage at this state. And since inactivation of LucA disables both fatty acid and cholesterol uptake, it is logical to conclude that fatty acids are being used by Mtb in resting macrophages. Therefore, metabolism of Mtb inside of the host is extremely dynamic: both in terms of nutrients and transporters used by Mtb.

Identification of a full lipid importing apparatus is necessary to shed light on the importance of certain nutrients in cells of specific immune status. It would be also intriguing to determine which cells are more permissive for bacteria unable to import lipids. Using mutants with inducible inactivation of LucA, MceG or specific lipid transporters for mouse infection, with subsequent evaluation of bacterial distribution between immune cells of different types might help to answer this question.

The central carbon and lipid metabolic pathways of Mtb have emerged as potential drug targets (Rhee et al., 2011; VanderVen et al., 2015), therefore understanding the bottlenecks or weaknesses in these pathways will assist TB

drug discovery. Additionally, the flux of fatty acids into TAG and central metabolism contributes to drug tolerance in Mtb (Baek et al., 2011), a phenotype that is further enhanced by immune pressure during *in vivo* infection (Liu et al., 2016). Targeting the specialized lipid metabolic pathways in Mtb that are involved in fatty acid and cholesterol utilization could be a viable strategy for the development of new drugs that reduce Mtb drug tolerance and augment current TB drug regimens. The data presented in this dissertation revealed previously unknown mechanisms of fatty acid and cholesterol assimilation by Mtb. A better understanding of the functional integration of Mtb's specialized metabolic pathways is required to acquire a fuller appreciation of Mtb pathogenesis.

References

Baek, S. H., Li, A. H., & Sasseti, C. M. (2011). Metabolic regulation of mycobacterial growth and antibiotic sensitivity. *PLoS Biology*, 9, e1001065.

Homolka, S., Niemann, S., Russell, D. G., & Rohde, K. H. (2010). Functional genetic diversity among *Mycobacterium tuberculosis* complex clinical isolates: Delineation of conserved core and lineage-specific transcriptomes during intracellular survival. *PLoS Pathogens*, 6, 1–17.

Huang, L., Nazarova, E., Tan, S., Liu, Y., & Russell, D. G. (2017). Host phagocyte lineages in the infected mouse lung exhibit different metabolic states and support differential growth of *Mycobacterium tuberculosis*. In preparation for submission.

Joshi, S. M., Pandey, A. K., Capite, N., Fortune, S. M., Rubin, E. J., & Sasseti, C. M. (2006). Characterization of mycobacterial virulence genes through genetic interaction mapping. *Proceedings of the National Academy of Sciences*, 103, 11760–11765.

Kelly, L. A., Mezulis, S., Yates, C., Wass, M., & Sternberg, M. (2015). The Phyre2 web portal for protein modelling, prediction, and analysis. *Nature Protocols*, 10, 845–858.

Lee, W., VanderVen, B. C., Fahey, R. J., & Russell, D. G. (2013). Intracellular *Mycobacterium tuberculosis* exploits host-derived fatty acids to limit metabolic stress. *Journal of Biological Chemistry*, 288, 6788–6800.

Liu, Y., Tan, S., Huang, L., Abramovitch, R. B., Rohde, K. H., Zimmerman, M. D., ... Russell, D. G. (2016). Immune activation of the host cell induces drug tolerance in *Mycobacterium tuberculosis* both *in vitro* and *in vivo*. *The Journal of Experimental Medicine*, 213, 809–825.

Mishra, B. B., Lovewell, R. R., Olive, A. J., Zhang, G., Wang, W., Eugenin, E., ... Sasseti, C. M. (2017). Nitric oxide prevents a pathogen-permissive granulocytic inflammation during tuberculosis. *Nature Microbiology*, 2, 17072.

Olive, A. J., & Sasseti, C. M. (2016). Metabolic crosstalk between host and pathogen: sensing, adapting and competing. *Nature Reviews Microbiology*, 14, 221–234.

Pandey, A. K., & Sassetti, C. M. (2008). Mycobacterial persistence requires the utilization of host cholesterol. *Proceedings of the National Academy of Sciences*, 105, 4376–4380.

Sassetti, C. M., & Rubin, E. J. (2003). Genetic requirements for mycobacterial survival during infection. *Proceedings of the National Academy of Sciences*, 100, 12989–12994.

Schnappinger, D., Ehrt, S., Voskuil, M. I., Liu, Y., Mangan, J. A., Monahan, I. M., ... Schoolnik, G. K. (2003). Transcriptional adaptation of *Mycobacterium tuberculosis* within macrophages: Insights into the phagosomal environment. *The Journal of Experimental Medicine*, 198, 693–704.